Minnesota Department of Transportation

RESEARCH SERVICES

Office of Policy Analysis, Research & Innovation

Assessment and Recommendations for the Operation of Standard Sumps as Best Management Practice for Stormwater Treatment (Volume 1)

Omid Mohseni, Principal Investigator
St. Anthony Falls Laboratory
University of Minnesota

February 2011

Your Destination...Our Priority

All agencies, departments, divisions and units that develop, use and/or purchase written materials for distribution to the public must ensure that each document contain a statement indicating that the information is available in alternative formats to individuals with disabilities upon request. Include the following statement on each document that is distributed:

To request this document in an alternative format, call Bruce Lattu at 651-366-4718 or 1-800-657-3774 (Greater Minnesota); 711 or 1-800-627-3529 (Minnesota Relay). You may also send an e-mail to bruce.lattu@state.mn.us. (Please request at least one week in advance).

Technical Report Documentation Page

1. Report No. MN/RC 2011-08	2.	3. Recipients Accession No.	
4. Title and Subtitle Assessment and Recommendations for the Operation of Standard Sumps as Best Management Practice for Stormwater Treatment (Volume 1)		5. Report Date February 2011	
		6.	
7. Author(s) Adam Howard, Omid Mohseni, John Gulliver, and Heinz Stefan		8. Performing Organization Report No.	
9. Performing Organization Name and Address St. Anthony Falls Laboratory University of Minnesota 2 Third Ave. SE Minneapolis, MN 55414		10. Project/Task/Work Unit No. CTS Project #2008082	
		11. Contract (C) or Grant (G) No. (c) 89261 (wo) 100	
12. Sponsoring Organization Name and Address Minnesota Department of Transportation Research Services Section 395 John Ireland Blvd., MS 330 St. Paul, MN 55155		13. Type of Report and Period Covered Interim Report	
		14. Sponsoring Agency Code	
15. Supplementary Notes http://www.lrrb.org/pdf/201108.pdf			

16. Abstract (Limit: 250 words)

Standard sumps are installed in many urban and suburban storm sewer systems. They may qualify as a best management practice (BMP) to pre-treat stormwater runoff by removing suspended sediment from the water. However, no data exist on the effectiveness of sediment removal by and maintenance requirements for sumps. Such data could justify giving pollution prevention credits to transportation departments, municipalities, counties and other local governments for the use of standard sumps.

To determine whether the standard sumps remove suspended sediments from stormwater runoff, two standard sumps with different sizes were tested in a laboratory setting to determine their removal efficiencies under low-flow conditions as well as the effluent concentrations under high-flow conditions. The removal efficiency tests included feeding a specific sediment size and concentration into the influent pipe and then collecting, drying and weighing the sediments removed by the sump at the test conclusion. The high-flow condition tests involved placing a commercial sediment mix inside the sump and assessing the amount of sediment remaining after the sump was subjected to high flows for a period of time.

At the conclusion of testing, removal efficiency functions as well as washout functions were developed for the sumps, which can be used to predict the performance of all standard sumps. In addition, an uncertainty analysis was conducted to aid with data interpretation.

17. Document Analysis/Descriptors Bedforms; Effluent concentration; Air entrainment; Particle size distribution; Sieve analysis; Performance measurement; Performance functions; Scaling; Settling power; Electric power supply		18. Availability Statement No restrictions. Document available from: National Technical Information Services, Springfield, Virginia 22161	
19. Security Class (this report) Unclassified	20. Security Class (this page) Unclassified	21. No. of Pages 109	22. Price

Assessment and Recommendations for the Operation of Standard Sumps as Best Management Practice for Stormwater Treatment (Volume 1)

Interim Report

Prepared by:

Adam Howard
Omid Mohseni
John Gulliver
Heinz Stefan

St. Anthony Falls Laboratory
University of Minnesota

February 2011

Published by:

Acknowledgements

Table of Contents

List of Tables

List of Figures

List of Symbols

A	Sump Area
A_p	Cross Sectional Area of Pipe Flow
A_w	Watershed Surface Area
a	Initial Slope of Removal Efficiency Function
b	Measure of Removal Efficiency Function's Curvature
$\overline{C}$	Average Concentration
C_r	Rational Equation Runoff Coefficient
D	Sump Diameter
D_z	Molecular Diffusion Coefficient
d	Particle Diameter
d_{50}	Median Particle Size
f_w	Wall Friction Coefficient
g	Gravitational Constant
Ha	Hazen Number
h	Sump Depth
h_{in}	Inlet Water Surface Elevation
h_{out}	Outlet Water Surface Elevation
h_L	*Head loss*
i	Rainfall Intensity
K_c	Adjustment Factor for Units
K_{en}	Entrance Loss Coefficient
K_{ex}	Exit Loss Coefficient
L	Watershed Hydraulic Length
l	Length Scale
n	Number of Observations
n_m	Manning's Roughness Coefficient
p	Number of Model Parameters
Pe	Péclet Number
Q	Flow Rate
R	Maximum Efficiency in the Removal Efficiency Function
r	Pipe Radius
S_o	Average Pipe
S	Average Watershed Slope
SG	Specific Weight of Sediment
t_c	Time of Concentration
U	Average Particle Velocity
U_{in}	Inflow Velocity
U_j	Inflow Jet Velocity
U_{out}	Outflow Velocity
U_s	Particle Settling Velocity
V_s	Sump Volume
W	Dry Weight of Sediment

z	Height Measurement
α	Stokes Law Correction for Turbulence
β	Constant of Integration
ε	Trap Efficiency
ε_z	Turbulent Diffusion Coefficient
κ	von-Karman Universal Constant
η	Removal Efficiency
$\bar{\eta}$	Mean Measured Removal Efficiency
η_i	Measured Removal Efficiency
η_{mi}	Modeled Removal Efficiency
ρ_w	Density of Water
ρ_s	Particle Density
τ_c	Sheilds Stress
ν	Kinematic Viscosity

Executive Summary

Standard sumps are installed in many urban and suburban storm sewer systems. They may qualify as a best management practice (BMP) to pre-treat stormwater runoff by removing suspended sediment from the water. However, no data exist on the effectiveness of sediment removal and maintenance requirements of the sumps. Such data could justify giving pollution prevention credits to transportation departments, municipalities, counties and other local governments for the use of standard sumps.

The goals of this study were to (1) evaluate four configurations of a flow-though standard sump for sediment capture and washout; (2) design a simple retrofit for standard sumps to improve sediment capture and decrease washout; (3) develop a performance function estimating the efficiency of standard sumps in removing suspended sediments; (4) develop another function estimating the sediment washout in standard sumps. This volume of the final report (Volume 1) only focuses on the performance of standard sumps. The second volume of the final report will be on the design and performance of the retrofit for improving the sediment capture and lowering the washout rate.

In order to determine whether standard sumps remove suspended sediment from stormwater runoff, two standard sumps of different size (4×4 ft (1.2×1.2 m), i.e. 4-ft (1.2 m) diameter by 4-ft (1.2 m) depth, 4×2 ft (1.2×0.6 m), 6×6 ft (1.8×1.8 m), and 6×3 ft (1.8×1.8 m)) were tested in a laboratory setting. Removal efficiencies under low-flow conditions as well as washout rates under high-flow conditions were measured. In the low-flow removal efficiency tests, sediments of known size distributions were fed at known rates into the influent pipe of the sump. At the conclusion of the test, the sediments removed by the sump were collected, dried and weighed. In the high-flow washout tests a commercially available sand gradation (e.g. F110 sand) was placed inside the sump and after passing water through the sump at high flows for a period of time, the amount of sediments remaining in the sump was measured. The sumps did remove suspended sediment at low flows, but at high flows the washout rate was substantial.

The data collected have been processed, and a sediment washout function and a removal efficiency function have been determined. These two performance functions together can be used as a tool to assess the performance of standard sumps as stormwater treatment devices and to determine their maintenance schedule. The table below presents the expected 1-yr and 2-yr storm removal efficiencies and the 10-yr storm washout effluent concentrations for all of the full scale sumps tested (size labeled as diameter × depth in feet) for two different particle size distributions. The results are obtained using the sediment washout and the removal efficiency functions. The two particle size distributions given in the table, OK110 and Mn/DOT Road Sand, have median particle sizes of 0.0046 in (116 μm) and 0.0137 in (347 μm), respectively. The OK110 sand has a d_{15} of 0.0039 in (98 μm) and a d_{85} of 0.0053 in (135 μm). It is important to note that the 1-yr, 2-yr and 10-yr storm events in the table have been computed for 10 and 20 acre watershed areas draining into 4-ft and 6-ft sumps, respectively, with a runoff coefficient of 0.7. It is evident that standard sumps can be only effective in treating stromwater runoff from small urban drainage areas, i.e. smaller than 4 acres.

Removal efficiency of standard sumps at expected 1-yr and 2-yr storm events and washout at expected 10-yr storm events

Sump Model	Particle Size Distribution	Water Temperature (F)	Removal Efficiency at 1-yr Storm Event (%)	Removal Efficiency at 2-yr Storm Event (%)	Washout at10-yr Storm Event (mg/L)
4x4	Mn/DOT Road Sand	50	16	12	6
4x4	OK110	50	3	2	240
4x2	Mn/DOT Road Sand	50	8	6	30
4x2	OK110	50	1	1	460
6x6	Mn/DOT Road Sand	50	4	2	270
6x6	OK110	50	1	0	820
6x3	Mn/DOT Road Sand	50	2	1	490
6x3	OK110	50	0	0	1100

1 Introduction

The standard sump within a manhole has been a key component in stormwater infrastructure. In addition to providing a location for pipe junctions and storm sewer maintenance access, the sump's detention time provides opportunity for the removal of some particulates and trash. Standard sumps are simple cylindrical tanks with vertical axis and varying sump depths. The inlet and outlet pipes are typically oriented straight across from each other, with a slight drop from inlet to outlet. However, it is not uncommon for a sump to have more than one inlet or outlet at various locations in the sump. Standard sumps may provide pre-treatment for Low Impact Development (LID) practices, removing sediment from the stormwater and retaining it. This requires non-routine maintenance activities at great cost (Kang, et al, 2008).

In recent decades, proprietary devices for the treatment of stormwater have become increasingly popular in dense urban communities to meet stormwater quality regulations. These regulations are a response to the 1987 amendments to the Clean Water Act (Smith 2001). Wisconsin has gone a step further by requiring 80% total suspended solid (TSS) removal in new developments and 40% TSS removal in redeveloped areas (Brzozwski 2006). While proprietary devices have proven effective for pre-treatment that removes inorganic particles larger than silt from stormwater runoff, their expense has led the Minnesota Department of Transportation (MnDOT) as well as cities and counties within Minnesota to seek other avenues to reach their stormwater pre-treatment goals.

From 2005 to 2007, a team from the St. Anthony Falls Laboratory at the University of Minnesota provided an in-depth laboratory and field performance analysis of several proprietary devices (Carlson et al., 2006; Wilson et al., 2009). The focus of these studies was to assess the removal of various sediment sizes from the influent. It was decided to follow the same testing procedure in the evaluation of standard sumps. The results of the standard sump studies can therefore be easily compared to those of the proprietary devices, and the cost effectiveness of the standard sump can then be determined. In addition to the evaluation of the sump as a sediment capturing device, washout tests have been conducted to determine the flows which cause removal of the previously captured sediment. Results of these tests can help develop guidelines for cleaning schedules.

The goals of this study are to (1) evaluate four configurations of a straight flow-though standard sump for sediment capture and washout; (2) design a simple retrofit for standard sumps to improve sediment capture and decrease washout; (3) develop a performance function for estimating the suspended sediment removal efficiency of standard sumps; (4) develop another function for estimating the sediment washout from standard sumps. This first volume of the final report focuses on the performance of standard sumps. The second volume of the final report will be on the design and performance of the retrofit for increasing the sediment capture and lowering the washout rate.

1.1 Terminology

Terminology for the description of sediment capture and washout by treatment devices varies widely and by study. It is typical to use the term treatment, performance, or removal efficiency to describe the ability of the sump to remove sediment from the influent and deposit it at the

bottom of the sump. Treatment and performance can be confused with the entire sediment capture and retention process. Thus, in this report, "removal efficiency" will be used to describe this portion of the process. It is also typical to use the terms retention, scour, re-suspension, or washout to describe the ability of the settling device to retain the previously captured sediment. It is possible for scour and re-suspension to occur in a settling device without the sediment actually leaving the device. The term retention also implies the previous capture of sediment. Thus, "washout" will be the term used in this report to describe the device's inability to retain previously captured sediment.

1.2   Previous Studies

The standard sump has been a common element of stormwater infrastructure throughout history. Settling chambers, or grit chambers, have been found in Pakistan from as early as 2500-2000 B.C. (Bertrand-Krajewski, 2003). Until the 1970s very little had been done to understand what sediment sizes and how much of each size is being captured in these sumps.

Many studies evaluating proprietary devices for stormwater treatment have been documented. However, data on the effectiveness of standard sumps is very limited. Settling basins represent devices which are hydraulically most similar to standard sumps. Butler et al. (1995) evaluated a gully pot (catch basin) in a laboratory setting for both washout and removal efficiency. For the laboratory analysis, sediment was fed upstream of the gully pot using a sediment feeder and effluent was quantified using a monitoring chamber which housed an infrared suspended solids sensor. Four discrete sediment sizes of 0.0025-0.0039 in (63-100 μm), 0.0039-0.0059 in (100-150 μm), 0.0059-0.0118 in (150-300 μm), 0.0118-0.0236 in (300-600 μm) were added to the water upstream of the device. The infrared sensor was not suitable for the larger two sediment sizes; therefore grab samples were also collected to quantify the effluent. It was found that the gully pot captured less than 25% of particles below 0.0024 in (60 μm). Particles above 0.0196 in (500 μm) however were hypothesized to have high removal efficiencies. A trap efficiency function (Equation 1.1) was developed using a mass balance approach.

$$\varepsilon = \frac{1}{1 + \dfrac{72 Q v}{\alpha \pi g d^2 D^2 (SG - 1)}} \tag{1.1}$$

In Equation 1.1, Q is flow rate, v is kinematic viscosity, α is a correction of Stokes Law for turbulence, g is the acceleration due to gravity, d is the particle diameter, D is the device diameter, and SG is the specific gravity of the particles. This formula requires the assumption of the gully pot being completely mixed, which was initially proposed by Fletcher and Pratt (1981).

More recently, Avila and Pitt (2008) evaluated the washout potential of a catch basin sump. Testing was conducted on a scale model. The data were used for calibration of a computational fluid dynamics (CFD) model. This study led to the conclusion that the rate of washout increases exponentially with decreasing depth and flow rate. Particles as large as 0.1870 in (4750 μm) were washed out of the sump when the flow rates were as high as 0.35 cfs (10 L/s), and the sump was shallow, i.e. 4 in (0.1 m) of water depth above the sediment deposit. Both Butler and Avila noted a decrease in washout rate over time. Butler attributed this to a grading of the bed, which

interlocks the bed particles. Avila's hypothesis involved bed armoring, where larger particles move to the top of the bed and subsequently protect the bed from further scour. Data for Avila's analysis was collected by measuring turbidity time series, suspended solids concentration, and particle size distributions at the outlet of the catch basin by sampling. Pitt (1985) found a stable condition (no net capture or washout of sediment) occurred when 60% of a catch basin's volume was filled with sediment. This has implications for maintenance of sumps when they are used for best management practice (BMP). Pitt's analysis (1985) was based on data collected by automatic flow-weighted samplers and by sonic depth gauges.

Kim et al. (2007) evaluated a hydrodynamic separator with and without cleaning for both treatment (removal efficiency) and scour (washout). In the removal efficiency tests a known particle size distribution was added to a clean sump, and sampling of the effluent concentration was used to determine sediment capture. Washout tests involved preloading the sump and sampling from the effluent to determine the amount of sediment removed. The lack of maintenance led to significant washout as well as changes in the pH and redox potential of the stagnant water in the device. These changes in pH and redox have implications for the release of pollutants which may have been considered trapped (Kim et al., 2007).

Settling (catch) basin studies can provide an understanding of the general sediment transport processes of scour and deposition in settling devices. However, actual removal efficiency and washout values for settling basins should not be compared to those of standard sumps due to a significant difference in flow regimes. Faram and Harwood (2003) evaluated catch basins, standard sumps, and simple and complex hydrodynamic separators using CFD. Each configuration had a diameter of 3.9 ft (1.2 m). The catch basin performed the poorest (removal efficiencies near zero) for particles finer than 0.0215 in (545 μm) at 2.1 cfs (60 L/s). The standard sump was able to capture some sediment with particle sizes larger than 0.0071 in (181 μm) at 2.1 cfs (60 L/s). These studies indicate catch basin sumps perform poorly for the capture and retention of the fine particulate under most flow conditions.

Wilson et al. (2009) measured the removal efficiency of four hydrodynamic separators in the field by utilizing a mass balance approach. Three discrete particle size ranges of 0.0035-0.0049 in (89-125 μm), 0.0099-0.0140 in (251-355 μm), and 0.0197-0.0232 in (500-589 μm) were input by a calibrated sediment feeder upstream of each device at a known rate. At the conclusion of each test the device was carefully cleaned and all deposited sediments were collected, dried, sieved and weighed. This same process was also successfully used by Carlson et al. (2006) and Mohseni et al. (2007) for laboratory evaluations of two other stormwater settling devices.

Mohseni et al. (2007) also evaluated the washout potential for a hydrodynamic separator. A mass balance approach was chosen for this study. The device was preloaded with sediment. The preloaded sediment depth in the device was measured using a ruler at many locations; the data provided the pre-test sediment volume. Following a high-flow test, the sediment depth was measured again, and the analysis of the data provided a value for the sediment washout. This process was also implemented by Saddoris et al. (2010) for the evaluation of the sediment washout from three hydrodynamic separators, which were tested in the laboratory. One of the devices was also tested in the field. In the field tests, the sediment depth was measured using a

ruler and/or laser levels. The laboratory tests were conducted by setting the devices on strain gauge load cells, which provided accurate monitoring of the device weight.

1.3   Sediment Sizes and Concentrations in Stormwater

Before evaluating the effectiveness of a standard sump for particulate removal, it is necessary to have an understanding of the size distributions and concentrations of sediments in stormwater runoff. Stormwater influent characteristics have been evaluated in many studies, but the results vary widely by location and evaluation technique. Maestre and Pitt (2005) provided a compilation and analysis of stormwater monitoring data. Their findings indicate stormwater TSS concentrations of 0.0089 lb/ft^3 (143 mg/L) for an urban summer rain and 0.0036 lb/ft^3 (58 mg/L) for other rains. Li et al. (2006) evaluated the particle size distribution in stormwater for the Los Angeles, CA, area. Their findings indicate that 97% of the sediment was less than 0.0012 in (30 μm) in diameter. Kim and Sansalone (2008) found that fine particulate matter, i.e. smaller than 0.0030 in (75 μm), accounted for 25% to 80% of the sediment by mass in stormwater. All of the data above were collected by sampling of stromwater influent and effluent.

The size distribution and specific weight of particles in stormwater which are trapped by stormwater BMPs have implications for nutrient removal. Vaze and Chiew (2004) found that most of the particulate total phosphorus and total nitrogen in stormwater are attached to particles from 0.0004 in (11 μm) to 0.0059 in (150 μm). This indicates particles as small as 0.0004 in (11 μm) have to be captured by BMPs if the goal is to remove particulate total phosphorus and nitrogen.

The literature analysis above suggests that significant amounts of sediment in stormwater runoff are smaller than 100 μm. Assessing stormwater BMPs, i.e. testing of particle removal below the 200 sieve size (0.0030 in, 75 μm) requires particle size distributions which are expensive to develop even in a laboratory setting. Particles larger than medium size sands will be captured by sumps with relative ease. Following this logic it is reasonable to assume that the evaluation of sumps should be made with particles in the range of fine particulates to medium sands. Influent concentrations of 0.0031-0.0094 lb/ft^3 (50-150 mg/L) also appear to be a reasonable range (Maestre and Pitt, 2005). An effluent concentration above 0.0031-0.0094 lb/ft^3 (50-150 mg/L) would indicate that a treatment device is no longer capturing particles, and may be subject to washout of previously captured particles.

It has been a common practice to evaluate stormwater BMPs by monitoring how they remove suspended sediment from the stormwater. Unfortunately, the use of samplers for monitoring influent and effluent has proven unreliable for the collection of some sediment particle sizes (Wilson et al., 2007, DeGroot et al., 2009). DeGroot et al. (2009) performed a detailed analysis of sampling procedures and results in a laboratory setting and found that samplers tend to misrepresent particles larger than fine silt. The samples typically had higher concentrations than the true mean concentration. This occurred mainly because the sampler is typically located near the bottom of the flow. Near the bottom of the flow, concentrations of inorganic sediment can be higher due to particle settling. The scaled comparison of two particle size distributions presented by DeGroot et al. (2009) show the highly variable results of sampling. The NURP distribution indicates that 90% of the particles are below 0.0039 in (100 μm), while Sansalone (2008) indicated that 90% of suspended sediments in stormwater were below 0.39 in (10,000 μm).

In order to avoid the problems associated with sampling, the mass balance approach used by Carlson et al (2006), Wilson et al (2009), Mohseni et al. (2007), and Saddoris et al. (2010) was adopted in this study to measure the removal efficiency and sediment washout of standard sumps.

2   Experimental Methods and Materials

2.1   Experimental Setup

Two full scale fiberglass sumps were constructed for testing by a local fiberglass manufacturer and placed on a test stand in the St. Anthony Falls Laboratory (SAFL) of the University of Minnesota in Minneapolis, Minnesota. The first sump evaluated was 4 feet (1.2 m) in diameter and 4 feet (1.2 m) deep (the height from the invert of the inlet pipe to the sump bed), and had 15-inch (0.38 m) inlet and outlet pipes at 0 and 180 degrees respectively, i.e. the sump was a straight flow-through sump. A false floor was placed in the sump to decrease the sump depth to 2 feet (0.6 m) for evaluating shallow sumps. There was a one percent drop between the inlet and outlet pipes.

The second sump was 6 feet (1.8 m) in diameter and 6 feet (1.8 m) deep with 24-inch (0.6 m) inlet and outlet pipes at 0 and 180 degrees, respectively. A false floor was also added to this configuration to create a 6 feet (1.8m) diameter by 3 feet (.9m) deep sump for some of the tests. Each sump was connected to the SAFL plumbing system which can supply Mississippi River water under up to 45 feet (14m) of head.

Flow was measured using a Pitot cylinder upstream of the sump. The 4 feet (1.2 m) sump also had a circular weir downstream of the test stand for verification. Due to the high-flow rates required for the 6 feet (1.8m) sump, two 12inch (0.3m) supply pipes were attached to the 24inch (0.6m) inlet pipe through a fabricated manifold. The flow rate was measured in each of these 12-inch (0.3 m) supply pipes using two Pitot cylinders. The use of the Pitot cylinders is described by Silberman (1947). The flow rate for both configurations was controlled using hydraulic gate valves in the supply pipes. Each sump's dimensions and design flow rates are given in Tables 2.1 and 2.2. Figures 2.1 and 2.2 are pictures of the 4 feet (1.2 m) and the 6 feet (1.8 m) fiberglass sumps, respectively.

Table 2.1. Dimensions of Sumps Tested

Sump	Inlet Invert From Floor (ft)	Outlet Invert From Floor (ft)	Sump Diameter (ft)	Pipe Inside Diameter (ft)
4x4	4	3.93	4	1.27
4x2	2	1.93	4	1.27
6x6	6	5.91	6	1.87
6x3	3	2.91	6	1.87
1x1	0.96	0.95	0.96	0.29

Figure 2.1. 4×4ft Sump and Test Stand

Figure 2.2. 6×6ft Sump and Tailwater Box

For performance testing, sediment was fed as a slurry from a Schenk AccuRate sediment feeder into the inlet pipe approximately one foot upstream of the sump. The feeder was located on the shop level of the laboratory, approximately 25 ft (7.6m) above the inlet. This provided the slurry with a high enough velocity to allow penetration into the flow within a short development length. The short development length eliminates loss of sediment in the inlet pipe. A manometer was connected to the device for recording of water surface elevations in the inlet pipe, the sump, and the outlet pipe.

For washout testing, the entire sump test stand was placed on precision strain gauge load cells from Tovey Engineering. The load cells allow the accurate measurement of weight before, during and after tests. The inlet and outlet connections, as well as all drainage ports and the slurry inlet location are removable. This allowed the sump to be weighed before and after the test without any outside influences.

Tests which included the 2 ft (0.6 m) deep or 3 ft (0.9 m) deep sumps required the construction of a false floor. This false floor was constructed of plywood. The actual floor surface of the sump was a ¼ inch (0.64 cm) plastic for the 4-ft (1.2 m) sump and epoxy-coated plywood for the 6-ft (1.8m) sump. The false floors were sealed to prevent any water or sediment penetrating underneath the false floors.

In addition to the full size models tested in the laboratory, a 1×1 ft (0.3×0.3 m) scale model of the 4×4 ft (1.2×1.2 m) sump was built to visualize the flow patterns and bed forms in the sump. This scale model was constructed of clear acrylic plastic at a scale of 1:4.17. Tap water was re-circulated using a 1 horsepower electric pump and two head tanks. The effluent from the model was passed through a 0.0008in (20μm) filter, and re-entered one of the head tanks. It was also possible to directly discharge the effluent into the laboratory drainage system while maintaining a constant head in the tank using the tap. This prevented the re-introduction of sediments into the influent. Appendix A provides additional information on the sump testing setup.

2.2   Testing Procedure

2.2.1   Sediment Removal Testing (Removal Efficiency)

For the 4-ft (1.2m) sump removal efficiency testing, flow rates of 0.6 cfs (17 L/s), 1.2 cfs (34 L/s), 1.8 cfs (51 L/s), and 2.4 cfs (68 L/s) were evaluated in triplicate. The 6-ft (1.8 m) sump was tested at flow rates of 1.8 cfs (51 L/s), 3.5 cfs (100 L/s), 5.3 cfs (150 L/s), and 7 cfs (198 L/s). Flow rates of 0.3 cfs (8.5 L/s), 0.4 cfs (11.3 L/s), and 0.5 cfs (14 L/s) were tested to ensure that a removal efficiency of approximately 100% is achieved. These flow rates were chosen with the goal of achieving removal efficiencies from approximately 0 to 100%. These discharges have been compared to design storm flow rates from a hypothetical, small, urban watershed in Appendix B.

The test duration was approximately one hour for the lowest flow and 18 minutes for the higher flows tests. For an approximate influent concentration of 0.0062-0.0125 lbs/ft^3 (100-200 mg/L) this requires 22 to 44 lbs (10-20 kg) of sediment input for each test. For each test, three relatively discrete particle sizes were mixed and fed into the inlet pipe.

The three median sediment sizes were, 0.0215in (545 μm) (i.e. 0.0197-0.0232 in, 500–589 μm), 0.0119 in (303 μm) (i.e. 0.0099-0.0140 in, 250–355 μm), and 0.0042 in (107 μm) (i.e. 0.0035-0.0049 in, 88–125 μm). The sieving operation is explained in Appendix C. The particle sizes were selected and sieved to avoid overlap of particle sizes in order to minimize scatter in the data (see Wilson et al., 2007). Approximately 40 data points were collected for each device. Appendix D gives a detailed description of the removal efficiency test procedure.

2.2.2   Sediment Washout Testing

Before a sediment washout test the sump was preloaded with sediment. High-flow rates were routed through the sump and the amount of sediment retained in the sump was measured. For these tests, a 12 inch (30.5 cm) deep sediment bed of U.S. Silica Sand F-110 with a median particle size of 0.0043 in (110 μm) was preloaded in the sump. Great care was taken to ensure that the initial conditions were identical for all tests. Samples of the loaded sediment were taken both before and after each of the tests conducted on the 4×4 ft (1.2×1.2 m) sump. These samples were used to determine the particle size distribution (PSD) and the bulk density of sediments retained in the sump. The difference between the initial and final PSDs and the bulk densities were determined to be inconsequential. Therefore, no samples were collected in the tests conducted on sumps of other sizes.

Before each test, the sediment surface was flattened and packed using a 20 lb (9 kg) roller. If new sediment was added to the previously tested deposit, it would all be stirred in an attempt to create a homogenous mixture. These tests were not intended to replicate the exact bed forms and sediment stratigraphy in the field. Since these are not known and can vary significantly from one location to another (due to natural variability in rainfall, soils and land use), it was decided to create a relatively homogenous deposit for all tests.

Two methods were used to measure the weight of sediment in the sump before and after each test. Stick measurements were taken to find the depth of sediment at 24 locations, and the average depth of the deposit was calculated from these data. With the measured bulk density of the samples, it was then possible to calculate the weight of deposit in the sump before and after each test. In the second method the weight of the deposit before and after each test was measured directly by precision strain gauge load cells. The load cells provided an accurate measure of weight throughout the test. A correction was made for the amount of water in the sump before and after the test. The latter was determined by use of a precision static monometer. The flow rates for the 4-ft (1.2 m) sump varied from 2.75 to 5.5 cfs (76 to 156L/s). The flow rates for the 6-ft (1.8m) sump varied from 5 to 19 cfs (142L/s to 538 L/s). Similar to the removal efficiency discharges, the flow rates for the washout tests were designed to reflect effluent concentrations for a wide range, i.e. 0.0012 to 0.062 lbs/ft^3 (20 to 1000 mg/L). The flow rates have been correlated to design storm discharges in Appendix B. See Appendix D for a detailed explanation of the retention testing procedure.

2.2.3   Scale Model Testing

Performance tests were also conducted on a 1×1 ft (0.3×0.3 m) scale model using the same methods as for the full scale tests. Sediment was added to the inflow from a small feeder upstream of the sump model. Two methods were used to add the sediment to the system. The first was to simply feed dry sediment into the flow approximately 13 in (0.3 m) upstream of the

device. The second method was to feed sediment as a slurry approximately 3 in (0.08 m) upstream of the device. The latter method more closely resembles the conditions in the full scale. The sump was cleaned prior to each test. At the end of each test, the sediment removed by the sump was collected, dried, and weighed. For these tests, only one sediment size, 0.0042 in (107 μm) was used, i.e. particles between 0.0035 in and 0.0049 in (88 μm and 125 μm). In addition to the sediment retained in the sump, sediment trapped in the pipe and in the feeder were also dried and weighed to obtain an accurate value of the influent concentration. Due to the low feed rates necessary for the model study, it was not possible to maintain a precise and constant inflow concentration throughout each test. Overall, influent concentrations in the model tests varied from 0.016 to 0.593 lbs/ft^3 (250 to 9500 mg/L), depending on the tested flow rate. The flow rates varied from 0.3 gpm (0.02 L/s) to 76 gpm (4.8 L/s).

The 1×1 ft (0.3×0.3 m) sump washout tests also followed a procedure similar to those in the full scale tests. Three inches (0.08 m), or about 18 lbs (8.2 kg) of U.S. Silica sand F-110 was initially placed in the sump. The sediment remaining at the conclusion of each test was collected, dried, and weighed. Initial testing used only one flow rate of approximately 89 gpm (5.6L/s). Subsequent tests were conducted at a variety of flows from 36 gpm (2.3 L/s) to 89 gpm (5.6 L/s).

3 Results

3.1 Results of Removal Efficiency Tests under Low-Flow Conditions

3.1.1 4-ft (1.2 m) Diameter by 4-ft (1.2 m) Depth

The first round of performance tests on the 4×4ft (1.2×1.2 m) sump began in January of 2009. The test results are plotted in Figure 3.1 in terms of removal efficiency versus discharge. The results indicate that the sump is effectively removing sediment from stormwater inflow.

Up to this point, all performance tests for removal efficiency had been conducted with low-flow rates measured at a downstream weir. The high flows required for the washout tests, made it necessary to replace the 15 in (0.38 m) wide downstream weir with a 24 in (0.61 m) weir. Instead of calibrating this weir, an alternative method for flow rate measurement using a Pitot cylinder in the supply pipes upstream of the device was implemented. This Pitot cylinder had been researched carefully (Silberman 1947) and proved to be effective. To ensure the results would be comparable and repeatable, a repeat series of tests was conducted on the 4×4 ft (1.2×1.2 m) sump in May 2009. In Figure 3.2 the results of the two test series are compared. In the repeat series all of the particle sizes had slightly higher removal efficiencies. The difference is suspected to be partly due to an increase in settling velocity because of an increase in water temperature.
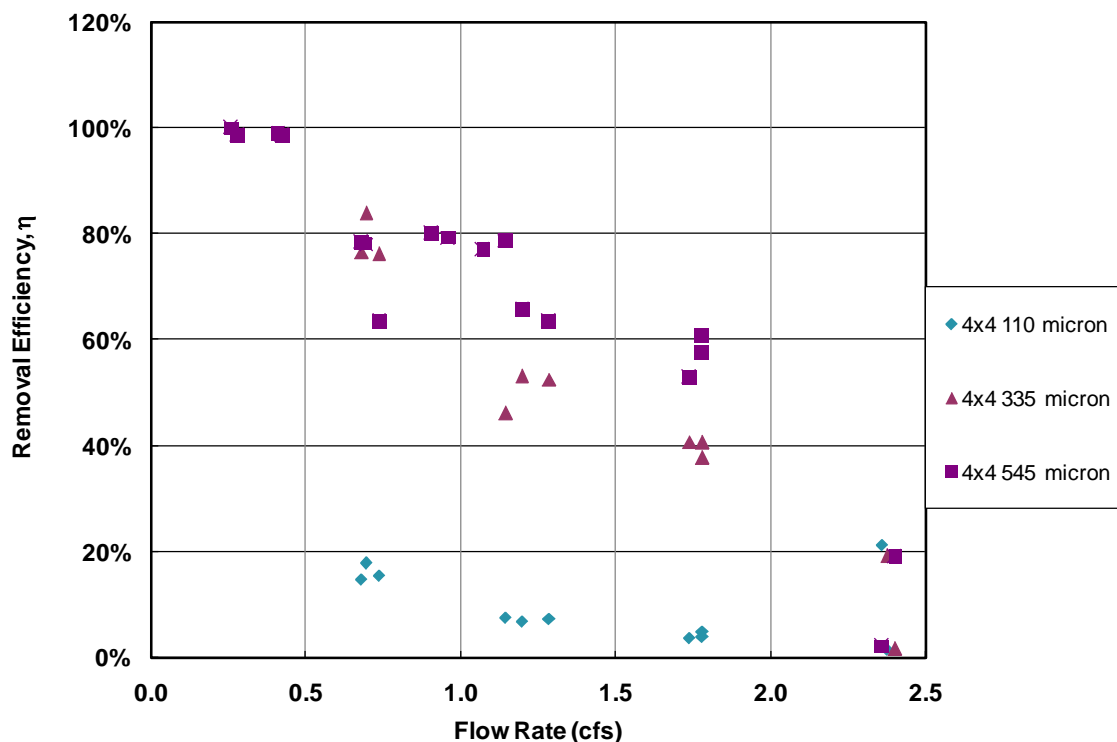
Figure 3.1. Removal Efficiency Results for the 4×4 ft Sump
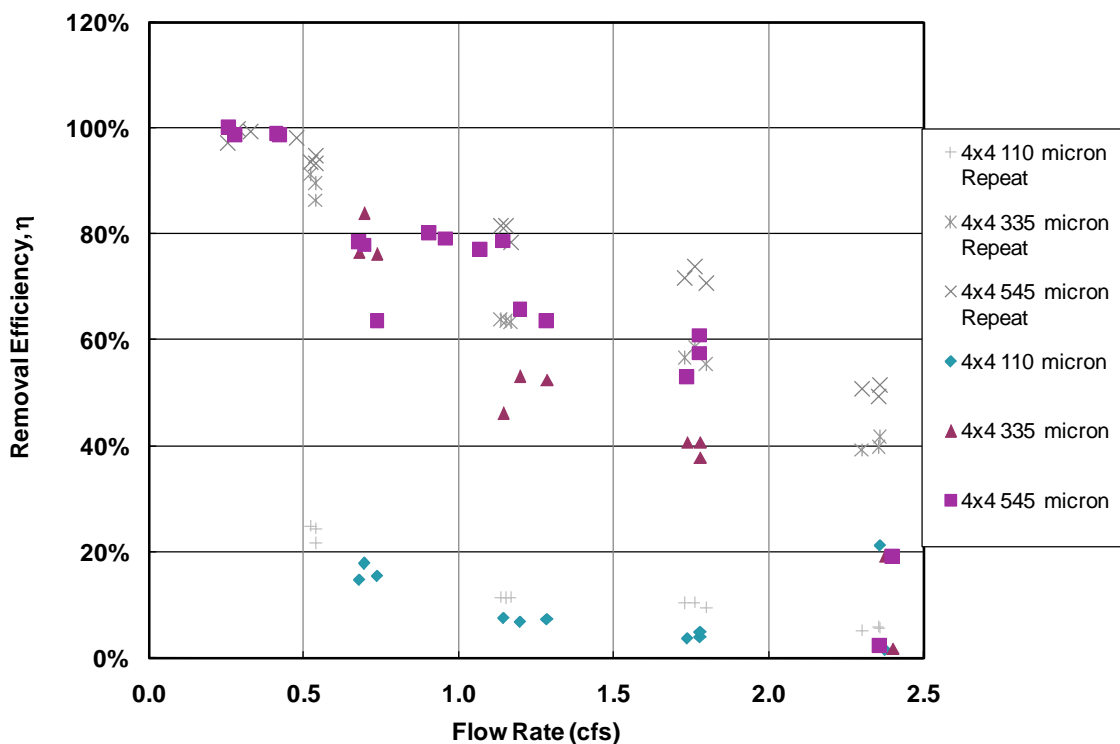
Figure 3.2. Comparison of the Original and the Repeat Tests of Removal Efficiency for the 4×4 ft Sump

3.1.2   4-ft (1.2 m) Diameter by 2-ft (0.6 m) Depth

Performance tests on the 4×2 ft (1.2×0.6 m) sump were conducted from March 23rd to April 16th 2009. The same series of 16 total tests were conducted, and the flow rates were measured using the Pitot cylinder. Figure 3.3 shows the results of this series of tests. When compared to the results from the 4×4 ft (1.2×1.2 m) sump given in Figure 3.1, there is a 5 to 10% decrease in the removal efficiency for the three particle sizes. This result is reasonable, considering that there is more chance for a particle to escape from a shallow sump due the sediment's proximity to the area of high energy associated with the flow path.
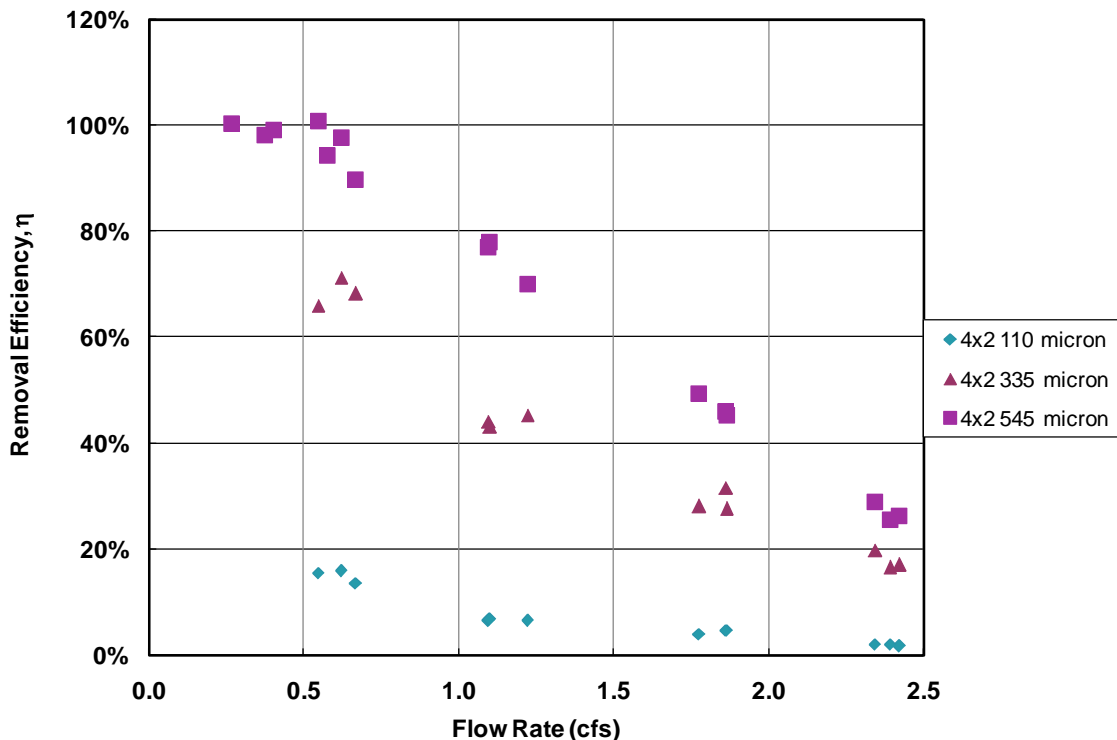
Figure 3.3. Removal Efficiency Results for the 4×2 ft Sump

3.1.3   6-ft (1.8 m) Diameter by 6-ft (1.8 m) Depth

Performance testing of the 6-ft (1.8m) sump began on August 28, 2009. The test procedure was the same as for the 4-ft (1.2 m) sump. The same particle size ranges were used, but the flow rates were higher as described in Section 2.2.1. The results of the removal efficiency tests for the 6-ft (1.8 m) sump are presented in Figure 3.4. As expected, for the same flow rate and particle size the 6-ft (1.8 m) sump performs about 40% better than the 4-ft (1.2 m) sump.
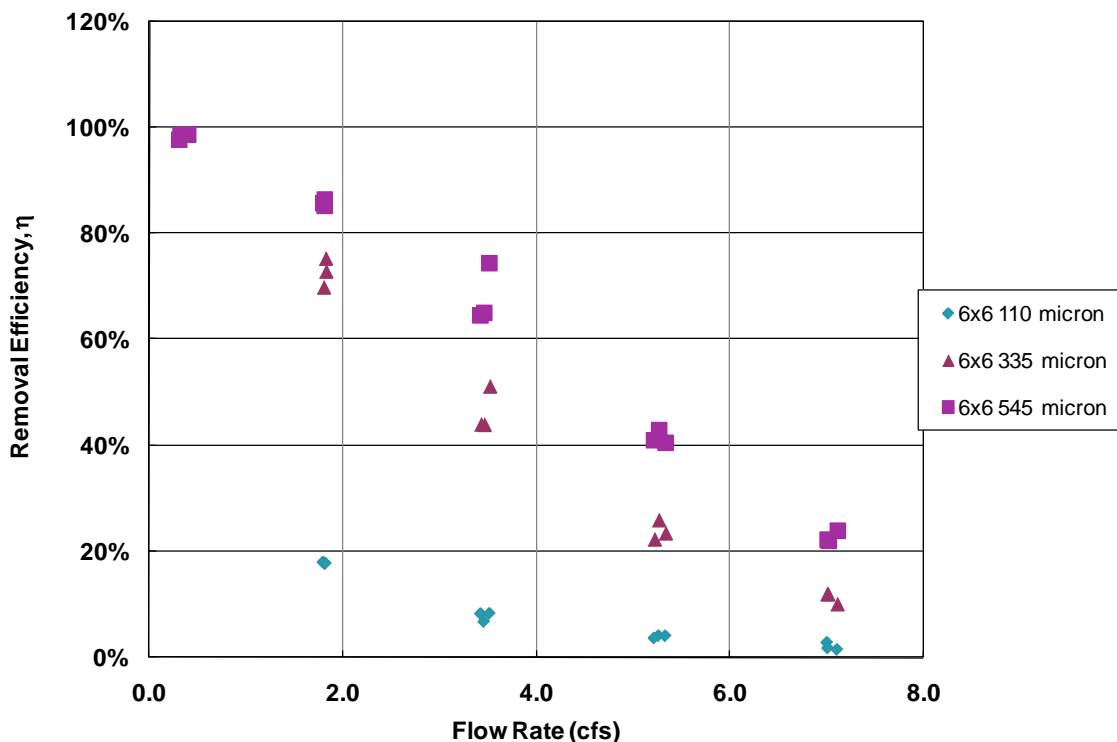
Figure 3.4. Removal Efficiency Results for the 6×6 ft Sump

3.1.4   6-ft (1.8 m) Diameter by 3-ft (0.9 m) Depth

Removal efficiency tests for the 6×3ft (1.8×0.9m) sump began on December 9th, 2009. The tests included the same particle sizes, flow rates, and influent concentrations as the tests previously conducted on the 6×6 ft (1.8×1.8 m) sump. Figure 3.5 provides the results of the 6×3 ft (1.8×0.9 m) removal efficiency tests. The comparison between the deep and the shallow 6-ft (1.8m) diameter sumps shows a 15 to 20% lower removal efficiency of the shallow sump for the same particle size and flow rate, i.e. the shallow sump will not perform as well as the deep sump.
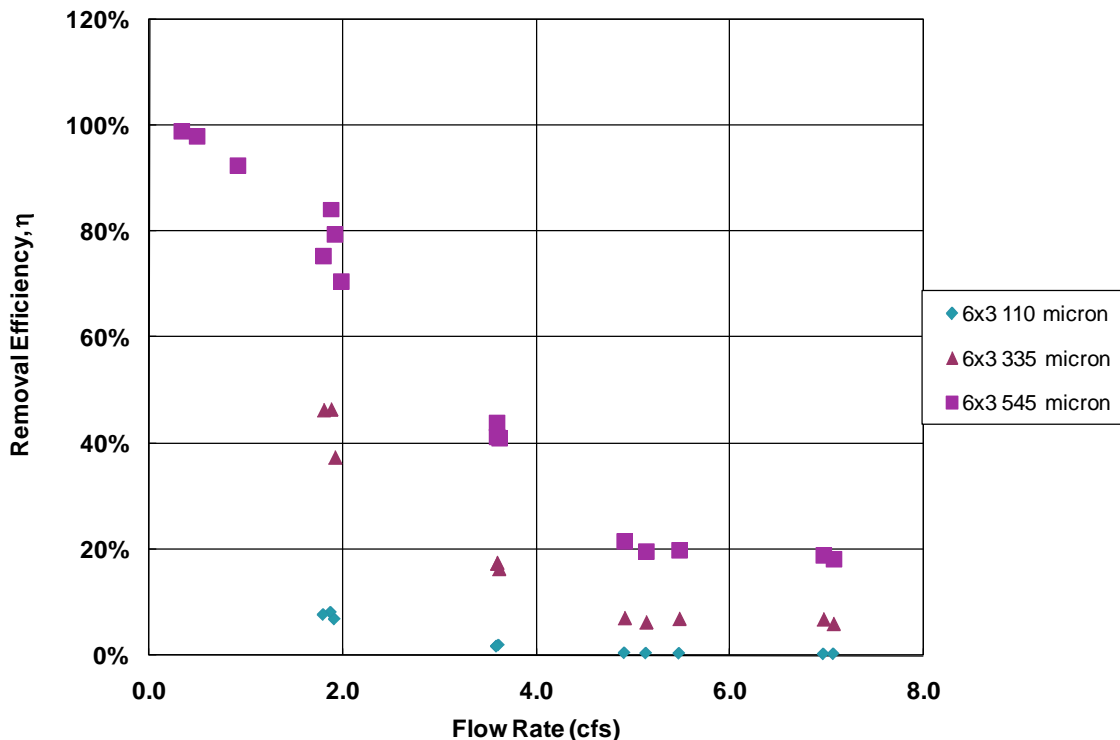
Figure 3.5. Removal Efficiency Results for the 6×3 ft Sump

3.1.5   Scale Model 1:4.17: 1-ft (0.3 m) Diameter by 1-ft (0.3 m) Depth

Extensive testing was conducted in the 1:4.17 scale model, i.e. a 1×1 ft (0.3×0.3 m) sump to explore the scaling of removal efficiency in standard sumps. Ideally, if a relationship can be developed between a small scale model and a full scale model, testing of removal efficiency can be conducted in a scale model at a lower cost of testing. Figure 3.6 is a plot of the removal efficiency results for the 1×1 ft (0.3×0.3 m) sump with one particle size, 0.0043 in (110μm). More information on the scaling relationship will be presented in the data analysis section.
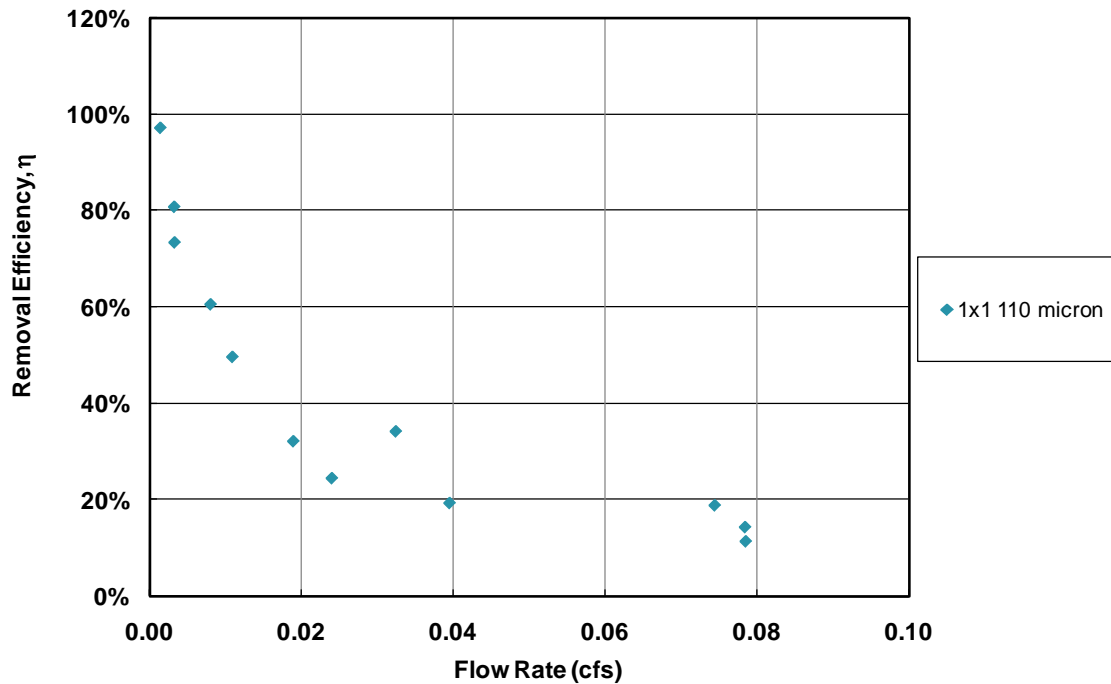
Figure 3.6. Removal Efficiency Results for the 1×1ft (0.3×0.3 m) Sump

3.2   Results of Washout Tests under High-Flow Conditions

3.2.1   4-ft (1.2 m) Diameter by 4-ft (1.2 m) Depth

The 4×4 ft (1.2×1.2 m) sump washout tests required a significant number of iterations to provide repeatable results, as is discussed in Appendix E. The curve connecting the final results has an exponential increase in effluent concentration until it reaches 4.8 cfs (136 L/s). At 5.5 cfs (156 L/s) a decrease in effluent concentration is exhibited; this is discussed in Section 3.3. The results of these washout tests are summarized in Figure 3.7 and Table 3.1. At flow rates above 4 cfs, a 4×4 ft (1.2×1.2 m) sump becomes a point source of suspended sediment with a minimum effluent concentration of about 0.0094 lbs/ft^3 (150 mg/L), assuming a median particle size of 110 microns in the sump. As flow rate rises to around 5 cfs (142 L/s) and higher, more sediment is expected to be washed out of the sump. However, as the flow rate exceeds 5 cfs (142 L/s), the washout rate drops. The drop in the washout rate is attributed to short-circuiting of the flow between the sump inlet and outlet and a weakening of the plunging flow into the sump.
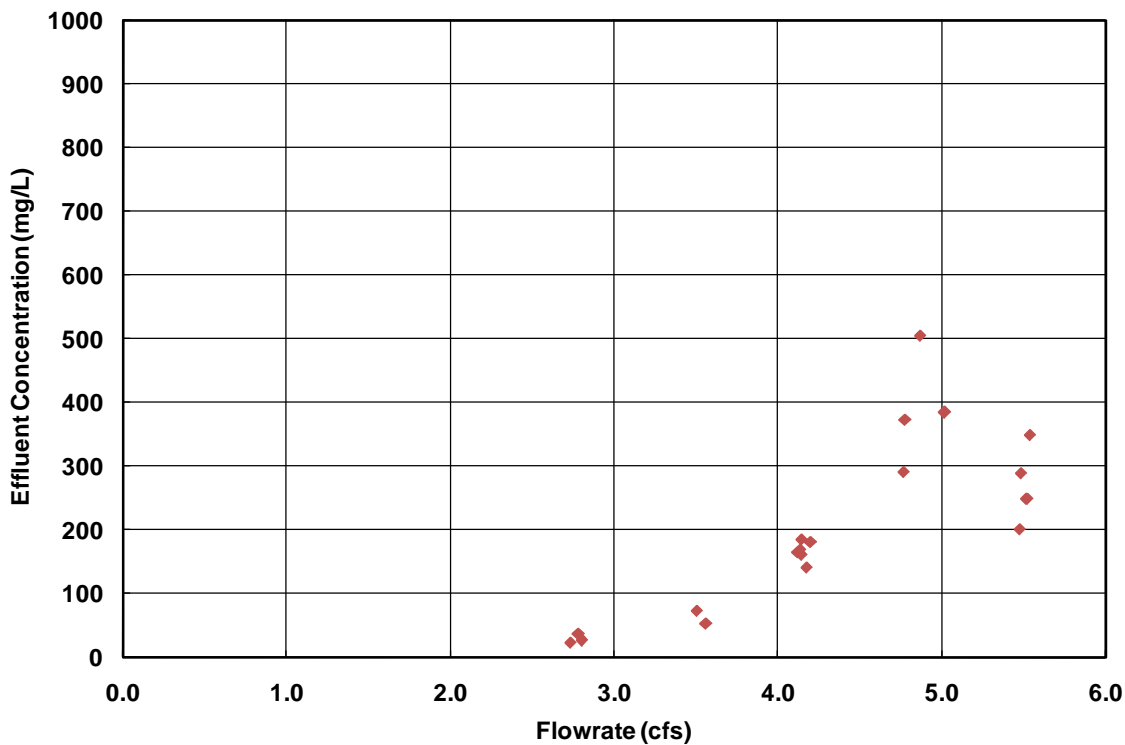
Figure 3.7. Washout Results for the 4×4 ft Sump

Table 3.1. Tabulated Washout Results for the 4×4 ft (1.2×1.2 m) Sump

Test No.	Actual Flow Rate (cfs)	Sediment Size (microns)	Dry Weight Removed (lbs)	Effluent Concentration (mg/L)
9	2.8	110	33	27
10	2.8	110	46	37
11	2.7	110	29	24
18	4.1	110	299	161
19	4.2	110	342	181
20	4.2	110	265	141
21	4.1	110	314	169
22	4.1	110	346	186
23	4.1	110	306	165
28	3.5	110	115	73
29	3.6	110	86	54
30	5.0	110	694	384
31	4.9	110	323	506
32	4.8	110	167	373
33	4.8	110	156	291
25	5.5	110	617	249
26	5.5	110	496	202
27	5.5	110	618	249
34	5.5	110	261	350
35	5.5	110	214	289

3.2.2   4-ft (1.2 m) Diameter by 2-ft (0.6 m) Depth

The results of the washout tests on the shallow 4×2 ft (1.2×0.6 m) sump are plotted in Figure 3.8 along with the results obtained for the deep 4×4 ft (1.2×1.2 m) sump. The washout rates from the 4-ft shallow sump are significantly higher than those from the 4-ft deep sump. The surface of the deposit in the shallow sump is closer to the high energy inflow jet, which increases sediment washout.
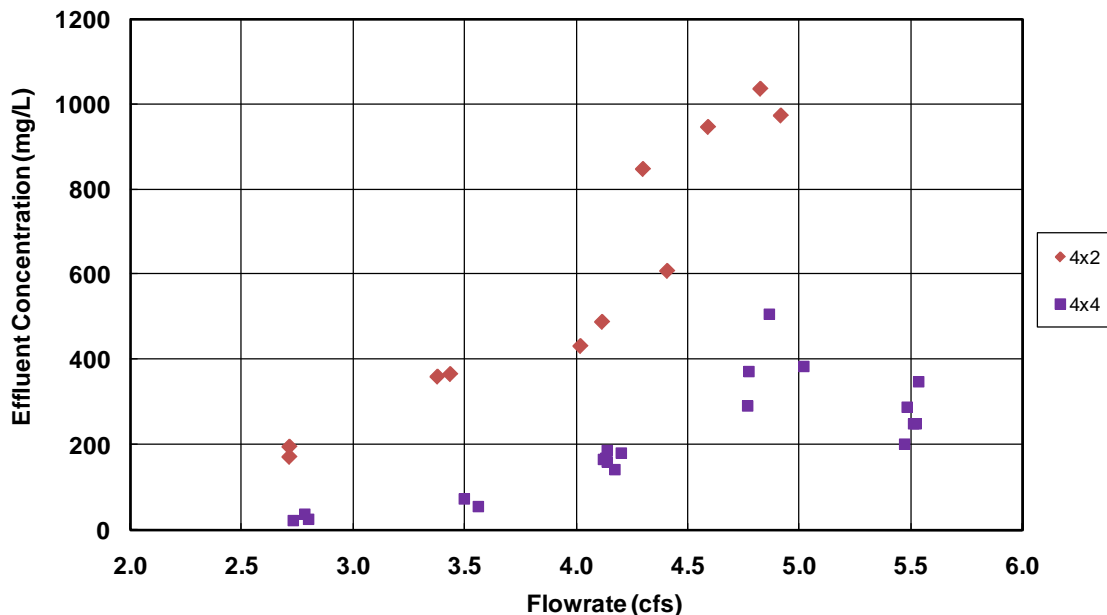
Figure 3.8. Comparison of the Washout Results (i.e. Effluent Concentrations) from the 4×4 ft (1.2×1.2 m) and 4×2 ft (1.2×0.6 m) Sumps

3.2.3   6-ft (1.8 m) Diameter by 6-ft (1.8 m) Depth

The results of the washout tests on the 6×6 ft (1.8×1.8 m) sump are presented in Figure 3.9. Figure 3.9 also includes the results of the washout tests conducted on the 4×4 ft (1.2×1.2 m) sump. The maximum effluent concentrations for the two sumps are very similar at approximately 0.031 lb/ft^3 (500 mg/L) for 110 micron particles. However the 6×6 ft (1.8×1.8 m) sump reaches this maximum effluent concentration at a flow rate of 16 cfs (453 L/s) as compared to a 5 cfs (142L/s) for the 4×4 ft (1.2×1.2 m) sump. The data at 16 cfs (453L/s) also show signs of short-circuiting with a significant drop of effluent concentration at 19 cfs (538L/s). This matches the data from the 4×4 ft (1.2×1.2 m) sump.
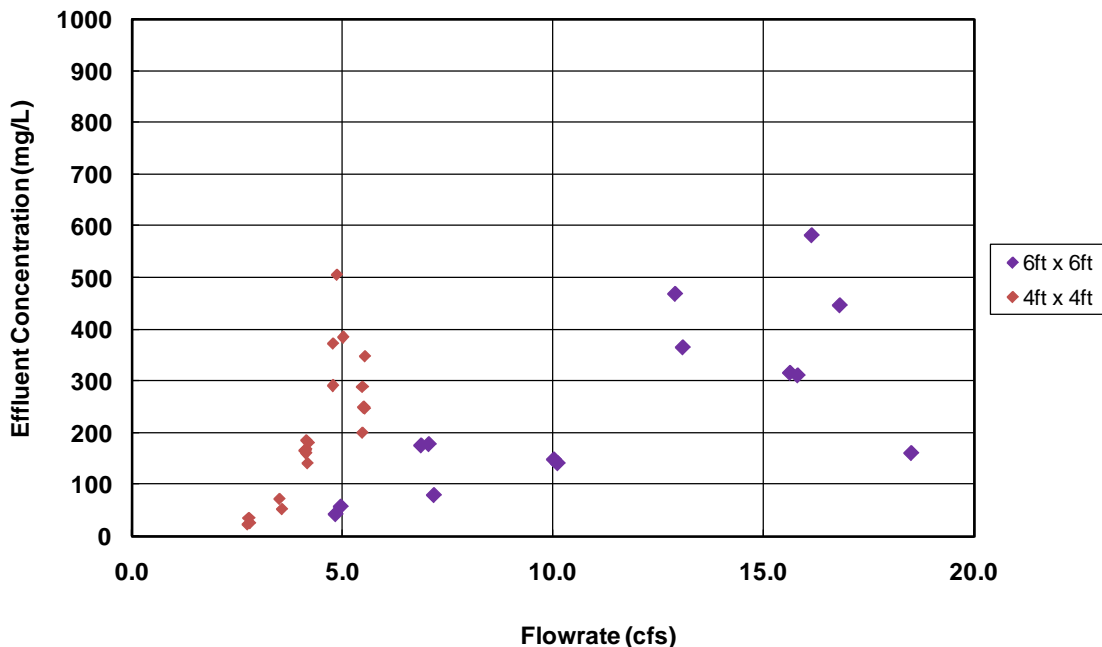
Figure 3.9. Comparison of Washout Effluent Concentrations Measured in a 6×6 ft (1.8×1.8 m) Sump and a 4×4 ft (1.2×1.2 m) Sump

3.2.4   6-ft (1.8 m) Diameter by 3-ft (0.9 m) Depth

After completing the washout tests on the 6×6 ft (1.8×1.8 m) sump, a false floor was placed at a 3-ft (0.3-m) depth in the sump and the sump was once again loaded with one foot of F-110 Silica Sand. Figure 3.10 presents the results of the washout tests on the 6×6 ft (1.8×1.8 m), a deep sump, and the 6×3 ft (1.8×0.9 m), a shallow sump. As was the case in the 4×4 ft (1.2×1.2 m) and 4×2 ft (1.2×0.6 m) comparison, the 6×3 ft (1.8×0.9 m) sump did not perform as well as the 6×6 ft (1.8×1.8 m) sump. For the same flow rate and particle size, the 6×3 ft (1.8×0.9 m) sump resulted in higher effluent concentrations than the 6×6 ft (1.8×1.8 m) sump. The decrease in sump depth makes more energy available for sediment washout of the deposit. Interestingly, the plot for the shallow sump shows a continuously increasing washout function, i.e. no sign of short-circuiting is evident in the 6×3 ft (1.8×0.9 m) sump. Even though short-circuiting may occur in a shallow sump, the data suggest that the deposit surface in shallow sumps is sufficiently close to the inflow jet to cause an increasing effluent concentration with the increasing flow rates tested.
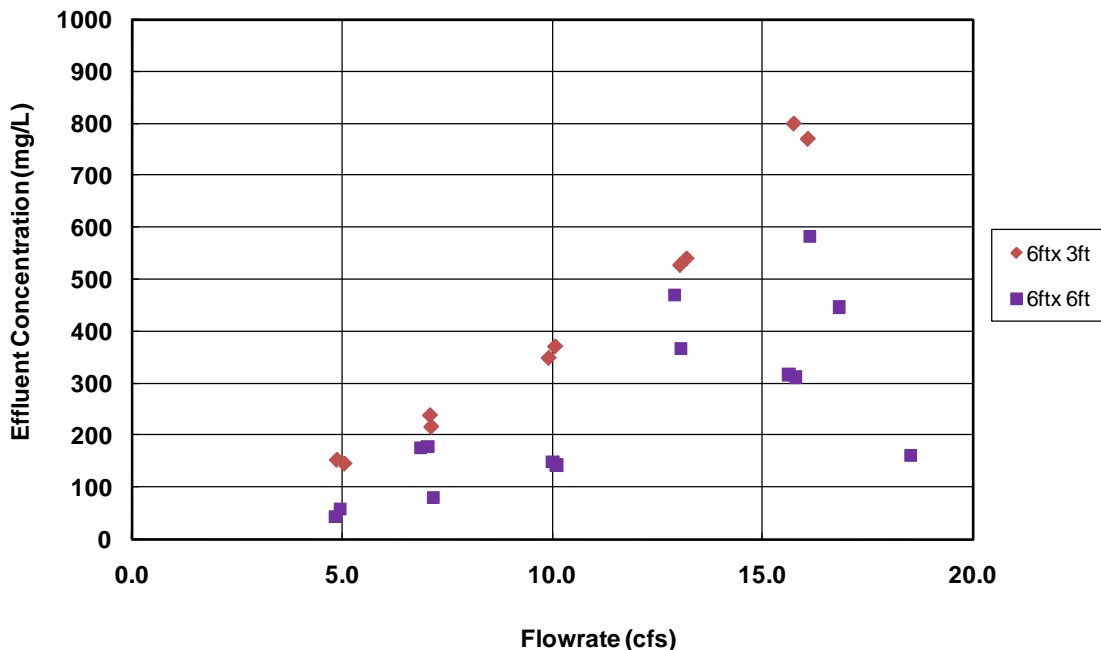
Figure 3.10. Comparison of Washout Effluent Concentrations Measured in a 6×6 ft (1.8×1.8 m) Sump and a 6×3 ft (1.8×0.9 m) Sump

Table 3.2. Tabulated Results of Washout Tests for the 6×3 ft (1.8×0.9 m) Sump

Test No.	Actual Flow Rate (cfs)	Sediment Size (microns)	Dry Weight Removed (lbs)	Effluent Concentration (mg/L)
1	4.9	110	197	154
2	5.1	110	165	145
3	7.1	110	254	240
4	7.1	110	231	217
5	9.9	110	260	349
6	10.1	110	308	371
7	13.0	110	387	529
8	13.2	110	400	541
9	16.1	110	557	770
10	15.7	110	566	800

3.3   Flow Patterns

In order to explain the processes involved in sediment washout and sediment capture within the sump, extensive velocity measurements using a 3-D Acoustic Doppler Velocimeter (ADV) were made and allowed detailed flow mapping in the sump. Flow rates of 2.4 cfs (68 L/s) and 4.8 cfs (136 L/s) were used for the ADV tests in both the shallow and deep sump configurations. Two different grid patterns were employed in these tests. The change in the grid patterns was related

to the change in the ADV type used in these tests. The ADV locations can be seen in Figure 3.11. Appendix F describes the complete flow pattern analysis.
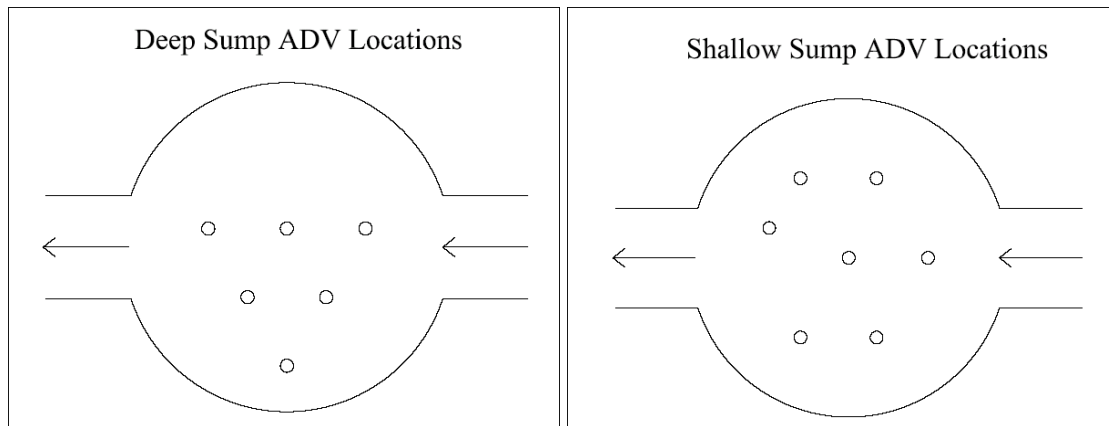
Figure 3.11. Deep and Shallow Sump ADV Locations

The first series of ADV tests was conducted at 2.4 cfs (68 L/s) in the deep sump using a Nortek Vectrino ADV with a side mounted probe which can sample at 250 Hz. The following three test series were conducted by a Sontek ADV with a down facing probe sampling at 10 Hz. The sampling time remained one minute for both probes. Figures 3.12 and 3.13 show the flow patterns for both the deep and shallow sumps. As water enters the sump there is a plunging action which creates downward velocities at the downstream end, upstream velocity near the sediment bed, and upward velocities at the upstream end. The plunging flow thus scours the deposit at the downstream side of the sump and deposits some of the scoured sediments at the upstream end of the sump. Figure 3.14 is a photo of the deposit after a washout test. In this photo, the flow direction is from right to left. The sediment is piled up at the upstream end, as can be seen in the photo the sediment deposit in the sump is severely scoured at the downstream end so that the sump floor is exposed.
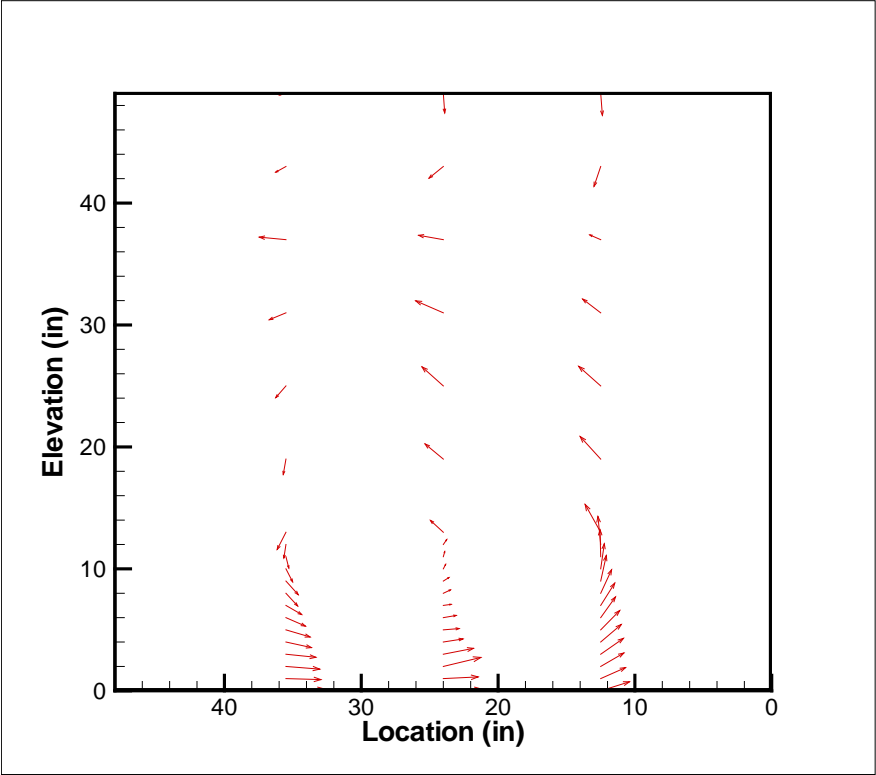
Figure 3.12. Velocities along the Centerline of a Deep Sump. Inflow is at a Depth of 48 inches
and from Right to Left
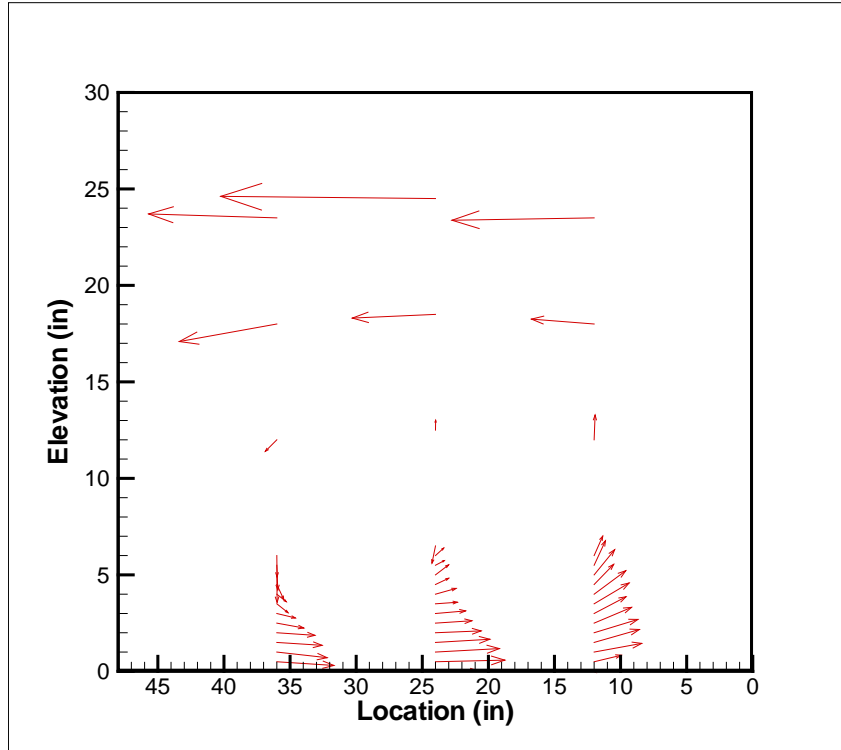
Figure 3.13. Velocities along the Centerline of a Shallow Sump. Inflow is at a Depth of 24
inches and from Right to Left

Figure 3.14. Overhead View of the Sediment Deposit in the Sump after a Washout Test. Inflow
during the Test Was from Right to Left

A review of the velocity data provides a partial explanation for the decrease in effluent concentrations at flow rates above 5 cfs (142 L/s) shown in Figure 3.7. At sufficiently high-flow rate, short-circuiting may occur in the sump, i.e. the flow from the inlet pipe may pass directly to the outlet pipe without plunging. Thus, the typical circulation pattern shown in Figure 3.12 no longer exists. To further verify this hypothesis, more velocity data were collected along the centerline of the sump at 4.5 cfs (127 L/s), 5 cfs (142 L/s), 5.5 cfs (156 L/s), and 6 cfs (170 L/s) flow rates. Figure 3.15 is a plot of the vertical component of velocity versus depth at a location 16 inches (41cm) upstream of the outlet pipe. The figure was transformed to a dimensionless format by dividing the measured velocities by the inflow jet velocity, and the depths by the height of the inlet invert above the bottom of the sump. At 4.5 cfs (127 L/s) and 5 cfs (142 L/s), the measured velocities remained negative along the entire height of the sump, i.e. at 16 inches (0.41m) upstream of the outlet, the flow direction was downward. This indicates a plunging flow and thus a circulation pattern along the entire height of the sump. At 5.5 cfs (156 L/s) and 6.0 cfs (170 L/s), the flow direction was positive, i.e. in upward direction in the top 20% of the sump and a weaker circulation pattern in the lower 80% of the sump. This demonstrates that at higher flow rates, the jet is moving from the inlet to the outlet pipe without plunging. The energy available for scour and resuspension is smaller.
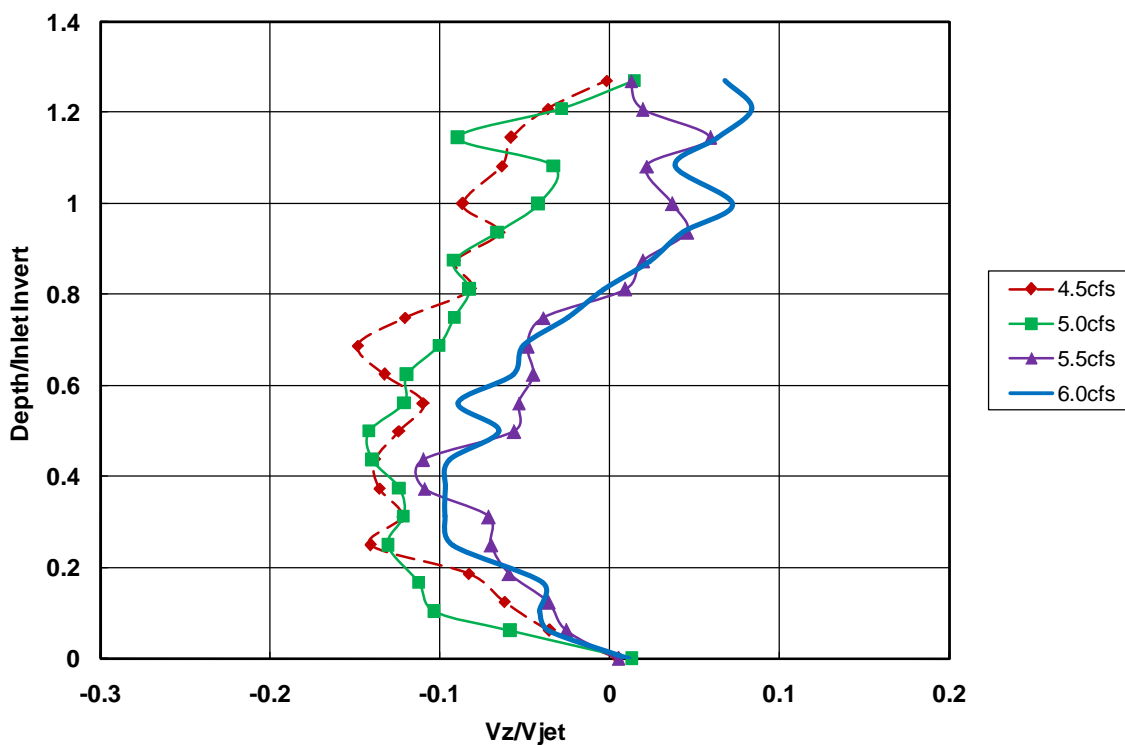
Figure 3.15. Normalized Vertical Velocity Profiles Measured 16 inches Upstream of the Outlet along the Centerline of the 4×4 ft (1.2×1.2 m) Sump

4 Data Analysis

4.1 Removal Efficiency and Péclet Number

Carlson et al. (2006) and Wilson et al. (2009) used a Péclet number to collapse sediment removal efficiency data for an entire range of flows, particle sizes, particle densities and flow viscosities tested. The Péclet number introduced by Wilson et al. (2009) is the ratio of settling to turbulent diffusion. The Péclet number is defined as

$$Pe = \frac{U_s * h * D}{Q} \tag{4.1}$$

In Equation 4.1, U_s is the particle settling velocity, h is the depth of the sump, D is the sump diameter, and Q is the flow rate. The settling velocity U_s in Equation 4.1 is calculated using Equation 4.2 from Cheng (1997) for the entire range of grain Reynolds numbers. When the measured removal efficiency is plotted versus the Péclet number, a removal efficiency function for a specific stormwater treatment device can be developed. Figure 4.1 is a plot of the removal efficiency versus Péclet number.

$$U_s = \frac{v}{d}\left(\sqrt{25 + 1.2\left(d\left(\frac{g\frac{\rho_s - \rho_w}{\rho_w}}{v^2}\right)^{\frac{1}{3}}\right)^2} - 5\right)^{1.5} \tag{4.2}$$
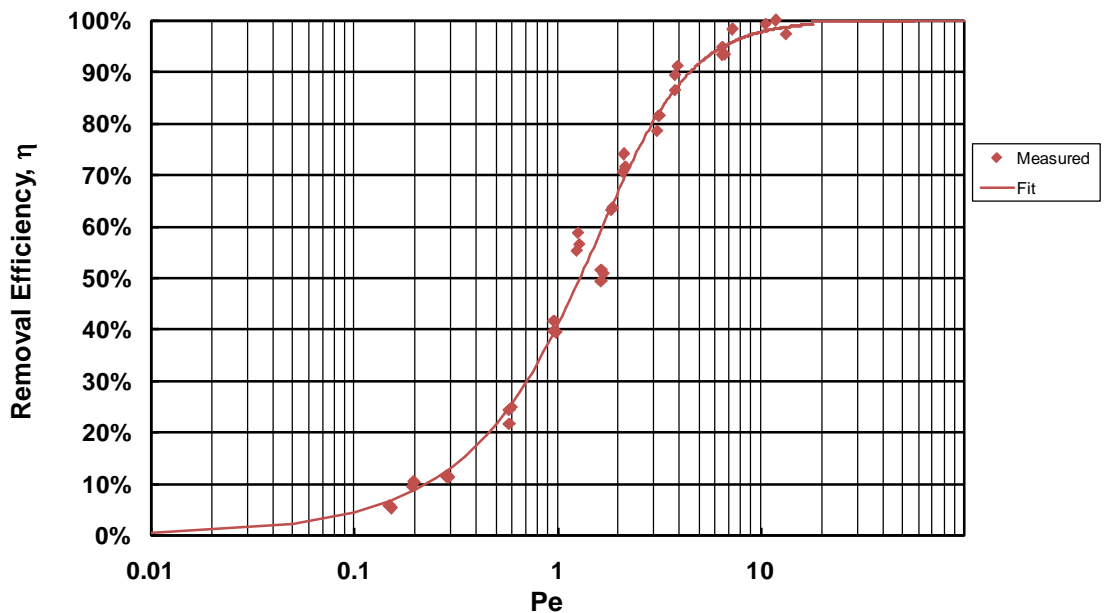
Figure 4.1. Removal Efficiency vs. the Péclet Number in 4×4 ft (1.2×1.2 m) Standard Sump.
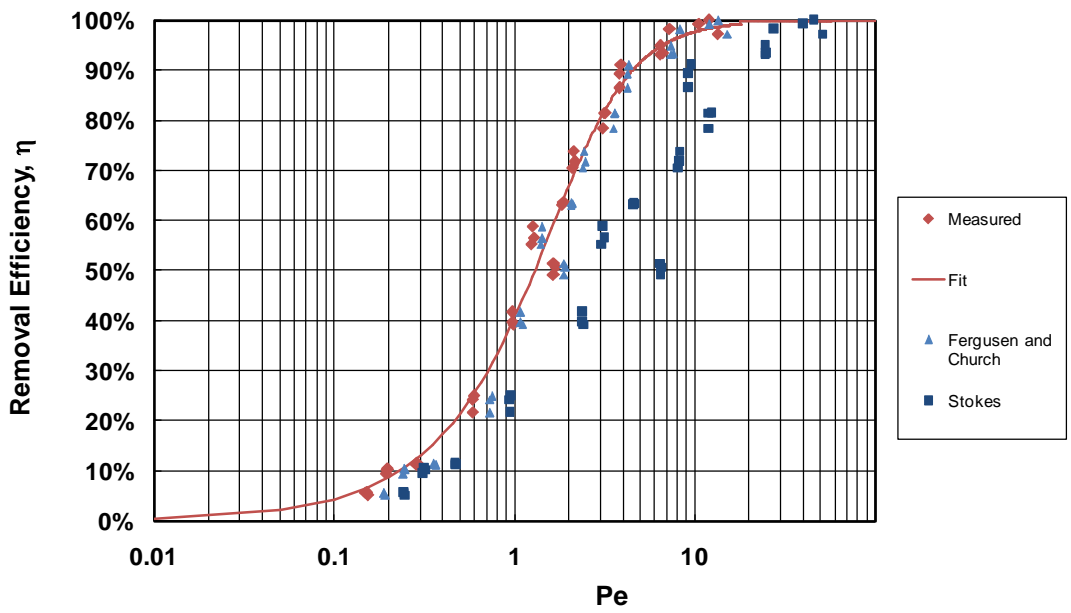
Figure 4.2. Removal Efficiency versus Péclet Number in 4×4 ft (1.2×1.2 m) Standard Sump Using Different Methods for Computing the Settling Velocity.

Figure 4.1 display the scattered data shown in Figure 3.2. It is evident that replacing flow rate Q by the Péclet number given by Equation 4.1, makes the data collapse on a single curve, i.e. all the data can be explained by a single function.

Settling velocity U_s is one important parameter in the Peclet number. It can be estimated using a variety of functions. Figure 4.2 displays the data from Figure 3.2 using three different settling velocity equations: (1) Equation 4.2 from Cheng (1997), an equation by Fergusen and Church (2004), and Stokes Law (Stokes, 1850). It is evident from Figure 4.2 that Stokes Law scatters the data more than the other two equations especially when it is applied to larger particles. The reason is that Stokes Law is for low grain Reynolds numbers. In order to avoid inconsistencies in the development of the removal efficiency function and future applications of the function, a settling velocity equation appropriate for the entire range of grain Reynolds numbers such as Cheng's (1997) or Fergusen and Church's (2004) equation should be used.

Equation 4.3 has been proposed to describe removal efficiency η as a function of Péclet number (Wilson et al., 2009).

$$\eta = \left[\frac{1}{R^b} + \frac{1}{(a\ Pe)^b} \right]^{-\frac{1}{b}} \tag{4.3}$$

In Equation 4.3, R, a, and b are fitted parameters, Pe is the Péclet number and η is the computed removal efficiency. To determine the goodness of fit of Equation 4.3 to the data, the Nash-Sutcliffe Coefficient (NSC) was calculated according to equation 4.4. An NSC of one represents a perfect fit, i.e. all measured data lie on the fitted curve.

$$NSC = 1 - \frac{\sum (\eta_i - \eta_{mi})^2}{\sum (\overline{\eta} - \eta_i)^2} \tag{4.4}$$

In Equation 4.4, η_i is the measured removal efficiency, η_{mi} is the computed (modeled) removal efficiency using equation 4.3, and $\overline{\eta}$ is the mean of the measured removal efficiencies. Besides the *NSC,* the Root Mean Square Error (RMSE) can be calculated by Equation 4.5 as another measure of the goodness of fit between the data and the value estimated from the fitted equation. *RMSE* is the average deviation of the fitted removal efficiency function from the measured data.

$$RMSE = \sqrt{\frac{\sum (\eta_i - \eta_{mi})^2}{n - p}} \tag{4.5}$$

In equation 4.5, n is the number of data points and p is the number of fitted parameters.

The Péclet number works well for predicting sediment capture in individual sumps or devices. A value of *NSC* for a single curve is typically between 0.96 and 0.98. However, there are limitations in employing the Péclet number for devices with various height (h) to depth (D)

ratios. Figure 4.3 is a plot of removal efficiency versus Péclet number for the 4×4 ft (1.2×1.2 m) sump and the 4×2 ft (1.2×0.6 m) sump.
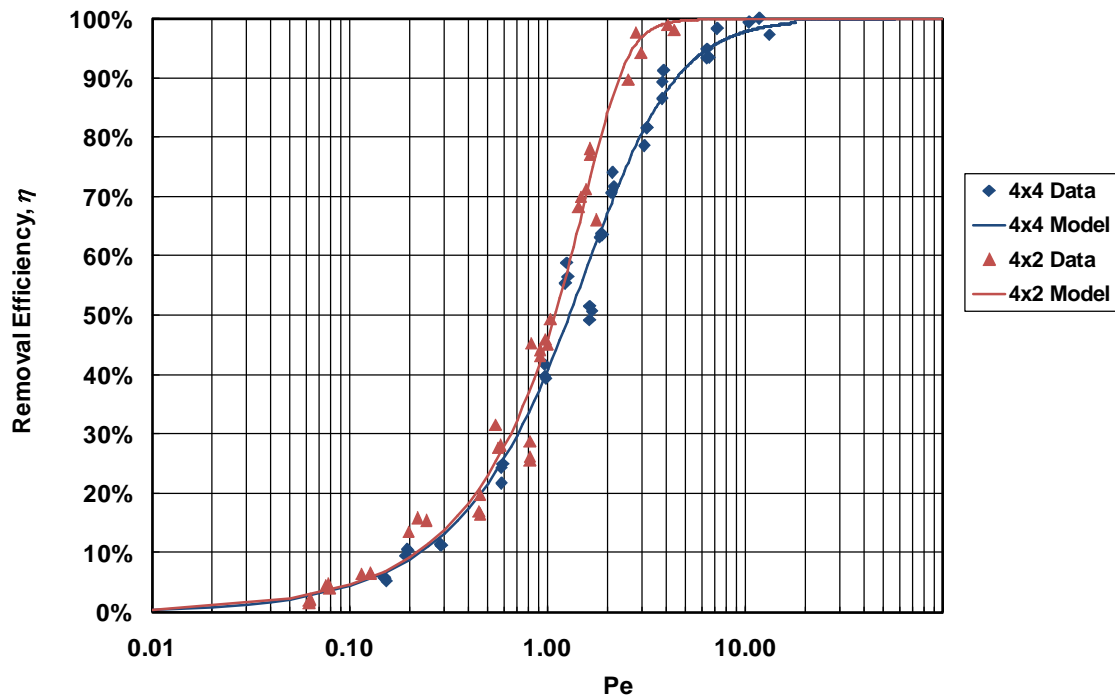
Figure 4.3. Removal Efficiency Functions of 4×4 ft (1.2×1.2 m) and the 4×2 ft (1.2×0.6 m) Sumps

Since the sump depth of a 4×2 ft (1.2×0.6 m) sump is half that of a 4×4 ft (1.2×1.2 m) sump the Péclet number is also halved for the same particle size and flow rate, This results in an efficiency reduction by up to 20% for the 4×2 ft (1.2×0.6 m) sump compared to the 4×4 ft (1.2×1.2 m) sump.

Carlson et al. (2006) indicated that the Péclet number performance function obtained for a stormwater treatment device can be applied to similar devices with approximately 20% distortion in its dimensions. Figure 4.3 shows that at a 50% distortion of a single dimension can make the performance function very different. Therefore, it seems that four different functions have to be developed for the four standard sumps tested in this study. Appendix G provides a detailed analysis of the Péclet numbers.

4.2 Sediment Washout and Péclet/Froude Number Parameter

Predicting the amount of washout from standard sumps is a challenging endeavor due to the highly variable flow patterns and the number of variables. As observed by Saddoris et al. (2010), washout from stormwater treatment devices under high-flow conditions is comprised of three processes: (1) scour or the motion of particles over the deposit, (2) entrainment (resuspension) of particles into the water column in the sump, and (3) lifting of particles up to the effluent pipe

(washout). The energy of water flowing into the sump has to do the work required for the above three processes.

To quantify washout in stormwater treatment devices, the supplied energy, and the required work for the above processes were studied. These scalars were estimated per unit of time, i.e. in terms of power.

The power supplied into the sump is

$$P_{sup} = \rho_w Q \frac{U_j^{\,2}}{2} \tag{4.6}$$

where ρ_w is the water density, Q is flow rate, and U_j is the inlet jet velocity. A significant amount of the supplied power is not utilized for sediment washout but dissipated in the turbulent flow. The dissipated energy is associated with the head loss in the sump; the head loss is comprised of the head loss at the inlet, at the exit, due to wall friction in the sump and the work required for sediment washout. Only a fraction of the power associated with the total head loss is used to cause washout from the sump. The power associated with the head loss can be estimated by Equation 4.7.

$$P_{loss} = gQh_L\rho_w \tag{4.7}$$

In Equation 4.7, h_L is the head loss through the sump; it is the difference in total head between the inlet and outlet of the sump as given by the energy Equation 4.8.

$$h_L = h_{in} + \frac{U_{in}^{\,2}}{2g} - \left(h_{out} + \frac{U_{out}^{\,2}}{2g} \right) \tag{4.8}$$

In Equation 4.8, h_{in} and h_{out} are the water surface elevations (or gage pressures) in the inlet and outlet pipes near the sump, respectively, and U_{in} and U_{out} are the flow velocities at the inlet and outlet. The power loss (Equation 4.7) includes the power which provides work on the sediment, and the power which is lost to heat by friction. In other words, the power used in sediment washout will be the total power lost minus the power lost to heat. The power lost to heat includes the wall friction and entrance and exit losses. The power lost to friction can be defined as

$$P_f = f_w \frac{l}{D} \rho_w Q \frac{U^2}{2} \tag{4.9}$$

where f_w is an average wall friction coefficient in the sump, l is the characteristic length, D is the sump diameter and U is a representative velocity in the sump. The power entrance and exit losses are,

$$P_{entrance} = \rho_w Q K_{en} \frac{U_{in}^{\,2}}{2} \tag{4.10}$$

where K_{en} is the entrance loss coefficient, and

$$P_{exit} = \rho_w Q K_{ex} \frac{U_{out}^2}{2} \tag{4.11}$$

where K_{ex} is the exit loss coefficient. The power available for sediment washout is thus,

$$P_{sed} = P_{loss} - \left(P_f + P_{entrance} + P_{exit} \right) \tag{4.12}$$

By measuring discharge and water depths at the inlet and outlet, the total power supplied and the total power lost to the sump due to heat and sediment washout can be quantified. Unfortunately, quantifying the power loss due to heat is not a trivial task, and therefore, quantifying the actual power available for sediment washout is not trivial either.

As stated earlier, sediment washout begins with incipient motion of the bed particles. The power required to initiate the motion of the particles can be approximated as

$$P_{sc} = \tau_c A U \tag{4.13}$$

In Equation 4.13, τ_c is the critical shear stress for the incipient motion of particles, A is the surface of the deposit and U is the average velocity of particles. This velocity can be approximated by the critical shear velocity as given in Equation 4.14.

$$U_{*sc} = \sqrt{\frac{\tau_c}{\rho_w}} \tag{4.14}$$

Replacing the critical shear stress with $\rho_w U_{*sc}^2$, Equation 4.13 can be rearranged into

$$P_{sc} = \rho_w U_{*sc}^3 A \tag{4.15}$$

Using the Shields diagram, one can estimate the critical shear stress for the movement of a particular sediment size with a given density (Vanoni 1975). The associated critical shear velocity can then be estimated and placed in Equation 4.15 to estimate the power necessary for bed load movement.

If there is still energy available following the bed load movement, it will be utilized for particle entrainment into the water column. The power required for particle entrainment can be parameterized as

$$P_{ent} = \rho_w U_{*ent}^3 A \tag{4.16}$$

In Equation 4.16, U_{*ent} is the critical shear velocity for particle resuspension and entrainment into the water which can be estimated using the results of research conducted by Akiyama and Stefan (1985) on turbidity currents. The critical shear velocity for entrainment occurs when the

suspended sediment concentration is near zero. Akiyama and Stefan (1985) defined the suspended sediment concentration by a dimensionless parameter, E_s, which is the sediment entrainment rate. Sediment entrainment approaches zero at a value of,

$$\frac{U_{*ent}}{U_s} R_p^{0.5} = 6 \tag{4.17}$$

In Equation 4.17, U_s is the particle settling velocity, U_{*ent} is the incipient sediment entrainment velocity, and

$$R_p = \frac{d\sqrt{SGgd}}{\nu} \tag{4.18}$$

In Equation 4.18, SG is the specific gravity of the sediment, d is the particle diameter, and ν is the kinematic viscosity of the fluid. Parker et al (1987) also provided a chart which can be used to find the constant on the right hand side of Equation 4.17. However Akiyama and Stefan (1985) have presented more data at lower values of E_s, making it easier to determine when sediment entrainment becomes insignificant. Inserting Equation 4.18 into Equation 4.17 and solving for U_{*ent} results in Equation 4.19

$$U_{*ent} = \frac{6U_s\sqrt{\nu}}{\sqrt{d\sqrt{SGgd}}} \tag{4.19}$$

The results of Equation 4.19 can then be used to estimate the power required for particle resuspension and entrainment into the water (i.e. Equation 4.16).

Once the sediment has become entrained, the next power required is the power to hold the sediment in suspension, or the settling power. If the remaining supplied power exceeds the settling power, then the particle can be lifted in the water column and transported towards the outlet pipe. The power for settling of a given mass of suspended particles is

$$P_{set} = \frac{\overline{C}aAg(SG-1)U_s}{SG} \tag{4.20}$$

In Equation 4.20 a is the height of the water column in which the particles are distributed, $\overline{C}$ is the average sediment concentration along the height a, and A is the sump cross sectional area. The average concentration of sediment in the sump is not known unless it is sampled. If washout occurs in a sump then the suspended sediment concentration in the sump may be assumed to be similar to the outflow concentration if the sump is well mixed. In addition, if sediment washout is to occur, a can be set equal to h, the height of the water column in the sump. In order to determine if a well-mixed condition exists in a standard sump under high-flow conditions, the one-dimensional vertical advection-diffusion equation under steady state condition (Equation 4.21) was analyzed for the sump.

$$-U_s \frac{\partial C}{\partial z} = \frac{\partial}{\partial z}\left(\left(D_z + \varepsilon_z\right)\frac{\partial C}{\partial z}\right) \tag{4.21}$$

Equation 4.21 is equivalent to

$$-U_s C = \left(D_z + \varepsilon_z\right)\frac{\partial C}{\partial z} \tag{4.22}$$

C in Equations 4.21 and 4.22 is the concentration at a given elevation, D_z is the molecular diffusion coefficient and ε_z is the mean turbulent diffusion coefficient and is defined as

$$\overline{\varepsilon_z} = \frac{1}{h}\int_0^h \varepsilon_z dz \tag{4.23}$$

Since the molecular diffusion, D_z, is much smaller than the turbulent diffusion, ε_z, D_z can be ignored and Equation 4.22 becomes

$$-U_s C = \overline{\varepsilon_z}\frac{\partial C}{\partial z} \tag{4.24}$$

After integration, Equation 24 is modified to

$$C = \beta e^{-U_s z/\overline{\varepsilon_z}} \tag{4.25}$$

In Equation 4.25, β is the constant of integration. Since C is the concentration at the height z, it is possible to compare the concentration near the top, i.e. at the invert of the outlet pipe, and the bottom of the sump. Equation 4.26 gives the ratio of the two concentrations.

$$\frac{C_{top}}{C_{bottom}} = \frac{e^{-U_s h /\overline{\varepsilon_z}}}{e^{-U_s h_b /\overline{\varepsilon_z}}} \tag{4.26}$$

In Equation 4.26, h is the elevation at the top of the sump (at the invert of the outlet pipe), and h_b is the elevation at the bottom of the sump, which can be set equal to zero, thus,

$$\frac{C_{top}}{C_{bottom}} = e^{-U_s h/\overline{\varepsilon_z}} \tag{4.27}$$

The Prandtl-von Karman equation can be used to approximate the average turbulent diffusion coefficient as

$$\overline{\varepsilon_z} = \kappa \Delta U_x f h \tag{4.28}$$

In Equation 4.28, $\kappa = 0.4$ is the von Karman constant, ΔU_x is the change in downstream velocity for the entire height of the vertical eddy in the sump, and f is the fraction of the total depth h which contains the large eddy. By incorporating Equation 4.28 into Equation 4.27, one obtains

$$\frac{C_{z=h}}{C_{bottom}} = e^{\frac{-U_s h}{k\Delta U_x fh}} = e^{\frac{-V_s}{k\Delta U_x f}}. \tag{4.29}$$

Using the velocity measurements taken at the center location in the 4×4 ft (1.2×1.2 m) sump (Figure 4.4), the ΔU_x and f are estimated to be about 3.5 ft/s (1.05 m/s) and 0.72, respectively. These values are relatively typical values in standard sumps under high-flow conditions. For a particle size with a d_{50} of 0.0043in (110μm), the settling velocity at 68°F (20°C) becomes 0.015ft/s (0.0046m/s). Using the above estimates and quantifying the right hand side of Equation 4.29, the left hand side of Equation 4.29 becomes

$$\frac{C_{z=h}}{C_{bottom}} = 0.985 \approx 1 \tag{4.30}$$

The result in Equation 4.30 indicates that the sump is well mixed and suspended sediment concentration is nearly uniform. For the small particle sizes considered this result is anticipated. Since the velocity profiles measured in the sump are fairly constant over a range of flow rates, the estimate in Equation 4,30 should hold true for fine sands and finer particles in general. The concentration at the sump outlet drops to 90% of the near bed concentration only when the particle size exceeds 340 microns. Therefore, a well mixed condition in the sump under high-flow conditions is a fair assumption.
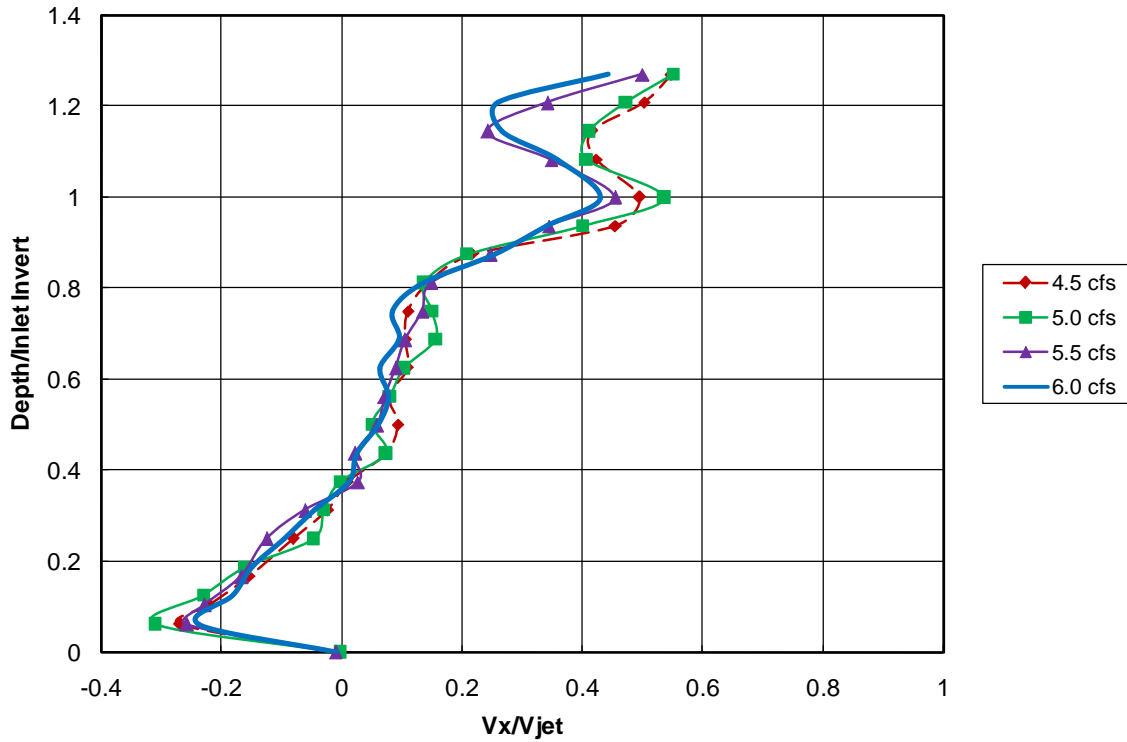
Figure 4.4. Velocity Measurements at Center Location in the 4-ft Standard Sump

If there is enough power available to begin sediment bed motion, to entrain sediment particles into the water column, and to overcome the settling of the resuspended sediments, washout becomes inevitable. To examine this, the powers parameterized in Equations 4.6, 4.7, 4.15, 4.16 and 4.20 have been quantified and tabulated in Table 4.1. To compare the measured values of power loss and power supplied, both equations included the hydrostatic pressure heads. Therefore, the power loss calculated in Table 4.1 utilizes Equation 4.31.

$$P_{\text{sup}} = g\rho_w Q \left(h_{in} + \frac{U_j^2}{2g} \right)$$ (4.31)

The term h_{in} in Equation 4.31 is the inlet water surface elevation.

In Table 4.1, the power supplied to the sump is significantly greater than any of the powers necessary for scour, entrainment, or to overcome settling. The power loss is about three orders of magnitude larger than the sum of the powers required for scour, entrainment and to overcome settling. This indicates that more than 99% of the power loss is due to the entrance, exit and frictional loss in the sump. When the power loss is about 10% of the supplied power, washout is very small, i.e. about 30 mg/L, which is within the measurement error of the experiments. As the power loss becomes a larger fraction of the supplied power, i.e. 15% and more, washout increases significantly.

The values tabulated in Table 4.1 clearly show that with very little power the sediment deposit can be disturbed and entrained into the water column. Bed forms may easily develop in standard sumps as well as in hydrodynamic separators before washout happens. This process was observed by Saddoris et al. (2010).

As is also evident in Table 4.1, head loss drops at the highest flow rates of 5.5 cfs (156 L/s), which is another indicator of the short-circuiting described in Section 3.3.

Table 4.1. Quantified Powers Involved in Sediment Washout for the 4×4 ft Sump

Actual Flow rate (cfs)	Supplied Power (lb.ft/s)	Head Loss (ft)	Power Loss (lb.ft/s)	Power for Scour (lb.ft/s)	Power for Entrainment (lb.ft/s)	Power for Settling (lb.ft/s)	Effluent Conc. (mg/L)
2.7	167	0.11	19	0.0023	0.0019	0.0005	24
2.8	171	0.10	18	0.0023	0.0019	0.0007	37
2.8	172	0.11	19	0.0023	0.0019	0.0005	27
3.5	250	0.13	28	0.0023	0.0033	0.0021	73
3.6	254	0.12	27	0.0023	0.0033	0.0016	54
4.1	320	0.13	34	0.0023	0.0020	0.0034	165
4.1	326	0.14	37	0.0023	0.0020	0.0034	169
4.1	327	0.15	38	0.0023	0.0019	0.0031	161
4.1	327	0.15	39	0.0023	0.0020	0.0038	186
4.2	330	0.14	38	0.0023	0.0019	0.0027	141
4.2	334	0.15	38	0.0023	0.0019	0.0036	181
4.8	434	0.25	74	0.0023	0.0034	0.0087	291
4.8	438	0.25	76	0.0023	0.0034	0.0110	373
4.9	449	0.25	75	0.0023	0.0034	0.0152	506
5.0	468	0.21	67	0.0023	0.0034	0.0121	384
5.5	526	0.10	34	0.0023	0.0021	0.0043	202
5.5	527	0.16	56	0.0023	0.0033	0.0085	289
5.5	531	0.12	41	0.0023	0.0021	0.0053	249
5.5	532	0.10	36	0.0023	0.0021	0.0053	249
5.5	534	0.16	54	0.0023	0.0034	0.0104	350

4.3   Washout Function

As shown above, washout is a function of power supplied and the power required to overcome the incipient motion of particles, particle entrainment into the water column and the power for lifting the particles. In Table 4.1, the power required for scour is shown to be constant for the F110 Silica Sand with a median size of 110 microns. The power for entrainment varies by no more than 80%, as effluent concentration increases 30 fold. The only power which increases relatively the same as effluent concentration is the power required to overcome settling, which can become an order of magnitude larger than the power required for scour. It seems that the ratio of power for particle settling to the power supplied can be a good indicator to explain the washout rate.

To develop a washout function, a dimensional analysis was carried out for standard sumps. Ignoring the power required for scour and entrainment, it was determined that the effluent concentration (C) during the washout is a function of gravity (g), water density (ρ_w), particle density (ρ_s), sump dimensions (h and D), settling velocity of particles (U_s), the influent jet velocity (U_j), and the flow rate (Q), i.e.

$$C = f\left(g, \rho_w, \rho_s, h, D, U_s, U_j, Q\right) \tag{4.32}$$

By converting Equation 4.32 to a number of dimensionless parameters (dimensional analysis) one obtains

$$\frac{C}{\rho_w} = \Phi\left(SG, Fr_j, Pe\right) \tag{4.33}$$

In Equation 4.33, SG is the specific gravity of particles, Fr_j is the Froude number of the influent jet velocity with a length scale which can be either the height or diameter of the sump, and Pe is the Péclet number given in Equation 4.1. It is important to note that in the dimensional analysis, one can use the Hazen number (Wilson et al., 2009) instead of the Péclet number. Before employing the data obtained in the testing to further develop Equation 4.33, it was determined that the dimensionless parameters in Equation 4.33 can also be obtained by assessing the ratio of the power required to overcome the particles settling to the supplied power

$$\frac{P_{set}}{P_{sup}} = \frac{2\overline{C}hAg(SG-1)U_s}{SG\rho_w QU_j^2} = \frac{\pi}{2}\frac{\overline{C}(SG-1)}{\rho_w\,SG} \bullet \frac{Pe}{Fr_j^2} \tag{4.34}$$

where,

$$Pe = \frac{U_s h d}{Q} \tag{4.35}$$

and

$$Fr_j^2 = \frac{U_j^2}{gD} \tag{4.36}$$

Equation 4.6 is utilized in the derivation of Equation 4.34 and represents an approximation of the power supplied. In Table 4.1, it is evident that before short-circuiting, washout rate increases as the ratio of these two powers increases; therefore, in the dimensional analysis (Equation 4.33) the washout rate must be a function of the ratio Pe/Fr_j^2. In addition, the length scale in the Froude number should be the diameter of the sump. Furthermore, the Péclet number in Equation 4.1, and not the Hazen number, should be used to explain the washout rate.

Subsequently, the dimensionless variable $\dfrac{\overline{C}(SG-1)}{\rho_w\,SG}$ was plotted versus Pe/Fr_j^2 using the data obtained from all tests. The plot is shown in Figure 4.5 and includes all the washout data obtained for the 6×6, 6×3, 4×4, 4×2, and 1×1 ft sumps. To develop a washout function, a three parameter decreasing function was fitted to the data in Figure 4.5. The function is given by Equation 4.37.

$$\frac{C(SG-1)}{p_w \, SG} = \frac{8.3 \times 10^{-6}}{\dfrac{Pe}{Fj^2}} + 4.7 \times 10^{-4} \, e^{-3.18 \frac{Pe}{Fj^2}}$$ (4.37)

The NSC of the fit is calculated to be 0.67.

It is evident from Figure 4.5 that Pe/Fr_j^2 is a suitable dimensionless parameter describing washout in standard sumps, and with a decent accuracy it can be applied to all sizes of standard sumps. The Pe/Fr_j^2 encompasses the effects of particle settling, the sump dimensions, the flow rate and the inflow jet velocity.
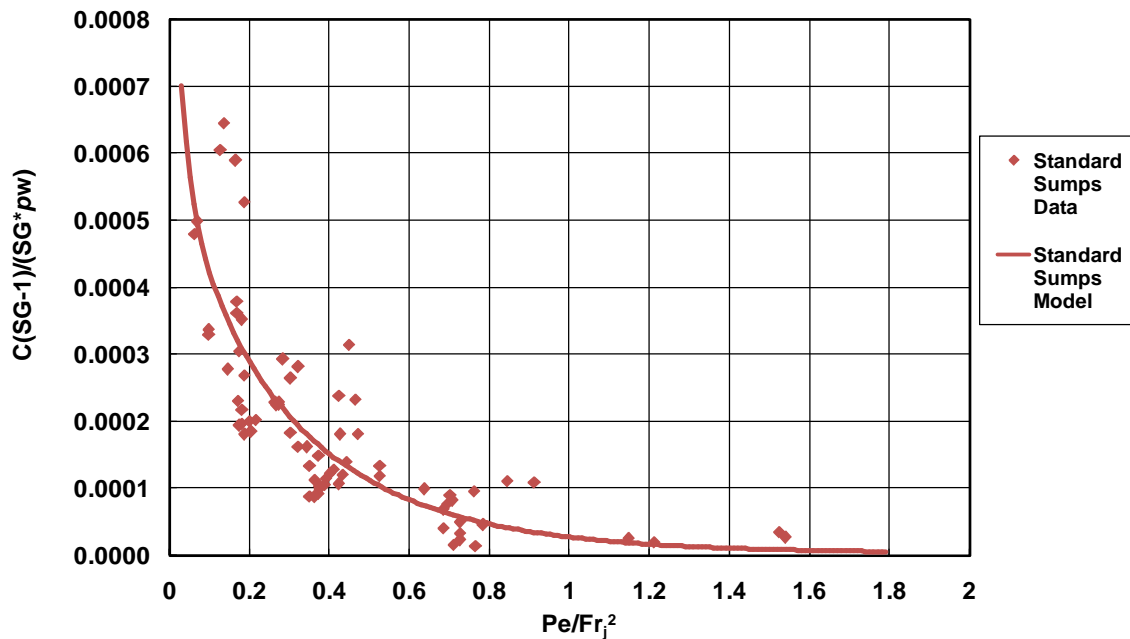
Figure 4.5. Washout Function for Standard Sumps

It is possible to develop separate charts for the geometrically similar devices, i.e. one for the 6×6, 4×4, and 1×1 ft, sumps and one for the 6×3 and 4×2 ft sumps. Nevertheless, Equation 4.37 is the three parameter fitted function to describe the washout rate (effluent concentration) in standard sumps as a function of Pe/Fr_j^2 under high-flow conditions.

Since the same parameters used in Equation 4.37 also affect the removal efficiency of standard sumps, the data obtained for removal efficiency from tests conducted on 6×6, 6×3, 4×4, 4×2, and 1×1 ft sumps, and previously plotted against flow rate in Figures 3.1, 3.3, 3.4, 3.5, and then against the Péclet number in Figures 4.1 and 4.3, were plotted a third time versus Pe/Fr_j^2. The results are shown in Figure 4.6. It is obvious that the parameter Pe/Fr_j^2 can be successfully used to explain the removal efficiency η of standard sumps.

When the three parameter function (Equation 4.3) is fitted to the removal efficiency data, Equation 4.38 is obtained.

$$\eta = \left(1 + \frac{1}{\left(0.0275 \dfrac{Pe}{Fr_j^{\,2}} \right)^{1.437}} \right)^{-\frac{1}{1.437}} \tag{4.38}$$

The NSC of Equation 4.38 is 0.942 and its RMSE is 8.1%.

When the powers for scour and entrainment are so small that they can be ignored in the performance function, and if the sump is well mixed, then it is immaterial where the sediment is being supplied into the sump and thus Pe/Fr_j^2 can be used to describe both the sediment washout and sediment removal efficiency.
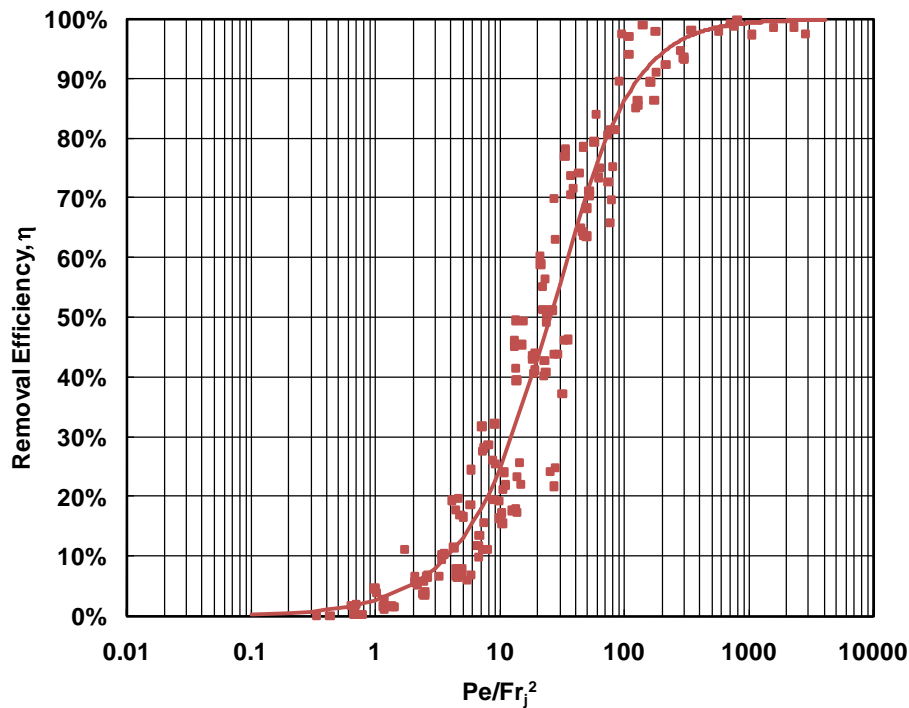
Figure 4.6. Removal Efficiency Function for Standard Sumps

5   Uncertainty Analysis

The fitted functions presented in Section 4 will be useful to determine the removal efficiency as well as the washout rates of standard sumps. It is necessary to determine the potential variability in these functions given the inherent variability in the data. The goal of this part of the study is to determine both upper and lower pointwise confidence bounds on the fitted functions (or models).

In case of normally distributed residuals, estimating confidence intervals of a fitted function would have been a straight forward procedure. However, the fitted functions (Equations 4.37 and 4.38) did not exhibit any normally distributed residuals. Therefore, it was decided to use the bootstrap method to develop the confidence intervals for the fitted functions.

The bootstrap method is a relatively new statistical tool and requires substantial computational power. Bradley Efron first proposed the bootstrap method in 1979 after working with the jackknife resampling technique (Lepage, 1992). Since then the bootstrap method has become widely used because of its ability to produce accurate results without knowledge of the data distribution. This is possible through the production of thousands of new data sets by sampling from the original data set. It is then assumed that these samples represent the entire range of possible values, from which a confidence interval can be developed. The majority of the research has focused on representing confidence in certain parameters including the mean, variance and standard deviation, and the particular model parameters. Although more complicated, finding the confidence intervals for each modeled point is possible. An example can be found in Rustomji and Wilkinson (2008).

The bootstrap method can be applied using three different sampling processes: parametric, non-parametric, and semi-parametric. The parametric bootstrap method requires the use of a known distribution, which makes this option impossible for the sump data. The semi-parametric bootstrap method involves sampling from the residuals which requires the error in the model to be consistent throughout the range of values. The non-parametric bootstrap method involves sampling from the original values, and requires no assumptions of the data distribution or of the model (Carpenter 2000). The non-parametric bootstrap method was used in this study to develop the confidence intervals. The process for determining pointwise confidence intervals using the non-parametric bootstrap method involves the following steps:
1. Sample from the observed data n values with replacement, or sample without replacement m out of n values to create a new bootstrap sample.
2. Fit the model to the new sample.
3. Repeat steps one and two 1000 to 2000 times.
4. Calculate the residual error of each new fitted value from the original fitted value.
5. Sort the residual errors and find the corresponding error values for the desired confidence region.
6. Add or subtract appropriate error values to their corresponding original fitted values.

Figure 5.1 is an example of a completed non-parametric bootstrap confidence interval from sampling with replacement. When sampling with replacement, the only difference between the sampled data and the original data is the presence of repeat data in the samples.

It is important to note that these confidence intervals are describing the uncertainty in the model, i.e., 95% of the lines fitted to the data will fall within these bounds. This is not saying that 95% of the observed data points will fall within these bounds. However, Figure 5.1 shows an increase in uncertainty in the model at lower Péclet numbers which is a reflection of the increased variability in the data at lower Péclet numbers. Figure 5.2 includes 180 of the fitted samples to show how they are distributed. Figure 5.3 was created by sampling without replacement from m out of n values. This process decreases the number of values available for the model to fit, which will increase the width of the bounds, thus representing the sensitivity of the model.
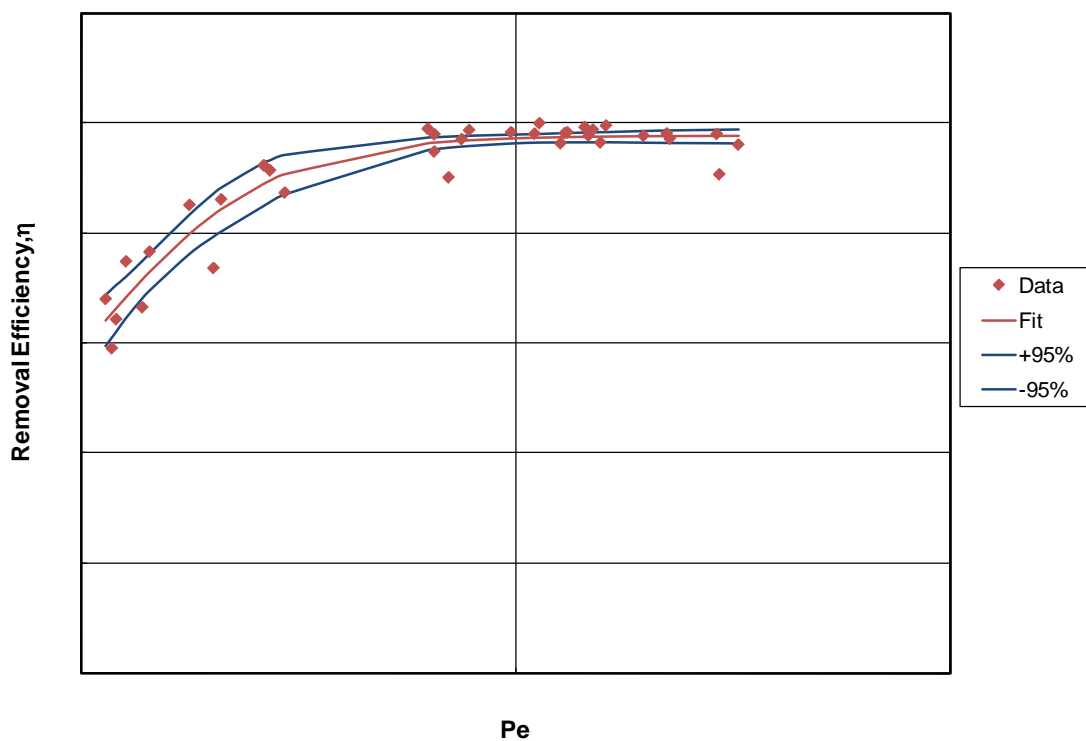
Figure 5.1. Bootstrap Non-Parametric Basic with Replacement
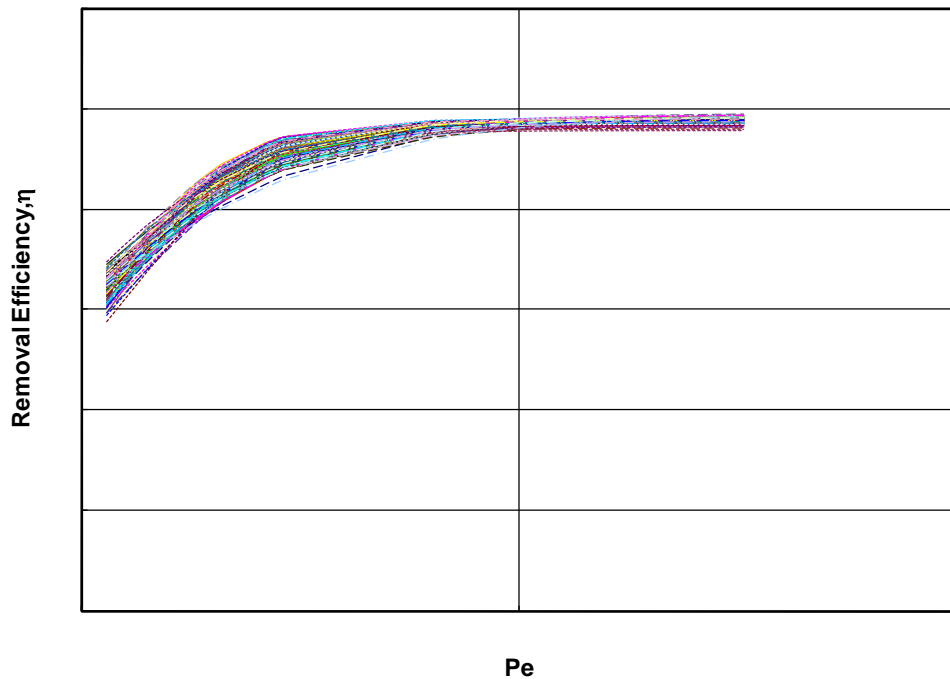
Figure 5.2. Bootstrap Non-Parametric Basic Samples
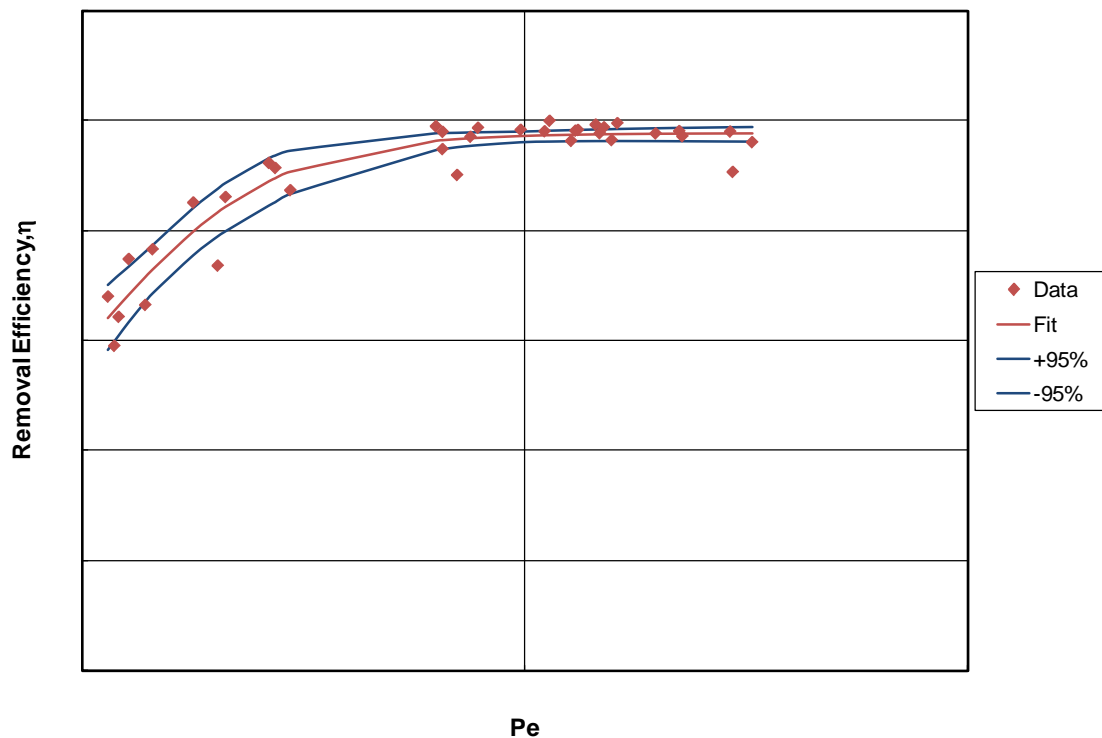
Figure 5.3. Bootstrap Non-Parametric Basic without Replacement

Figures 5.4 and 5.5 are plots of the removal efficiency and washout functions with their modeled 95% confidence intervals. The increased scatter in the high-flow washout data has produced the wider intervals. Even though the confidence intervals are describing the variability in the fitted model, the increased scatter in the data is reflected in the wider intervals.
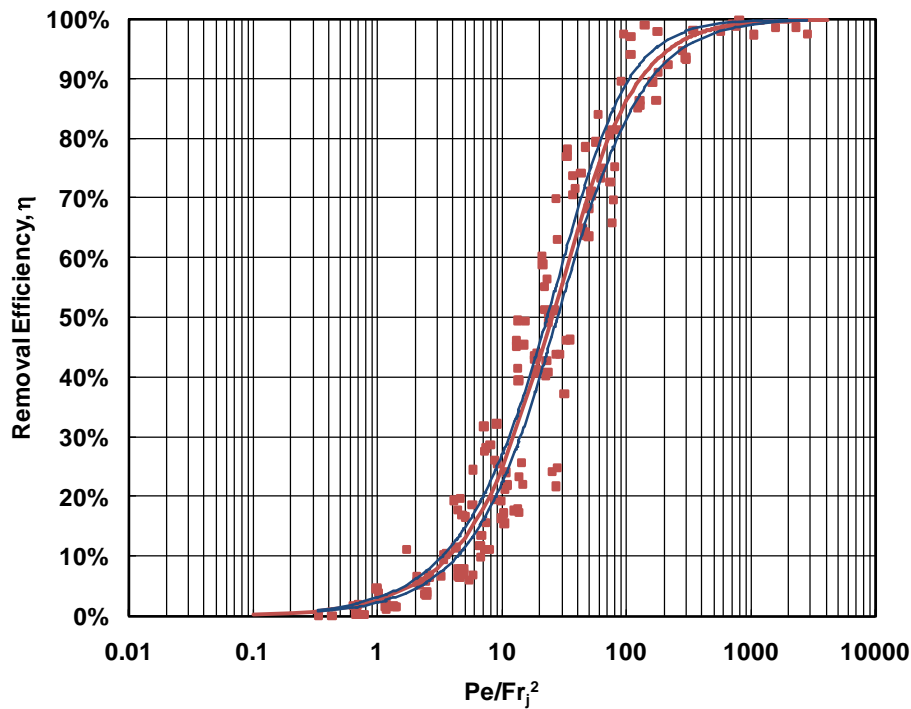
Figure 5.4. Standard Sumps: Measured Removal Efficiency Data, and the Corresponding Fitted Function with its 95% Confidence Intervals
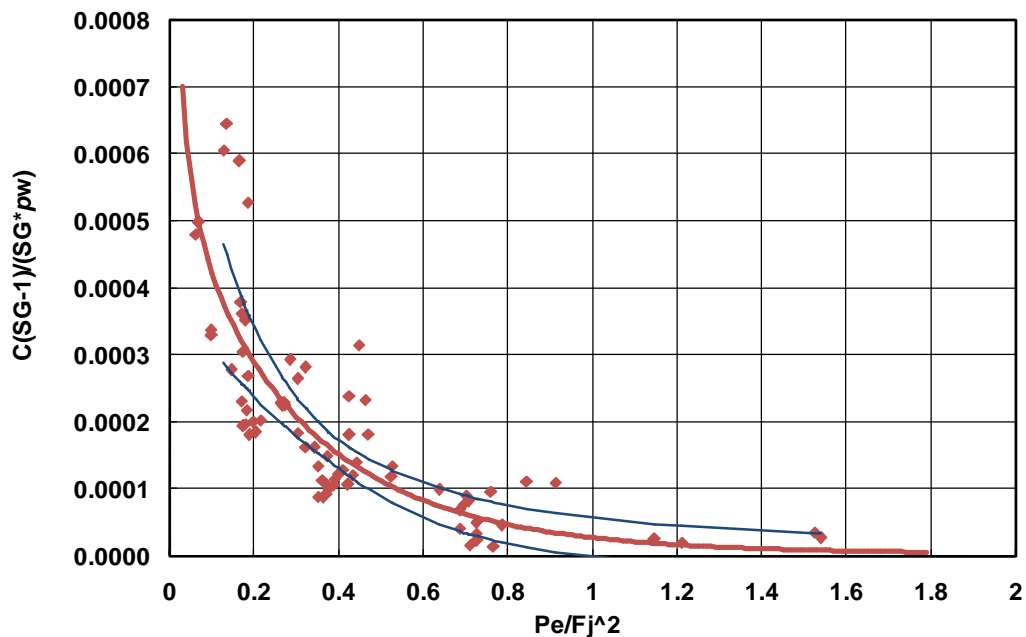
Figure 5.5. Measured Washout Rates (non-dimensional) in Standard Sumps versus Pe/Fr_j^2 and the Corresponding Fitted Function with its 95% Confidence Intervals

6 Application of Performance Functions

6.1 Removal Efficiency

Using the plot of removal efficiency versus the dimensionless parameter given in Figure 5.4, it is possible to predict the removal efficiency of a particular standard sump (depth and diameter are given) in capturing a specific particle size distribution from the influent, on a given day of the year (i.e. water temperature) and at a given storm event (i.e. flow rate). It is also possible to design a standard sump to meet a particular removal efficiency goal with the knowledge of the influent particle size and flow rates.

For example, it may be desired to design a standard sump to remove 20% of a 0.0043 in (110 μm) particle size at a flow rate of 0.6 cfs (17 L/s). A 20% removal efficiency for the standard sump requires a Pe/Fr_j^2 value of 7.82. If the water temperature is 44 ^{o}F (7 ^{o}C), the settling velocity becomes 0.0149 ft/s (0.0045 m/s). If the inlet pipe diameter is 15 inches (38 cm) wide and is laid at a 1% slope, the inflow velocity will be approximately 1.6 ft/s (0.49 m/s) for a flow rate of 0.6 cfs (17L/s). Using Equation 4.38, the only unknowns will be the height and diameter of the sump. For this case, the volume of the sump, $h*D^2$, would be 25 ft^3 (0.71 m^3). The sump would need to be at least 2.9 feet (0.9 m) deep and 2.9 feet (0.9 m) wide in diameter to satisfy these requirements.

To complete the sizing of a standard sump requires the development of runoff hydrographs at the outlet of watershed draining into the sump for an extended period of time. Based on the runoff time series and the potential particle size distribution in stormwater runoff, the annual sediment loading to the sump can be determined. When the annual loading is routed through the removal efficiency function, a minimum length scale can be determined based on a regulatory suspended sediment removal goal.

In another example, the removal efficiency for a given sump depth and diameter can be predicted based on the particular watershed characteristics. Table 6.1 presents the results of such an example. Table 6.1 was created by utilizing the watershed characteristics calculated in Appendix B, and the subsequent design flow rates. To complete this example, a value must first be found for the Pe/Fr_j^2 (Equations 4.35 and 4.36) relationship. Two particle size distributions were chosen to calculate settling velocity for Pe/Fr_j^2, OK110 (d15=0.0039 in (98 μm), d50=0.0046 in (116 μm), d85=0.0053 in (135 μm)) and MN/DOT Road Sand (d50=0.0137 in (347 μm)). The d50 particle size was chosen to represent the MN/DOT Road Sand distribution and a value for the OK110 distribution was calculated by assuming 30% of the particle distribution is represented by the d15, 30% is represented by the d85, and 40% is represented by the d50. Using these assumptions, a value for Pe/Fr_j^2 can then be calculated by inserting the particle settling velocity (calculated using Equation 4.2), 2-yr or 1-yr design flow rate from Appendix B and corresponding pipe jet velocity, and the particular sump depth and diameter. The calculated Pe/Fr_j^2 value will then be placed into Equation 4.38 to return a prediction for removal efficiency.

6.2 Washout

There are certain constraints and limitations in the application of the washout function presented in Section 4 (Equation 4.37). At values of Pe/Fj^2 greater than 2.3 the washout function is no longer valid. This is the point where the power supplied becomes small enough that no particles

can be entrained from the sediment deposit into the water column in the sump. In addition, if the particle size becomes large, the sump will no longer be well mixed, and the calculation of settling power is no longer valid.

The fitted model presented in Figure 5.5 can be used to predict sediment effluent concentrations for a standard sump for any particle size distribution, particle specific weight, water temperature, sump model (i.e. depth and diameter), sump inlet pipe size, and flow rate. Additionally, Equation 4.37 can be used for the design of a standard sump if a target effluent concentration has to be met. This process is similar to the one presented above for the removal efficiency function.

For example, the goal may be to limit the effluent concentration to 0.012 lbs/ft³ (200 mg/L) during the 10-year storm event. If the 10-year storm peaks at 19 cfs (538 L/s), the inlet pipe is 24 in (0.61m) in diameter, then the inflow velocity will be approximately 6.7 ft/s (2.04 m/s). Additional necessary variables are particle size, water temperature, and specific gravity, which are assumed to be 0.0043 in (110 μm), 50 °F (10 °C), and 2.65 respectively, in this example. Using the input data, the settling velocity becomes 0.017 ft/s (0.0052 m/s). Using the maximum effluent concentration and the input data, the dimensionless effluent concentration, $C^*(SG-1)/(\rho_w^*SG)$, becomes 0.000125 which results in a Pe/Fr_j^2 value of 0.47 from the model in Figure 5,5. The only unknowns are now the sump height and diameter, h^*D^2, which is equal to 722 ft³ (20.4 m³). Thus, the minimum values for the height and diameter of the sump will each be 9 ft (2.7 m).

Similarly to the second example presented in Section 6.2, it is also possible to calculate a predicted effluent concentration for a high-flow design storm, i.e. the 10-year design storm flow rate calculated in Appendix B. The Pe/Fr_j^2 value will be calculated in the same way as the example in Section 6.2, except with the 10-year design storm discharge and corresponding jet velocity. The calculated Pe/Fr_j^2 value will then be placed into Equation 4.37 which can be solved for concentration. Table 6.1 below provides the results of this analysis for the same particle size distributions mentioned in Section 6.2. It is important to note, Table 6.1 is based on an assumed watershed. Watersheds with different design discharges and particle size distributions will produce different results.

Table 6.1. Predicted design storm removal efficiencies and effluent concentrations for various sump sizes and particle distributions (based on theoretical watersheds calculated in Appendix B).

Sump Model	Particle Size Distribution	Water Temperature (F)	Removal Efficiency at 1-yr Storm Event (%)	Removal Efficiency at 2-yr Storm Event (%)	Washout at 10-yr Storm Event (mg/L)
4x4	Mn/DOT Road Sand	50	16	12	6
4x4	OK110	50	3	2	240
4x2	Mn/DOT Road Sand	50	8	6	30
4x2	OK110	50	1	1	460
6x6	Mn/DOT Road Sand	50	4	2	270
6x6	OK110	50	1	0	820
6x3	Mn/DOT Road Sand	50	2	1	490
6x3	OK110	50	0	0	1100

6.3   *Practical Application of Results*

In Sections 6.1 and 6.2, the examples presented show how to utilize each fitted performance function separately to size a standard sump for a particle diameter, and a flow rate. However, the overall removal efficiency of a device is dependent on how a device removes a variety of sediment sizes found in stormwater runoff under a variety of flow conditions. In addition, the washout occurring during infrequent storm events reduce the overall efficiency of the device. Therefore, in order to practically size a standard sump, it is deemed necessary to route a number of runoff hydrographs (a runoff time series) through the sump and to determine the overall removal efficiency for the entire period of the runoff time series. If the runoff time series is comprised of several years of 15-minute flow rates from the drainage basin, the results will give more or less a realistic performance of the sump which can subsequently be used to estimate the mean annual removal efficiency of the sump.

This method of sizing the sump has to be done iteratively, i.e. a sump size is selected and evaluated for the period of record and the estimated mean annual removal efficiency will be compared with the target efficiencies. If the target efficiency is not met, a larger standard sump has to be selected or the sump has to be installed further upstream in the drainage basin, i.e. the area of the drainage basin has to be reduced.

6.3.1   *Removal Efficiency Simulation*

The process explained above, requires continuous simulation of runoff from the drainage basin of interest. The resulting runoff hydrographs will then be incorporated into the standard sump performance functions. This process is possible through the use of the computer model SHSAM, (Mohseni et al., 2009; see also www.barr.com). The removal efficiency functions developed for standard sumps have been modeled in SHSAM. SHSAM simulates 15-minute runoff events from 15-minute precipitation events and then computes the influent suspended sediment load from the drainage basin and finally estimates the amount of sediment removed by the device. In near future, the washout function of standard sumps (Equation 4.37) will be incorporated in SHSAM

to simulate the complete performance of standard sumps and the corresponding maintenance requirements.

Table 6.2 is an example of the input data used in SHSAM to size a standard sump for a hypothetical watershed. The precipitation data are 15-minute rainfall events recorded at the weather station in Northfield, MN, from 1991-2007. In the example shown in Table 6.2, it is assumed that the particle size distribution of suspended sediments in runoff is either similar to the particle size distribution used by the New Jersey Department of Environmental Protection (NJDEP) or the Mn/DOT Road Sand. The results of the model are summarized in Table 6.3.

Table 6.2. Example of Input Data for Sizing Standard Sumps

Parameter	Value/Description
Precipitation	Northfield, MN, 1991-2007
Temperature	Northfield, MN, 1991-2007
Particle Size Distribution	NJDEP or Mn/DOT Road Sand
Watershed Size (acres)	5
Impervious Area (%)	20
Hydraulic Length (ft)	527
Curve Number (Pervious Area)	68
Influent Concentration (mg/L)	200
Sump Cleaning	Once per year

Table 6.3. Standard Sump Removal Efficiency Performance for the Parameters Provided in Table 6.2

Sump Model	d_{50} of the PSD (μm)	Total Load (lbs)	Total Load Removed (lbs)	Removal Efficiency (%)
4×4	67	17206	4593	26.7
4×4	347	17206	13097	76.1
4×2	67	17206	3799	22.1
4×2	347	17206	11647	67.7

The data shown in Table 6.3 is the summary of 17 years (1991 to 1997) of simulated sediment load upstream of the sump (Total Load) and the total amount of sediment removed by the sumps. The 0.0026 in (67 μm) particle size given in the second column of Table 6.3 is the d_{50} of the NJDEP particle size distribution and the 0.0137 in (347 μm) particle size is the d_{50} of the Mn/DOT Road Sand. The 4×4 ft sump consistently achieves higher removal efficiencies than the 4×2 sump. In addition, the smaller particle size in stormwater results in lower removal efficiencies, i.e. between 22% and 27%.

Figure 6.1 is the output chart from SHSAM for the 4×4 ft sump with the Mn/DOT Road Sand particle size distribution showing the time series of sediment loading and sediment removal for the entire period of 1991-2007.

In addition to the data provided above, SHSAM also provides yearly loading, capture, and removal efficiencies. Table 6.4 provides the results of the 4×4 ft sump for each year assuming the Mn/DOT Road Sand particle size distribution in stormwater runoff. From Table 6.4 it is

evident that the annual removal efficiency can vary from 62% to 94% during the period of 1991-2007.

The final column in Table 6.4 provides the depth of deposit at the end of each year before the annual clean-up. SHSAM will also provide the required number of sump clean-up. For this example, i.e. the watershed and particle size, the deposit in the sump never reached a depth of one foot (the assumed maximum depth of deposit in the sump), so it was only necessary to clean the sump once a year. If the goal was to only clean the sump when the deposit became one foot deep, then the sump should be cleaned once every 1.6 years for this example. For a 4×2 ft sump to be installed at the outlet of the same watershed and assuming the NJDEP particle size distribution in stormwater runoff, the sump is required to be cleaned once every 5.6 years because the sump does not remove any significant amount of sediment load from runoff. Thus, the required maintenance is highly dependent upon the particle size distribution in stormwater runoff, the sump size, and the climate and the watershed characteristics.
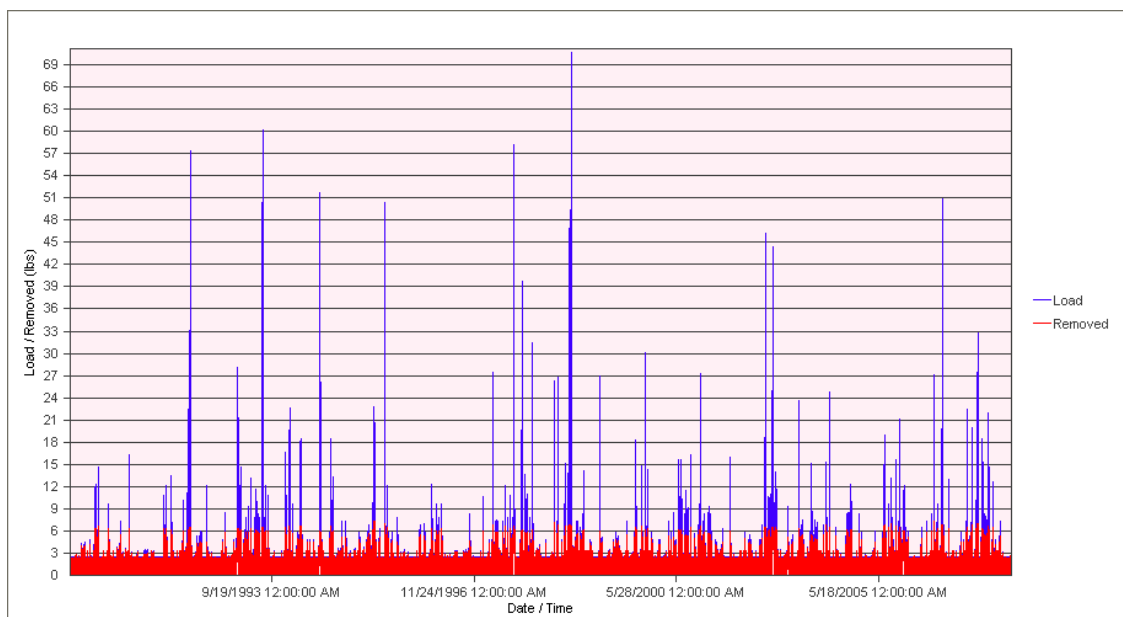
Figure 6.1. Sediment Load from the Watershed Presented in Table 6,1, and the Amount of Sediment Removed by the 4×4 ft Standard Sump, Assuming the Mn/DOT Road Sand Particle Size Distribution in Stormwater Runoff.

Table 6.4. Yearly Removal and Deposit in a 4×4 ft Standard Sump Assuming Mn/DOT Road
Sand Particle Size Distribution in Stormwater Runoff

Year	Removal Efficiency (%)	Annual Load (lbs)	Load Removed (lbs)	Deposit (in)
1991	92	965.8	888	8.49
1992	70	1258.6	881.6	8.43
1993	70	1476.8	1028	9.83
1994	72	1321.6	955.8	9.14
1995	80	940.2	748.2	7.16
1996	94	803.6	752.5	7.2
1997	69	1503.7	1038.4	9.93
1998	62	1447	901	8.62
1999	88	926.8	811.4	7.76
2000	81	1142.7	930	8.9
2001	92	363.9	335.6	3.21
2002	62	1091.6	671.6	6.42
2003	83	828.6	690.2	6.6
2004	88	356.5	315.5	3.02
2005	84	936.8	786.9	7.53
2006	76	787.7	596	5.7
2007	73	1054.5	766.6	7.33

6.3.2   *Washout Simulation*

SHSAM currently does not simulate sediment washout because the washout functions have not
been incorporated into the model yet. However, it is possible to predict the washout potential in a
standard sump by assuming that once the sump effluent concentration becomes larger than the
influent concentration no net sediment will be captured in the sump. At this point, it is suspected
that significant quantities of sediment will be washed out of the sump.

By employing the standard sumps washout function (Equation 4.37), a critical discharge can be
estimated for a particular sump assuming an effluent concentration equal to or larger than the
influent concentration (in this example of 0.0125 lbs/ft^3, 200 mg/L). This critical discharge will
also be dependent on the particle size and water temperature. The 15-minute watershed runoff
modeled by SHSAM (e.g. Figure 6.2) can be used to quantify the number of times the discharge
through the sump exceeds the critical discharge. Thus the occurrence of large washout rates can
be predicted for the period of simulation. The results of this analysis are presented in Table 6.5.
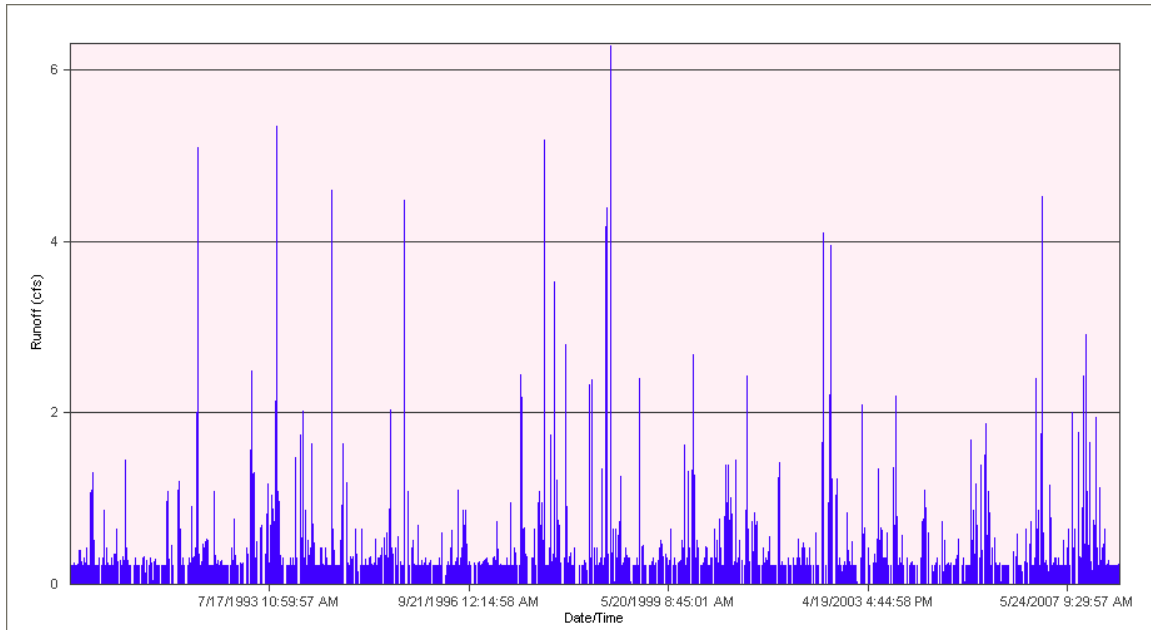
Figure 6.2. Simulated Runoff Time Series for the Watershed Assumed in Table 6.1.

Table 6.5. Critical Discharge for Various Sump Sizes and Particle Distributions

Sump Model	Sediment d_{50} (μm)	Effluent Concentration (mg/L)	Pe/Fr_j^2	Critical Discharge (cfs)	No, of Times the Critical Discharge Exceeded in Figure 6.2
4×4	67	200	0.478	3.0	33
4×4	347	200	0.478	10.8	0
4×2	67	200	0.478	2.1	70
4×2	347	200	0.478	8.1	0

From Table 6.5, it is evident that an increase in particle size requires a higher critical discharge to result in an effluent concentration of 0.0125 lb/ft^3 (200 mg/L). Thus the number of times the critical discharge is exceeded is significantly lower for the larger particle size than the larger particle size, i.e. 33 times for the 4×4 ft sump with the small particle size (67 μm) and 0 times for the 4×4 ft sump with the large particle size (347 μm). A similar trend can be noted for the change in depth. The effluent concentration in a 4×2 ft sump will exceed 0.0125 lb/ft^3 (200 mg/L) 70 times over the 17 years of simulation for the small particle size, while in a 4×4 ft sump, effluent concentration only exceeds the 0.0125 lb/ft^3 (200 mg/L) 33 times for the same particle size and duration.

6.3.3   Comparison of Standard Sumps to Proprietary Devices

From a design engineering perspective, it is desirable to compare the performance of standard sumps for sediment collection to that of proprietary hydrodynamic separators. Wilson et al. (2007) and Carlson et al. (2006) used the same method of testing and also the same procedure to develop removal efficiency functions for five other devices. The washout functions, however, have not been developed for those devices yet. Therefore, the comparison will only be conducted using the Péclet number removal efficiency analysis (Section 4.1). Figure 6.3 displays the removal efficiency function of standard sumps next to the removal efficiency functions of

Stormceptor STC 4800, CDS PMSU20_15, Environment 21 V2B1 Model 4, BaySaver 1K, and Vortech Systems Model 2000. It is important to note that the removal efficiency functions of the proprietary devices shown in Figure 6.3 are based on testing only one size of each device. Therefore, it is anticipated that the overall removal efficiency functions of all sizes are somewhat different. Nevertheless, it is evident that standard sumps are approximately 20% less efficient than most proprietary devices.
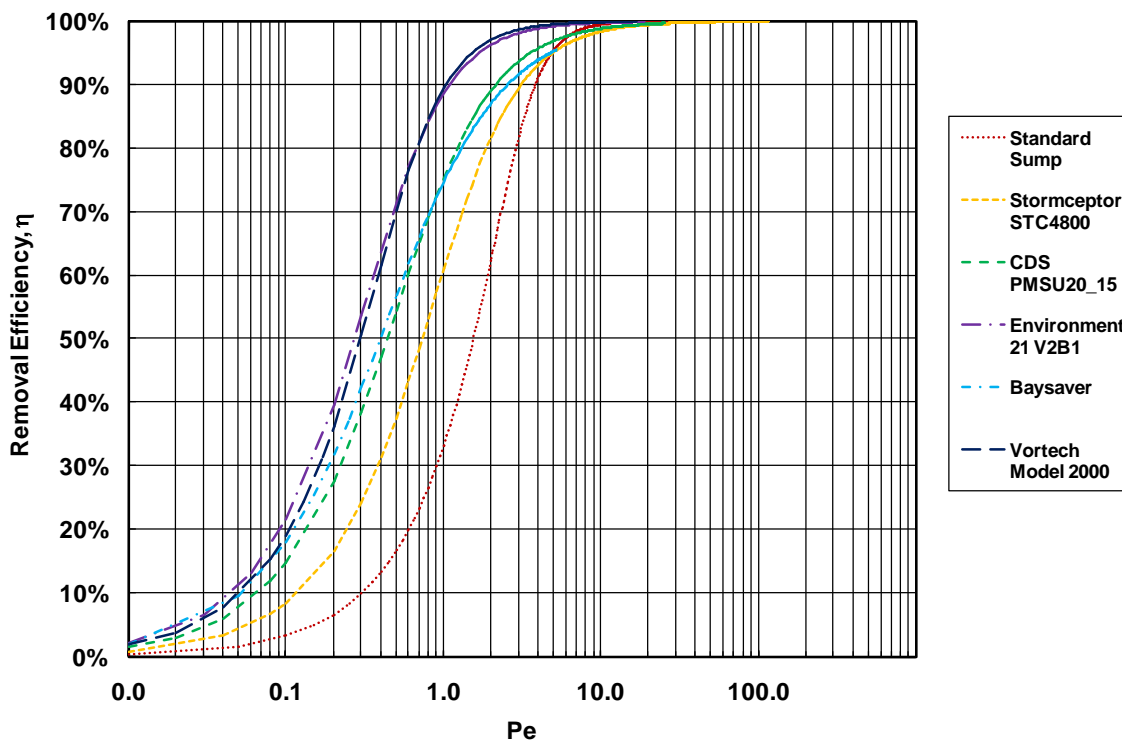
Figure 6.3. Removal Efficiency Functions of Standard Sumps, Stormceptor, CDS, Vortech Systems, Environment21, and BaySaver

7   Summary and Conclusions

In this study we have evaluated the ability of standard sumps to capture particles larger than silt carried in stormwater runoff, and to retain them without washout. Tests were conducted for five different sump configurations, 4×4 ft (1.2×1.2 m), 4×2 ft (1.2×0.6 m), 6×6 ft (1.8×1.8 m), 6×3 ft (1.8×0.9 m), and 1×1ft (0.3×0.3 m).

A full scale removal efficiency test typically produced 40 data points collected during 15 tests. The sediment size was divided into three narrow distributions, 0.0035-0.0049 in (89-125 μm), 0.0099-0.0140 in (251-355 μm), and 0.0197-0.0232 in (500-589 μm). The maximum tested flow rate for assessing the removal efficiency was 2.4 cfs (68 L/s) for the 4-ft (1.2 m) sump and 7.0 cfs (198L/s) for the 6-ft (1.8 m) sump.

A full scale washout test typically produced 15 to 20 data points, each point representing an individual test for one particle size (110 μm). The maximum tested flow rate was 5.5 cfs (156L/s) for the 4-ft (1.2 m) sump and 19.0 cfs (538 L/s) for the 6-ft (1.8 m) sump.

The results of this study provide insight into the processes involved in sediment capture and retention in standard sumps. Removal efficiency testing has proven that the sump sizes listed above are effective at collecting sediment at low-flow conditions from small urban drainage basins, i.e. smaller than 4 acres. The major drawback of the sump is its inability to retain the captured sediment under high-flow rates. This is especially evident in the test results for the shallow sumps. A decrease in depth increases the potential for sediment washout. Frequent maintenance of the standard sump is necessary to be an effective stormwater pre-treatment device for sediment.

During the washout tests it was noted that sediment was being scoured, moved upstream, and deposited just below the inlet pipe. This flow pattern was verified by measuring velocities in the sump. The results indicate rotation exists with downstream flow at the water surface, downward flow due to the plunging effect, upstream flow near the sediment bed, and upwelling at the upstream end of the sump.

The Péclet number is an effective parameter for the prediction of stormwater settling device removal efficiency in a given sump. However, the Péclet number is not necessarily a parameter for accurately scaling of standard sump performance, i.e. if a specific standard sump tested, and a removal efficiency function is developed for that sump, that resulting function cannot necessarily be used for other sump sizes.

A washout function has been developed to predict washout from all standard sumps. The washout function employs a parameter representing the ratio of the settling power to the power supplied to the device which can accurately predict effluent concentration for a particular flow rate, device diameter and depth, inlet pipe diameter, water temperature, sediment size, and sediment specific weight. The washout function is accurate as long as the power supplied is greater than the power required for scour, entrainment, and lifting of the particles. It is also necessary for the sediment size of the deposit to be smaller than medium sand to ensure complete mixing.

The performance and required maintenance of standard sumps is highly dependent on the watershed characteristics, weather conditions (precipitation and temperature), and sediment loading. In order to develop a maintenance schedule for a given standard sump, runoff from the drainage basin upstream of the standard sump should be simulated using a continuous runoff model. The simulated runoff time series with the performance functions presented in this report can be utilized to determine the required maintenance frequency of the sump.

The table below presents the expected 1-yr and 2-yr design storm removal efficiencies and the 10-yr design storm washout effluent concentrations for all of the full scale sumps tested (size labeled as diameter × depth in feet) for two different particle size distributions. The data was created using the sediment washout performance function and the removal efficiency performance function. The two particle size distributions given in the table, OK110 and Mn/DOT Road Sand, have median particle sizes of 0.0046 in (116 μm) and 0.0137 in (347 μm), respectively. The OK110 sand has a d_{15} of 0.0039 in (98 μm) and a d_{85} of 0.0053 in (135 μm). It is important to note that the 1-yr, 2-yr and 10-yr storm events in the table have been computed for 10 and 20 acre watershed areas draining into 4-ft and 6-ft sumps, respectively, with a runoff coefficient of 0.7. It is evident that standard sumps can be only effective in treating stromwater runoff from small urban drainage areas, i.e. smaller than 4 acres.

Table 7.1. Removal efficiency of standard sumps at expected 1-yr and 2-yr storm events and washout at expected 10-yr storm events

Sump Model	Particle Size Distribution	Water Temperature (F)	Removal Efficiency at 1-yr Storm Event (%)	Removal Efficiency at 2-yr Storm Event (%)	Washout at 10-yr Storm Event (mg/L)
4x4	Mn/DOT Road Sand	50	16	12	6
4x4	OK110	50	3	2	240
4x2	Mn/DOT Road Sand	50	8	6	30
4x2	OK110	50	1	1	460
6x6	Mn/DOT Road Sand	50	4	2	270
6x6	OK110	50	1	0	820
6x3	Mn/DOT Road Sand	50	2	1	490
6x3	OK110	50	0	0	1100

References

AGSCO. "Silica Sand Product Particle Distributions." Wheeling, IL. http://agsco.thomasnet.com/Asset/Silica%20Sands.Flours.Tech.Data%20Sheet.0709.pdf. Accessed October 2009.

Akiyama, J. and H. Stefan. "Turbidity Current with Erosion and Deposition." *Journal of Hydraulic Engineering*. 111(12): 1473-1496. 1985.

American Society of Civil Engineers (ASCE). *Sedimentation Engineering*. ASCE Manuals and Reports on Engineering Practice-No. 54. Washington, D.C. 1975

Avila, H. and R. Pitt. "Evaluating Scour Potential in Stormwater Catchbasin Sumps Using a Full-Scale Physical Model and CFD Modeling." *Proceedings of the Water Environment Federation, WEFTEC*. pp. 6958-6977. Chicago, IL. 2008.

Bertrand-Krajewski, J.-L. "Sewer Sediment Management: Some Historical Aspects of Egg-Shaped Sewers and Flushing Tanks." *Water Science and Technology*. 47(4): 109-122. 2003.

Brzozwski, C. "BMP Testing Protocols: Wisconsin Steps Forward." *Stormwater Journal*. October 2006.

Butler, D. and S.H.P.G. Karunaratne. "The Suspended Solids Trap Efficiency of the Roadside Gully Pot." *Water Research*. 29(2): 719-729. 1995.

Carlson, L., O. Mohseni, H. Stefan, and M. Lueker. *Performance Evaluation of the BaySaver Stormwater Separation System*. St. Anthony Falls Laboratory Project Report # 472. 2006.

Carpenter, J. and J. Bithell. "Bootstrap Confidence Intervals: when, which, what? A practical Guide for Medical Statisticians." *Statistics in Medicine*. 19: 1141-1164. 2000.

Cheng, N. "A Simplified Settling Velocity Formula for Sediment Particle." *Journal of Hydraulic Engineering*. 123(2): 149-152. 1997.

DeGroot, G.P., J.S. Gulliver, and O. Mohseni. "Accurate Sampling of Suspended Solids." *World Environmental and Water Resources Congress Proceedings*. pp. 807-813. Kansas City, MO. 2009.

Faram, M.G. and R. Harwood. "A Method for the Numerical Assessment of Sediment Interceptors." *Water Science and Technology*. 47(4): 167-174. 2003.

Ferguson, R.I. and M. Church. "A Simple Universal Equation for Grain Settling Velocity." *Journal of Sedimentary Research*, 76(6): 933-937. 2004.

Fletcher, I.J. and C.J. Pratt. "Mathematical Simulation of Pollution Contributions to Urban Runoff from Roadside Gully Pots." *Urban Stormwater Quality, Management & Planning*. pp. 116-124. 1981.

Gupta, R.S. *Hydrology and Hydraulic Systems*. Waveland Press, Inc. Long Grove, IL. 2001.

Huff, F.A. and J.R. Angel. *Rainfall Frequency Atlas of the Midwest*. Midwest Climate Center, National Oceanic and Atmospheric Administration. Champaign, IL. 1992.

Kang, J.H., P.T. Weiss, C.B. Wilson, and J.S. Gulliver, "Maintenance of Stormwater BMPs: Frequency, Effort and Cost." *Stormwater*. 9(8): 18-28. 2008.

Kim, J. and J.J. Sansalone. "Event-Based Size Distributions of Particulate Matter Transported During Urban Rainfall-Runoff Events." *Water Research*. 42: 2756-2768. 2008.

Kim, J., S. Pathapati, B. Liu and J. Sansalone. "Treatment and Maintenance of Stormwater Hydrodynamic Separators: A Case Study." *Proceedings of the 9th Biennial Conference on Stormwater Research and Watershed Management*. Orlando, FL. 2007.

Lepage, R. and L. Billard. *Exploring the Limits of Bootstrap*. Wiley, Inc. New York, NY. 1992.

Li, Y., S. Lau, M. Kayhanian, and M.K. Stenstrom. "Particle Size Distribution in Highway Runoff." *Journal of Environmental Engineering*. 131(9): 1267-1276. 2005.

Mohseni, O. and A. Fyten. *Performance Assessment of Modified ecoStorm Hydrodynamic Separator*. St. Anthony Falls Laboratory, Project Report # 495B, University of Minnesota. Minneapolis, MN. 2007.

Maestre, A. and R. Pitt. "A Compilation and Analysis of NPDES Stormwater Monitoring Information." The National Stormwater Quality Database, Version 1.1, U.S. EPA Office of Water. Washington, D.C. 2005.

Miller, R.W. *Flow Measurement Engineering Handbook*. McGraw-Hill, Inc. New York, NY. 1989.

Minnesota Department of Transportation, Office of Bridges and Structures. *Minnesota Drainage Manual*. St. Paul, MN. August 30, 2000.

Pitt, R. *Characterizing and Controlling Urban Runoff through Street and Sewerage Cleaning*. U.S. EPA Water Engineering Research Laboratory. Cincinnati, OH. 1985.

Rustomji, P. and S.N. Wilkinson. "Applying Bootstrap Resampling to Quantify Uncertainty in Fluvial Suspended Sediment Loads Estimated Using Rating Curves." *Water Resources Research*. 44:1-12. 2008.

Saddoris, D.A., K.D. McIntire, O. Mohseni, and J.S. Gulliver. *Hydrodynamic Sediment Retention Testing*. Mn/DOT Research Services Report #2010-10. St. Paul, MN. 2010.

Silberman, E. *The Pitot Cylinder*. St. Anthony Falls Hydraulic Laboratory, Circular No. 2. University of Minnesota. Minneapolis, MN. 1947.

Smith, E. "Pollutant Concentrations of Stormwater and Captured Sediment in Flood Control Sumps Draining an Urban Watershed." *Water Resources*. 35: 3117-126. 2001.

Stokes, G.G. "On the Effect of Inertial Friction of Fluids on the Motion of Pendulums." *Transactions of the Cambridge Philosophical Society*. 9(II): 8. 1851.

U.S. Silica, Berkeley Springs, WV. SIL-CO-SIL 250 Product Data. http://www.u-s-silica.com/PDS/Ottawa/OttSCS2502000.PDF. Accessed October 2009.

Vaze, J. and F.H.S. Chiew. "Nutrient Loads Associated with Different Sediment Sizes in Urban Stormwater and Surface Pollutants." *Journal of Environmental Engineering*. 130(4): 391-396. 2004.

Wilson, M.A., J.S. Gulliver, O. Mohseni, and R.M. Hozalski. *Performance Assessment of Underground Stormwater Devices*. St. Anthony Falls Laboratory, SAFL Project Report #494, University of Minnesota, Minneapolis, MN. pp. 1-94. 2007.

Wilson, M., O. Mohseni, J. Gulliver, R. Hozalski, and H. Stefan. "Assessment of Hydrodynamic Separators for Stormwater Treatment."*Journal of Hydraulic Engineering*. 131(5). 2009.

Young, D., B.R. Munson, and T.H. Okiishi. *A Brief Introduction to Fluid Mechanics*. John Wiley and Sons, Inc. New York, NY. 2004.

Appendix A.   Sump Setup

A.1.   4-ft (1.2 m) Sump Setup

Construction of the 4ft (1.2m) by 4ft (1.2m) sump was started on December 29, 2008. The sump was placed on a wood base which was mounted on a steel frame. The steel frame was in the shape of a triangle, which allowed it to rest on three load cells, one at each corner. Several bulkhead fittings were placed on the sump to allow draining water at various elevations and to connect the shop vacuum for sediment collection. Upstream, the device was connected to a 15ft (4.6m) long section of 15inch (0.38m) ribbed plastic pipe at a 1% slope by a rubber Firnco gasket. The water supply came from a 12inch (0.31m) hydraulic gate valve. Two 12inch (0.38m) PVC 90 degree bends and one vanstone flange brought the flow from the valve to a 12 to 15 inch (0.3 m to 0.38 m) expansion. The connections to the ribbed plastic piping were by Mar-Mac adhesive. Downstream of the sump the 15inch (0.38m) ribbed plastic pipe was connected to the sump using a rubber Firnco connection. The pipe carried the flow approximately 10ft (3m) at a 1% slope to a 45 degree drop, then another 10 ft (3 m), to where it emptied into the laboratory's exit channel. At the end of the pipe was a 15inch (0.38m) circular weir with a pressure transducer for measuring water depth and flow rate. The equation used to calculate flow rate was

$$\frac{Q}{g^{0.5}d_p^{2.5}} = cw\left(\frac{H}{d_p}\right)^n \tag{A.1}$$

where d_p is the diameter of the pipe, H is the water depth in the pipe, and cw and n are calibration parameters based on the relationship of the weir height to the water depth in the pipe. During high-flow tests the pipe was flowing completely full, making equation A.1 ineffective. To overcome this difficulty a Pitot cylinder was installed upstream of the in the supply pipes by Silberman (1947). Since the supply pipes are vertical it can be assumed that the pipe is always flowing completely full. By measuring the pressure difference between the static tap and the dynamic tap in the Pitot cylinder, the flow rate can be determined assuming a turbulent velocity profile. The velocity profile used (Pai 1935, Miller 1989) was

$$\overline{V_f} = \frac{V_{max}}{1+1.44\sqrt{f}} \tag{A.2}$$

where f is calculated using the Colebrook equation (Young 2004). The pressure difference was measured using a Rosemount digital pressure differential device. Figure A.1 is a drawing of the 4-ft (1.2 m) sump and Figure A.2 is a collage of photos of the 4-ft (1.2 m) sump setup.
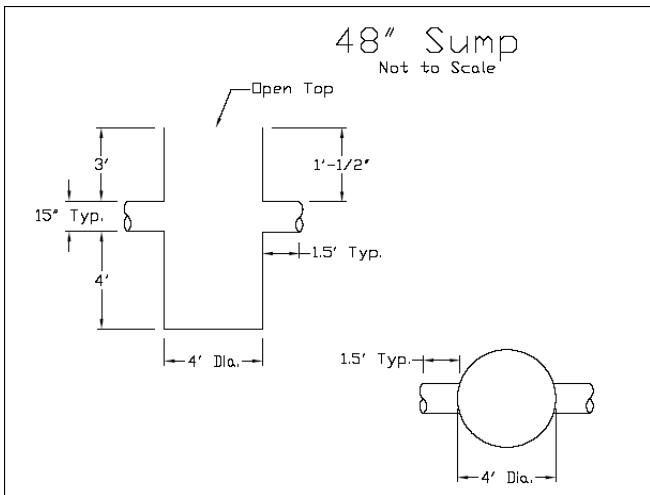
Figure A.1. 4×4 ft Sump Design Drawing

Figure A.2. 4-ft Sump Setup

A.2.   6-ft (1.8 m) Sump Setup

The 6-ft (1.8m) sump was set up similarly to the 4-ft (1.2 m) sump. However, due to its large size there were several differences. The device rested on a wooden platform which was placed on a square steel frame. This frame rested on four load cells, one on each corner. Due to the high cost of 24 inch (0.61m) pipe, the water was discharged into a tail box 1.5 ft (0.38m) downstream of the device. The tail box had an opening in the floor to drain water directly into the exit channel. Upstream of the device, 10 ft (3 m) of 24 inch (0.61m) PVC pipe brought water from a fabricated manifold to the inlet pipe. Two 24 inch (0.61m) rubber Firnco fittings where used to connect both ends of the 10ft (3m) pipe section. Because of the high-flow requirement of the 6ft (1.8m) sump, two 12 inch (0.30m) supply pipes where required. Each supply pipe had its own hydraulic gate valve and two 12 inch (0.3 m) 90 degree bends. The two 12inch (0.30m) pipes were then connected to a fabricated manifold which combined the flow into one 24inch (0.61m) pipe. Connections to the gate valves and manifold were completed using four vanstone flanges. Flow was measured using two Pitot cylinders, one in each supply pipe. Figure A.3 is a design drawing of the 6-ft (1.8m) sump and Figure B.4 is a collage of photos showing the 6-ft (1.8m) sump setup.
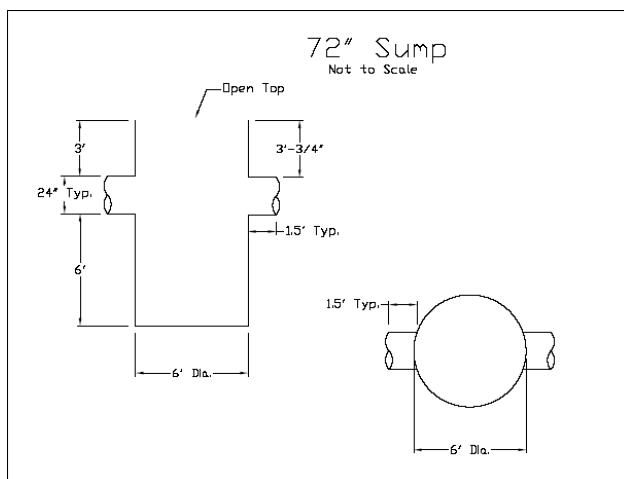
Figure A.3. 6-ft Sump Design Drawing

Figure A.4. 6-ft Sump Setup

A.3. False Floor Setup

A false floor was constructed for testing in both the 4-ft (1.2m) and 6-ft (1.8m) sumps. In both cases, the false floor was constructed building a frame to the desired height and then adding a plywood surface on top of the frame. This plywood surface was cut to fit the diameter of the sump, and needed to be very precise in order to reduce leakage.

Both false floors were sealed using vulcum sealant. The 4-ft (1.2m) sump false floor had another surface of 1/4in (0.64cm) plastic placed on top of the plywood. The 6-ft (1.8m) sump did not have the plastic surface, but was instead painted with an epoxy paint. Figure A.5 is a design drawing of the typical framing for the false floors.
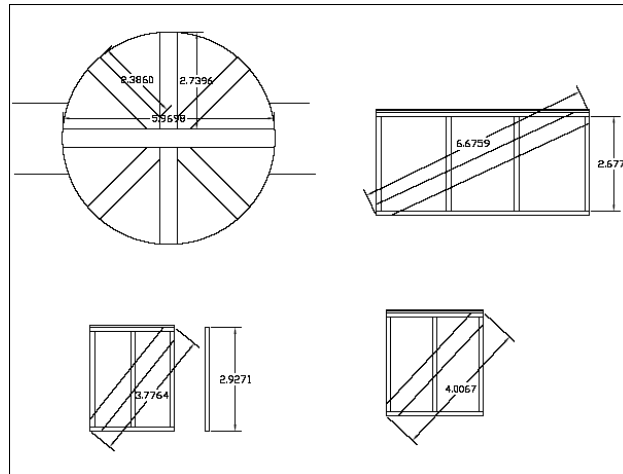
Figure A.5. 6-ft Sump False Floor Support Frame

A.4. 1×1 ft (0.3×0.3 m) Scale Model Setup

The 1×1 ft (0.3×0.3 m) scale model provided water to the sump by recirculation. Two head tanks were connected to a one horsepower electric pump. The first head tank was the larger of the two, and provided the water volume necessary to maintain a constant head. The second, smaller head tank was connected to the pump and had a 0.0008in (20μm) filter at its top. Water would leave the second head tank, enter the pump and be raised to the elevation of the 1×1 ft (0.3×0.3 m) scale model. From there, water would flow by gravity back to the second head tank where it would first go through the filter before entering the tank. The last connection before entering the filter was a 90 degree bend which was free to move. This allowed the outlet pipe to be moved to discharge either into the smaller head tank and filter and into the laboratory's exit channel, or into a bucket resting on a scale. This bucket was used to measure the flow rate by finding the weight of water accumulated in the bucket over a set amount of time. The flow rate was set using a gate valve located between the pump and the sump inlet pipe. Most of the scale model was constructed of PVC, however, the sump itself and the influent and effluent pipes were constructed using clear acrylic plastic. Figure A.6 is a picture of the 1×1 ft (0.3×0.3 m) scale model setup.

Flow rates below 20 gpm (1.3 L/s) were conducted without re-circulating the water. In this case, the sump effluent was routed directly into the laboratory's exit trough, and the head tanks would be kept full using two hoses from the tap water. This eliminated the sediment from the effluent re-entering the model.

For the removal efficiency tests, the sediment was fed into the inlet pipe using a small sediment feeder. The feeding configurations included dry feeding at 13 in (0.33 m) upstream, dry feeding 3 in (0.076 m) upstream, or slurry feeding 3 in (0.076 cm) upstream.

Figure A.6. 1×1 ft (0.3×0.3 m) Scale Model Complete Setup

Appendix B.   Design Storm Discharges for Tested Standard Sumps

Discharges for storm sewers are typically characterized in terms of design storm frequencies. Thus, it is necessary to quantify the results from the standard sumps analysis to typical design storm discharges for a particular watershed and region. The Minneapolis, MN/St. Paul, MN metro area was chosen as a representative environment for this analysis. It is important to note, for testing, it was necessary for the range of discharges utilized to cover the full range of removal efficiencies. Thus, the discharges chosen for the removal efficiency testing did not necessarily represent any design storm discharges. However, the design storm discharges can be correlated to the data collected through use of the fitted performance functions. To complete this analysis, the 10-year design storm was chosen to be the maximum storm event for the high-flow washout tests. If runoff from the 10-year design storm would result in 80% pipe full, then a representative flow rate can be found using Manning's equation,

$$Q = \frac{K_c}{n_m} * A_p * \left(\frac{A_p}{P_w}\right)^{\frac{2}{3}} * S_o^{\frac{1}{2}} \tag{B.1}$$

In Equation B.1, K_c is an adjustment for units (1.49 for U.S. Customary Units and 1 for SI Units), n_m is the Manning resistance coefficient, A_p is the flow cross sectional area in the pipe, P_w is the wetted perimeter, and S_o is the pipe slope. For this situation, a value of 0.014 for n, corresponding to a concrete pipe, and a slope of 0.01 ft/ft (m/m) was used. Using the 4-ft (1.2 m) sump as an example, a completely full 15-in (38 cm) pipe has a cross sectional area of 1.23 ft^2 (0.114 m^2), which results in a 80% pipe full cross section of 0.984 ft^2 (0.091 m^2). The equation for the circular segment area is,

$$A_p = \pi r^2 - \frac{r^2(\theta - \sin\theta)}{2} \tag{B.2}$$

were r is the pipe radius, and θ is the central angle created by two radii passing through to the location were the water surface meets the pipe wall. The angle θ can then be solved for since A_p is the value for the 80% pipe full cross sectional area. The wetted perimeter is thus found using equation B.3,

$$P_w = 2\pi r - r\theta \tag{B.3}$$

All of the values necessary for finding the 80% pipe full flow rate using Manning's equation are now quantified. Using Equation B.1, the 10-year design flow rate is estimated to be 5.5 cfs (156 L/s) for the 4-ft (1.2 m) sump with a 15-in (38 cm) inlet pipe and 19 cfs (538 L/s) with a 24-in (61 cm).

Since a design discharge is now known, it is possible to work backwards using the rational method to provide an estimate for the drainage basin area,

$$Q = C_R i A_w \tag{B.4}$$

In Equation B.4, C_R is the runoff coefficient (0.7 for an urban watershed), i is the rainfall intensity, and A_w is the watershed area. The storm intensity, i, is dependent on the time of concentration, which is a function of the watershed hydraulic length and the design storm, none of which are known. Due to the large number of unknowns, an iterative process was used to find

an appropriate hydraulic length, time of concentration, and intensity for the 10-year design storm. To start this process a time of concentration, or storm duration, was assumed and then from the intensity-duration-frequency (IDF) tables provided by Huff and Angel (1992) the rainfall intensity for the 10-year storm was determined. A typical hydraulic length was then calculated using the Kirpich equation (Gupta 2001), Equation B.5. The Kirpich equation was developed for overland flows in rural areas, but it has been shown to be also applicable to small urban drainage basins.

$$t_c = 0.0078 \frac{L^{0.77}}{S^{0.385}}$$
(B.5)

In Equation B.5 t_c is the time of concentration, L is the hydraulic length of the drainage basin, and S is the average slope of the overland area (0.01 ft/ft for this example). The rainfall intensity value, flow rate for 80% pipe full, and runoff coefficient, were then placed in the Equation B.4 to determine the watershed area. The hydraulic length obtained from Equation B.5 was then compared to the calculated watershed area to ensure reasonable values. The representative watershed area for the 4-ft (1.2 m) sump was calculated to be 10.2 acres (4.1 hectares).

Now that the representative watershed area was determined, it was possible to estimate the 1-year or 2-year design discharge. To complete this, rainfall intensity for the 1- or 2-year design storm was found from the IDF tables (Huff and Angel, 1992) for the time of concentration/design storm duration used for the 10-year storm (the time of concentration is relatively constant for all storm durations since the hydraulic length, slope, and surface characteristics remain the same). The 1- or 2-year design discharge was then found by inserting the respective rainfall intensity, watershed area found for the 10-year storm and the runoff coefficient into the rational equation. This process was completed separately for the 6-ft (1.8 m) sump and the 4-ft (1.2m) sump. Table B.1 provides the results and assumptions from the maximum treatment rate analysis.

Table B.1. Maximum Treatment Rate Design Parameters

Sump Model	Design Storm	Runoff Coefficient	Hydraulic Length (ft)	Time of Concentration (min)	Rainfall Intensity (in/hr)	Design Flow Rate (cfs)	Watershed Area (acre)
4-ft	10-yr	0.7	1120	10	0.77	5.5	10.2
4-ft	2-yr	0.7	1120	10	0.56	4.0	10.2
4-ft	1-yr	0.7	1120	10	0.47	3.4	10.2
6-ft	10-yr	0.7	4665	30	1.37	19.1	19.9
6-ft	2-yr	0.7	4665	30	0.98	13.7	19.9
6-ft	1-yr	0.7	4665	30	0.82	11.4	19.9

Appendix C.   Sieving Operation

C.1. Particle Size Distributions of Manufactured Sediments

Suspended sediments were purchased from two manufacturers (U.S. Silica Company and AGSCO Corporation) which supplied particle size distributions for their products. The particle size distributions for the manufactured sediments used are given in Figure C.1. A size distribution and evaluation of F-110 as determined by SAFL personnel is given in Figure C.2 below. F-110 was used extensively in testing for both washout tests and for the creation of the smallest particle size range in the removal efficiency tests. AGSCO 40-70 and 20-40 where used specifically for creation of the two larger particle size ranges in the removal efficiency tests.

C.2. Size Distributions Desired for Tests

The particle size distributions which were fed into the sump for the removal efficiency tests were chosen to depict the range of sediment sizes in stormwater as discussed in the introduction. Three distinct particle size ranges were created through sieving at the laboratory. The three particle sizes where mixed in equal parts and added to the influent. Following each test, the sediment collected in the sump would be dried and sieved back into its respective particle size ranges.

Each of the three particle size ranges where created from different manufactured sediment, each of which has a particle size distribution provided above. The three particle size ranges and their representative initial manufactured designation is as follows: The smallest particle size was created by sieving F-110 or AGSCO 140-270 with sieves 0.0035in to 0.0049in (89μm to 125μm), with a median value of 0.0042in (107μm). The medium particle size was created using AGSCO 40-70 with sieves 0.0099in to 0.014in (251 μm to 355 μm), with a median value of 0.0119in (303μm). The largest particle size was created using AGSCO 20-40 with sieves 0.0197in to 0.0232in (500 μm to 589 μm), with a median value of 0.0215in (545 μm). The narrow particle size bands allowed one sieve to remain unused between each particle size to ensure no overlap occurred. For example, if the particle sizes where too close in size, it would be possible for sediment which was initially in one particle range to end up in another particle range when sieved following the completion of a test. This is due to the inherent error associated with the sieving process. Wilson et al. (2007) provides a detailed description of the steps which lead to the creation of this sieving process.

C.3. Sieving Operation

Sieving was a major endeavor in the removal efficiency tests. One worker was always sieving either to prepare for the next removal efficiency test series or to analyze the data from the previous removal efficiency test series. The sieving of material which would be input to the sump influent (pre-sieving) was conducted using the large shaker table at the laboratory. Pre-sieving the larger two particle sizes went fairly smoothly with approximately 50% of the sediment sieved becoming waste, i.e. the particles which passed through the top sieve (125μm for the smallest particle range) and remained on the bottom sieve in the stack (89μm for the smallest particle range) where collected, while the sediment caught on the top sieve (125μm for the smallest particle range) or passing through the smallest particle size (89μm for the smallest particle range) would be termed waste and discarded. Pre-sieving the smaller particle size with F-110, however, was very time consuming, with approximately 85 to 90% of the sediment sieved going towards waste and only 15 to 10% actually being used. If AGSCO 140-270 was used in

place of F-110 to produce the smallest particle size, slightly better performance of 75 to 80% waste was achieved. Post-sieving of the sediment collected in the sump was completed through use of a smaller ro-tap sieving device.

The typical sieving process using the shaker table is as follows:

1) Place lower number (small diameter sieve) on shaker table first with the corresponding sieve above it.
2) Place approximately 3 quarts of feed sediment (out of specified bag) into top sieve and start shaker. Run shaker table for 5-6 minutes.
3) Stir the sediment in the top tray 1-2 times during sieving as the sediment will tend to clump on one side.
4) After shutting the sieve off empty both sieves into their respective buckets. Material passing through both sieves can be thrown away.
5) Use scrub brush to clean out sieves (this is more important for the 2nd and 3rd pairs as sediment is more likely to clog).
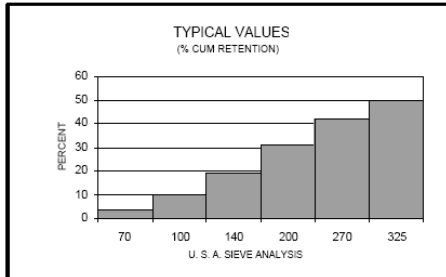6) Repeat steps (1-5)

PRODUCT DATA

U.S. SILICA
Sands of Time

SIL-CO-SIL® 250

GROUND SILICA

PLANT: OTTAWA, ILLINOIS

TYPICAL VALUES
(% CUM RETENTION)

| USA STD SIEVE SIZE | | TYPICAL VALUES | | |
| | | % RETAINED | | % PASSING |
MESH	MICRONS	INDIVIDUAL	CUMULATIVE	CUMULATIVE
70	212	3.5	3.5	96.5
100	150	6.0	9.5	90.5
140	106	9.5	19.0	81.0
200	75	12.0	31.0	69.0
270	53	11.0	42.0	58.0
325	45	8.0	50.0	50.0

TYPICAL PHYSICAL PROPERTIES

HARDNESS (Mohs) 7
MELTING POINT (Degrees F) 3100
MINERAL .... QUARTZ
pH.. 7

REFLECTANCE (%) 78
YELLOWNESS INDEX.. 4.8
SPECIFIC GRAVITY 2.65

TYPICAL CHEMICAL ANALYSIS, %

SiO_2 (Silicon Dioxide)...................................... 99.8
Fe_2O_3 (Iron Oxide)... 0.035
Al_2O_3 (Aluminum Oxide)................................. 0.05
TiO_2 (Titanium Dioxide).................................. 0.02
CaO (Calcium Oxide)...................................... 0.01

MgO (Magnesium Oxide)... <0.01
Na_2O (Sodium Oxide)... <0.01
K_2O (Potassium Oxide).. 0.02
LOI (Loss On Ignition)... 0.1

December 15, 1997

DISCLAIMER: The information set forth in this Product Data Sheet represents typical properties of the product described; the information and the typical values are not specifications. U.S. Silica Company makes no representation or warranty concerning the Products, expressed or implied, by this Product Data Sheet.

WARNING: The product contains crystalline silica - quartz, which can cause silicosis (an occupational lung disease) and lung cancer. **For detailed information on the potential health effect of crystalline silica - quartz, see the U.S. Silica Company Material Safety Data Sheet.**

U.S. Silica Company   P.O. Box 187, Berkeley Springs, WV 25411-0187   (304) 258-2500

Figure C.1. SCS 250 Particle Size Distribution

AGSCO CORPORATION

TECHNICAL DATA

AGSCO SILICA SAND
TYPICAL SCREEN ANALYSIS ... (continued)
(Percent Retained)

US SIEVE	12-20	16-30	20-40	(#1) 35-50	(#2) 40-70	50-80	(#7) 70-100	(#10) 100-140	(#16) 140-270
12	0.1								
14	1.3								
16	10.3								
18	44.2	1.4							
20	40.4	35.7	2.3						
25	3.5	58.0	19.7	0.3					
30	0.2	4.7	28.0	2.0	0.3				
35		0.2	30.3	20.5	5.2				
40			15.8	35.3	16.5	2.7			
50			3.6	32.7	37.0	39.3	8.2		
60			0.3	4.7	14.2	23.8	16.3	3.2	
70				2.2	9.3	16.2	22.3	4.6	
80				2.3	5.5	9.1	24.0	11.6	
100					4.8	5.4	13.5	19.8	
120					7.2	3.5	9.3	20.3	5.1
140							3.6	23.9	22.7
170							2.5	7.0	26.5
200							0.3	5.3	24.4
230								3.5	13.4
270								0.8	5.9
325									2.0
	100.0	100.0	100.0	100.0	100.0	100.0	100.0	100.0	100.0

AFS Grain Number	10	16	25	35	47	50	66	94	144
Effective Size (mm)	.85	.71	.43	.30					

SILICA FLOUR
(Percent Retained)

US SIEVE	140	200	325
100	T		
140	1	T	
200	6	3	
270	10	7	T
325	8	7	2
Passing 325	75	83	98
	100	100	100

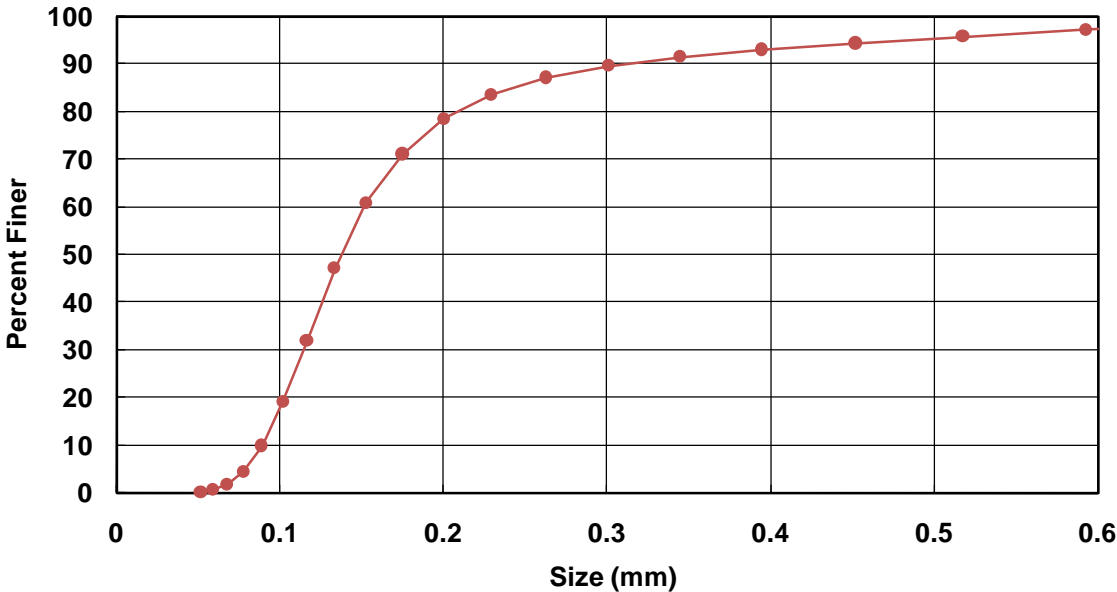**Figure C.2.** AGSCO 140-270, 40-70, and 20-40 Particle Distributions

Figure C.3. U.S. Silica F-110 Particle Size Distribution as Evaluated at St. Anthony Falls Laboratory

Appendix D.   Testing Procedures

D.1. Removal Efficiency Testing Procedure

D.1.1. Setup

Sediment is fed as a slurry into the inflow about one foot upstream of the sump. The slurry is created by the release of dry sediment from a precision sediment feeder into a pipe where it is combined with tap water. The slurry falls twenty five vertical feet before it enters the inflow pipe to the sump at the top. The vertical fall allows the sediment slurry to penetrate the entire water column before it enters the sump. The sump itself is outfitted with three bulkhead fittings which are located on the side of the sump. Bulkhead fittings provided a location for small diameter pipe (1.5 in diameter PVC pipe for example) to connect to the inside of the sump with no leakage. One larger fitting was located one foot above the sump floor, another smaller fitting was two inches above the floor. These two fittings provide a means to drain the sump below the outlet elevation. The third fitting, also located about one foot above the sump floor, was sized for connection to a vacuum hose. Thus the vacuum could sit outside of the sump, similar to a central vacuum unit in a home.

D.1.2. Pre-Test

Before testing even begins the necessary sediment must be sieved and the sump must be completely clean. Three narrow particle size ranges are sieved on a large shaker table as described in Appendix C. Equal parts of each of the three particle sizes are loaded into the feeder. The total sediment (all three particle sizes combined) is usually 33 to 44 lbs (15 or 20 kg) for each test. The goal of the total influent concentration is around 200 mg/L, and the sediment feeder is set to achieve this concentration for the selected water inflow rate. Concentration may vary for higher flow rates.

D.1.3. Test Run

To start the test, the inflow is first brought up to the desired inflow rate. Once the flow is properly set and has reached a steady-state, the tap water for the slurry can be turned on, followed by the sediment feeder. The time at which the feeder is started is recorded. The test is now free to run for the planned duration. During the test, various records are kept. The flow rate is checked and recorded periodically to be averaged at the end of the test. The flow rate variations are typically about ±0.05 cfs (1.4 L/s). The inflow, tank, and outflow manometer readings giving the water elevations are taken. Instrumentation for the monitoring of both water and air temperatures is used.

A test duration between 20 and 50 minutes, depending on flow rate, is the usual goal. When the feeder runs out of sediment, the time is recorded, and the feeder can be shut off. It is important to make sure that all of the sediment placed in the feeder has been used. The sediment pipe is flushed to ensure that no sediment has been trapped in the feed pipe and the flow is stopped. After shutting down flow, the sump is allowed to sit undisturbed to allow all particles to settle out of the water column. The time required for this is dependent on the settling velocity of the smallest particle size and the height of the water column. Settling time typically is around 15 minutes. Draining can begin at the conclusion of this waiting period. The time is recorded for the sediment feed start, feed stop, end of flush, flow stop, and when draining begins.

D.1.4. Post-Test

During the post test draining and sediment collection, every possible precaution is taken to ensure that all of the sediment in the sump is collected. Draining of the sump begins from the upper drain port located one foot above the device floor. The first flush from this drain port is collected in a five gallon bucket in case sediment has been trapped in the bulkhead fitting. The rest of the drain water can be discarded. With the outlet located one foot above the floor, sediment will not be pulled out with the drain water. Once the upper drain has stopped flowing, the lower drain is opened. This drain may remove sediment from the sump, it is therefore emptied into a series of clean 30 gallon trash barrels. After each barrel is full, sediment is allowed to settle (about 5 minutes) then the water is carefully decanted from the top and discarded. Any sediment will remain in the bottom of the trash can. Once the lower drain has stopped flowing, the sediment remaining in the device can be removed by a wet/dry vacuum. Each time the vacuum is full, it is emptied into the barrels. After all of the sediment is emptied from the vacuum, it is thoroughly cleaned over the barrels so that no sediment is lost. The vacuum, hoses, pales, and boots are thoroughly cleaned before the beginning of the test to ensure that contamination is not a problem.

After waiting for all particles to settle in the barrel, each barrel can be decanted. After continued decanting, the captured sediment can be consolidated into a tray and placed in an oven for drying. Once the sediment in the oven is dry, it can be sieved and divided into its original three particle size ranges. The weight of each particle size is then recorded and used to find the removal efficiency.

D.2. Washout Testing Procedure

D.2.1. Setup

Retention is the opposite of washout. Retention testing is accomplished by weighing of the sediment mass in the sump which is placed on precision strain gauge load cells. These load cells allow for accurate monitoring of the weight of the sump throughout the test. In addition to the load cells, the sump has constant monitoring of both water and air temperature. Both the inlet and outlet pipes are connected to the sump by rubber fittings which can be disconnected during the weighing process.

D.2.2. Pre-Test

Before testing begins, the initially clean sump is loaded with one foot of sediment. Each bag of sediment loaded into the sump is weighed on an external scale. The total weight of sediment loaded is compared to the load cell reading before and after loading for calibration of the load cells. The discrepancy between the two weights is usually 0.4 to 0.5% for 3,000 pounds (1,360kg) loaded.

After the sediment has been loaded, the surface of the sediment bed is flattened and packed to a known density of around 108 lbs/ft^3 (1,730 kg/m^3) for U.S. Silica F-110. This is completed in order to ensure a repeatable initial condition for all tests. Once the sediment bed has been properly prepared, the sump is slowly filled halfway with water. The sump is then disconnected from both its upstream and downstream pipes in order to eliminate the weight influence of these

pipes. The weight of the whole device is then recorded using the load cells, and the water elevation is recorded using a manometer mounted on the side of the sump.

D.2.3. Test Run

Once the upstream and downstream pipes have been reconnected, the sump is slowly filled the rest of the way with water. Once the water reaches the outlet invert the flow rate is raised to its proper level and the time is recorded. The device can now be tested for the predetermined duration. The duration of the test depends on the predicted rate of sediment washout. If too much sediment is removed the floor of the sump will become exposed and the test may not be repeatable. If too little sediment is removed, the accuracy of the load cells may be an issue.

During the test various parameters are monitored and recorded. These parameters include the flow rate, manometer readings for the inlet pipe, sump, and outlet pipe, and water and air temperatures. When the test duration has been reached the flow is shut off and the sump is allowed to sit for 15 minutes to allow the suspended sediment to settle.

D.2.4. Post-Test

Following the 15 minute settling time, the sump is drained to the halfway level and the manometer and load cell readings are again recorded. The new weight reading is adjusted based on the pre- and post-manometer readings to take into account the weight difference due to differing water levels. The sump is then drained and the sediment which was washed out can be replaced with new sediment for another test.

Appendix E.   High-Flow Washout Analysis

E.1.   Initial Washout Test Series in 4×4 ft (1.2×1.2 m) Sump

Washout (retention) was tested at higher flow rates than removal efficiency. The retention test series with the sump that had a 4ft (1.2m) diameter by 4 ft (1.2 m) depth included 35 tests. The discharges in each of the first six tests were 2.75 cfs (78 L/s), 4.18 cfs (119 L/s), and 5.5 cfs (158 L/s). These six tests essentially became pilot tests. The initial goal was to pre-load the sump with 6 inches (0.15m) of F-110 sediment and each run to last 60 minutes. After each test, the deposit in the sump was replenished with F-110 to return to the original 6 inch (0.15 m) initial condition. The weight of sediment in the sump was determined either from sediment depth (stick) measurements, load cells, or both. Flow rate was measured using a circular weir for the first 6 tests and a Pitot cylinder in the supply pipe for the remaining tests.

Analysis of the first 6 tests revealed that finer particles might be washed out during the test leaving the larger particles behind. This preliminary result was derived from the varying amounts of washout as the flow rate increased. Tests 9 through 17 gave results that countered the earlier findings. It was therefore decided to conduct the tests in series of three over a two hour period and with an 8 inch (0.20 m) deep deposit. Each flow rate would begin with a fresh load of F-110 and each subsequent test in the series would have sediment replenished, mixed with the remaining, and then sampled. The samples were sieved and the bulk density of the deposit for each test was determined. Therefore, a better knowledge of initial and final sediment in the sump was available. Despite of these changes, inconsistencies were exhibited in the tests. For some tests, as sediment was washed out during the test, a portion of the floor was exposed which limited the wash out rate. To overcome this problem, tests 18 through 27 were conducted similar to the previous 9 tests except that the initial deposit depth in the sump was increased to 12 inches (31 cm). The increase in initial sediment depth prevented the exposure of the sump floor and increased the repeatability of the test results.

All tests up to number 27 were conducted for three flow rates only. Tests 28 to 35 were designed to fill in the flow rate gaps. The first 27 tests were conducted in February and March, while the final eight tests were conducted in May and June. There was nearly a 30 ^{o}F difference in water temperature between the two sets of tests. The final curve has an exponential increase in effluent concentration, i.e. increasing washout rate until the flow reaches 4.8 cfs (136 L/s). At 5.5 cfs (156 L/s) a decrease in effluent concentration was recorded.

E.2.   Initial Washout Test Series in 4×2 ft (1.2×0.6 m) Sump

With most of the issues from the first round of retention tests in the deep (4-ft, 1.2-m) sump settled, the shallow (2 ft, 0.6 m) sump retention tests went quickly. The major issue in this series of tests was the high rate of scour. As already stated, it was important to ensure that the floor of the sump did not become exposed. Tests 1 through 9 in the shallow sump were conducted in the same way as in the deep sump. Each test was conducted for two hours with 12 inch (0.3 m) of F-110 sediment loaded. The sediment was mixed, flattened, and rolled before each test. Samples were taken before and after each test to determine the particle size distribution and the bulk density. The proximity of the sediment layer at the bottom of the sump to the inflowing jet resulted in high rates of scour, which left the floor of the sump exposed for tests 3 through 9. The load cell data gave an estimate of the time for the floor to become exposed. Therefore new shorter tests were conducted. The duration of the tests varied from 2 hours for 2.75 cfs (78 L/s)

flow to 12 minutes for the 5 cfs (142 L/s). No tests were conducted above 5cfs (142 L/s) due to the high error associated with the short duration.

E.3. Bulk Density Analysis

A significant effort was made to determine the bulk density of the sediment in the sump. The goal was to ensure that the same bulk density was reached for the sediment in the sump both before and after the retention tests. The sediment was completely stirred and repacked using a 20 lbs (9kg) PVC roller. The duration and pattern used for packing was varied until one sequence was found which gave repeatable bulk density values. The bulk density in the sump was calculated by first filling the sump with a known weight of sediment. Water was then added to the sump. Once the sediment was packed and the bed leveled, stick depth measurements were taken at 24 locations in the sump. The average of these measurements was then taken to be the depth of sediment in the sump. Knowing the cross sectional area of the sump it was now possible to determine a bulk density for the sediment in the sump. Thus, as long as the stirring, packing, and leveling protocol was followed, the same bulk density could be achieved both before and after each test. An average bulk density of 107.4 lbs/ft^3 (1,720 kg/m^3) was determined for the material used. The typical variability in the bulk density was ±0.6 lbs/ft^3 (9.6 kg/m^3)

There were also concerns regarding the change in the particle size distribution of the sediment deposit after each washout test, i.e. as the finer particles were washed out the remaining deposit could have a different bulk density. This required developing a testing protocol to determine the bulk density of the deposit before and after each test. A series of bulk density tests was conducted in a small 6 inch (0.15 m) by 18 inch (0.46m) tray. These tests were repeated many times, using samples taken from the known bulk density tests described above. Each repeat test used either a different weight roller, or the roller was passed over the sediment a different number of times. The testing protocol (and its subsequent weighted roller and number of times rolled) which produced a repeatable result and mirrored the result from the full scale sump tests was chosen to be the optimal protocol. It was now possible to take samples before and after a test to determine the bulk density of each in situ sample. The corresponding bulk density could be applied to the volume of sediment deposit found from the stick depth measurements to calculate the weight of sediment in the sump before and after each test. The weight found using the stick depth measurements was then compared to the load cell measurements. Table E.1 compares all of the results for the 4×4 ft (1.2×1.2 m) sump which had both stick depth measurements and weight measurements. A rough measure of maximum error using the initial sediment weight of 1,250 lbs (567 kg) is 3% between the two measurement techniques.

Table E.1. Comparison of Weight Measurement Techniques for Washout Testing

Test No.	Actual Flowrate (cfs)	Starting Bulk Density (lbs/ft³)	Ending Bulk Density (lbs/ft³)	Dry Weight Removed (lbs)	Effluent Conc. (mg/L)	Dry Weight Removed (lbs)	Effluent Conc. (mg/L)	Weight Error
9	2.8	106.2	106.1	39	31	33	27	0%
10	2.8	106.1	106.7	62	50	46	37	1%
11	2.7	106.7	106.8	33	27	29	24	0%
12	4.1	106.8	106.3	308	165	306	164	0%
13	4.1	107.3	105.5	215	117	173	94	3%
14	4.1	105.1	104.9	220	119	216	117	0%
15	5.5	106.0	100.1	650	264	631	257	2%
16	5.5	101.1	105.1	376	153	404	164	2%
17	5.5	103.6	105.3	323	131	329	134	0%
20	4.2	104.8	106.2	258	138	265	141	1%
23	4.1	104.5	105.6	251	135	306	165	4%
27	5.5	103.7	103.2	637	257	618	249	2%
28	3.5	108.9	111.1	108	69	115	73	1%

Appendix F.   Velocity Measurements

A significant number of velocity measurements were made in the sump using an Acoustic Doppler Velocimeter (ADV). The results provided great insight into the complex flow patterns which occur in a sump. Measurements were made at flow rates of 2.4cfs (68L/s) and 4.8cfs (136L/s) in the shallow and deep 4-ft (1.2 m) sump. Velocity measurements were also made along the centerline of the 4-ft (1.2 m) deep sump at closely spaced flow rates of 4.5 cfs (127 L/s), 5.0 cfs (142 L/s), 5.5 cfs (156 L/s), and 6.0 cfs (170 L/s).

Two different ADV's were used for the data collection. A Nortek Vectrino 3D ADV was used for the 2.4 cfs (68 L/s) data which was collected in the 4-ft (1.2m) deep sump. This ADV could collected data at a rate of 250Hz. The rest of the data was collected using a Sontek 3D ADV with a collection rate of 10Hz. Axes for all of the tests are defined as follows: X-axis is along the flow path, Y-axis is perpendicular to the flow path, and the Z-axis is vertical.

The ADV measurements captured the powerful water circulation pattern in the sump, which causes the movement of sediment across the sediment bed in upstream direction, i.e. opposite to the incoming flow direction, where the sediment would be either deposited or suspended. If suspended, the particles are likely lifted up to the inlet and outlet elevation, and discharged with the effluent from the sump. Besides the main circulation pattern along the x-z plane, there are more complex circulation patterns along the x-y and y-z planes. These circulation patterns are highly variable depending on flow rate and other random conditions. Figures F.1 through F.4 are plots of velocity vectors which capture some of the complex flow characteristics in the 4ft deep standard sump.
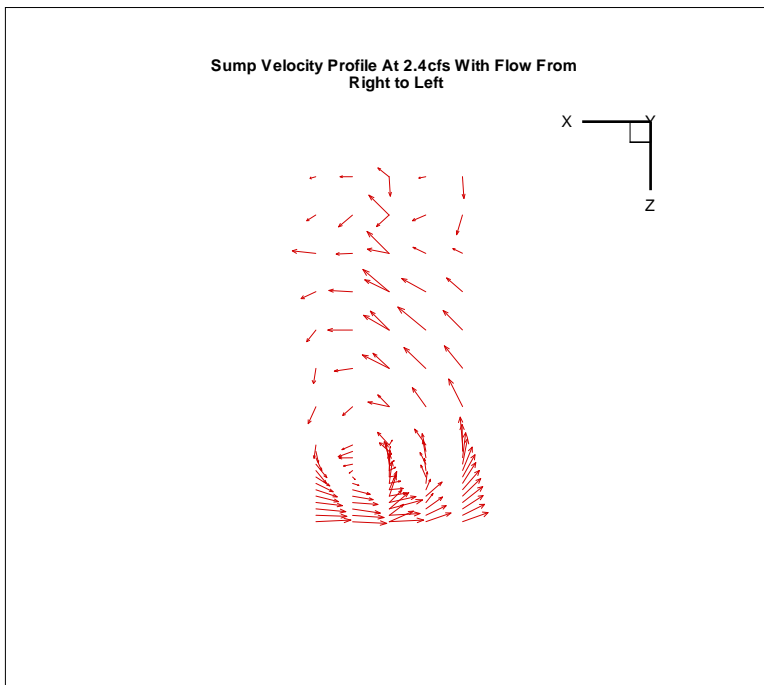
Figure F.1. Measured Velocity Vectors Illustrating the Flow Pattern in a Vertical Plane Aligned with the Inflow Direction (X-Z Plane) and Through the Center of a 4ft Deep Sump. Inflow is Near the Top and from Right to Left.
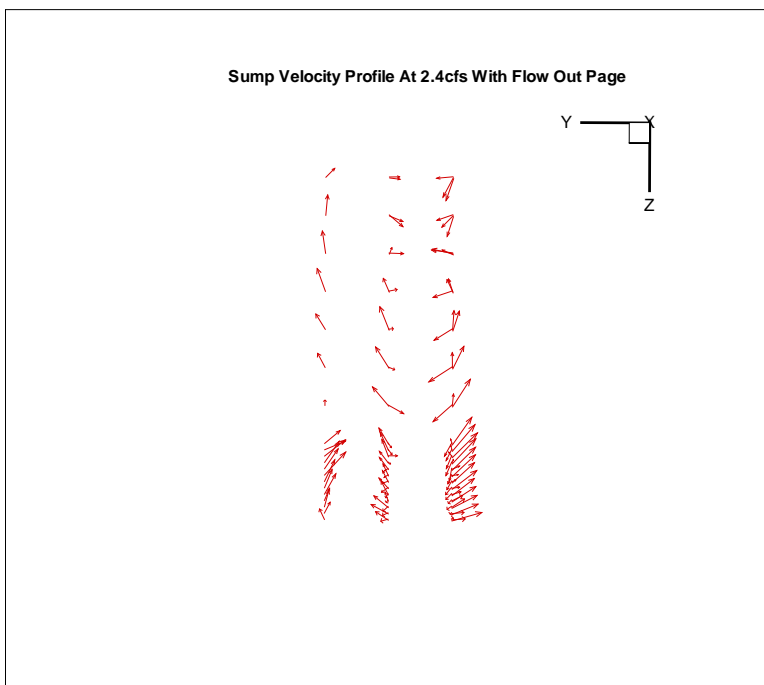

Figure F.2. Measured Velocity Vectors Illustrating the Flow Pattern in a Vertical Plane Perpendicular to the Inflow and Through the Center of a 4ft (1.2m) Deep Sump (Y-Z Plane). Inflow is Near the Top and Perpendicular to the Plane Shown. The Centerline of the Sump Corresponds to the Furthest Right Measurements.
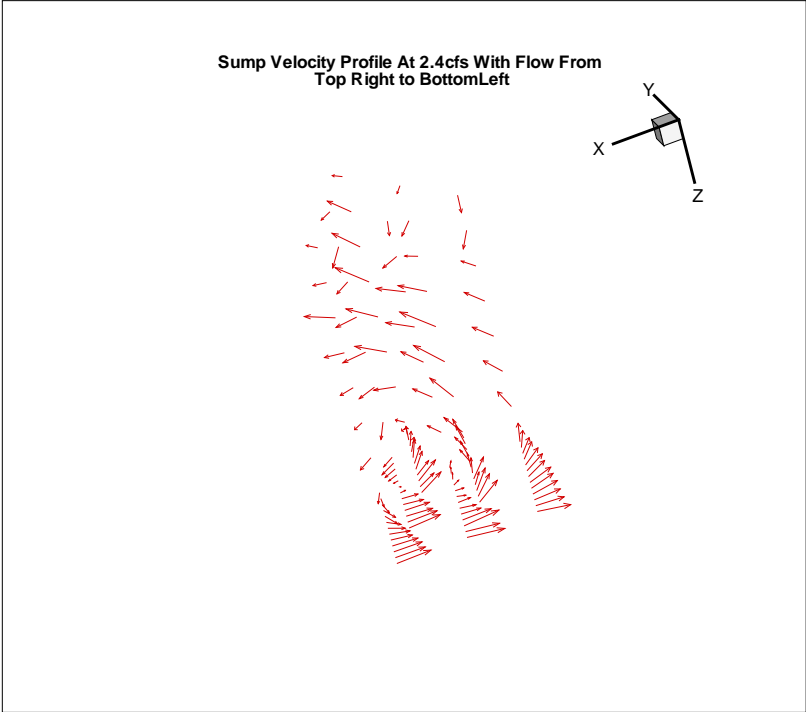
Figure F.3. 3D View of Measured Velocity Vectors Illustrating the Flow Pattern in a Vertical Plane (X-Z Plane) Through the Center of a 4ft (1.2m) Deep Sump. Inflow is Near the Top Along the X-axis.
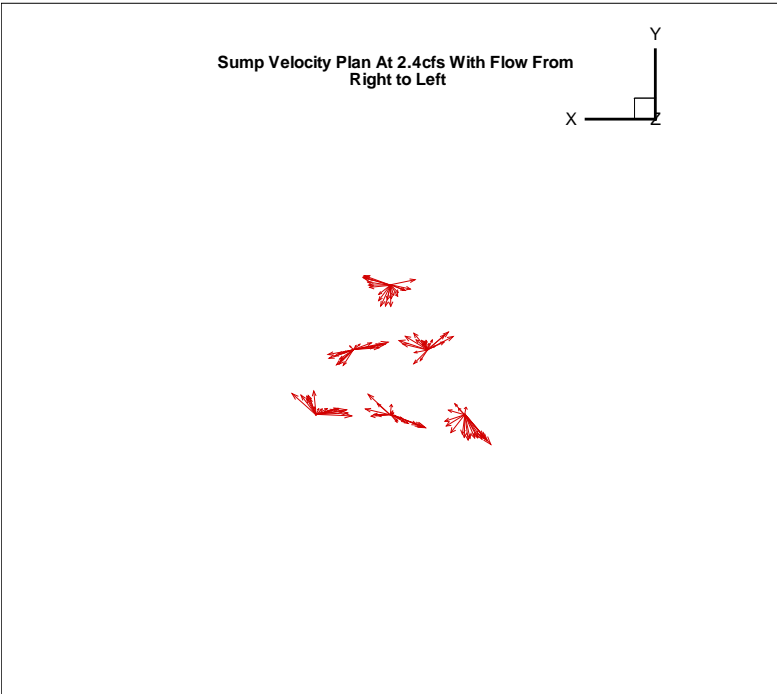
Figure F.4. Measured Velocity Vectors Illustrating the Flow Pattern Looking Down onto a Horizontal Plane (X-Y Plane), The Inflow is along the X-Axis, and the Flow Centerline is at the Bottom of the Plot.

Appendix G.   Péclet Number Evaluation

G.1. Comparisons of Removal Efficiency Results for Different Sump Designs and Tests Using the Péclet Number

In Section 4.1 the Péclet number (Equation 4.1) was shown to be an effective predictor of the sediment removal efficiency for each individual sump configuration. However, when comparisons were made between different sump designs the Péclet number provided confusing results. This appendix provides the individual charts for removal efficiency versus the Péclet number, and comparisons among different sump designs. Figures G.1 through G.5 are of each for an individual sump configuration.
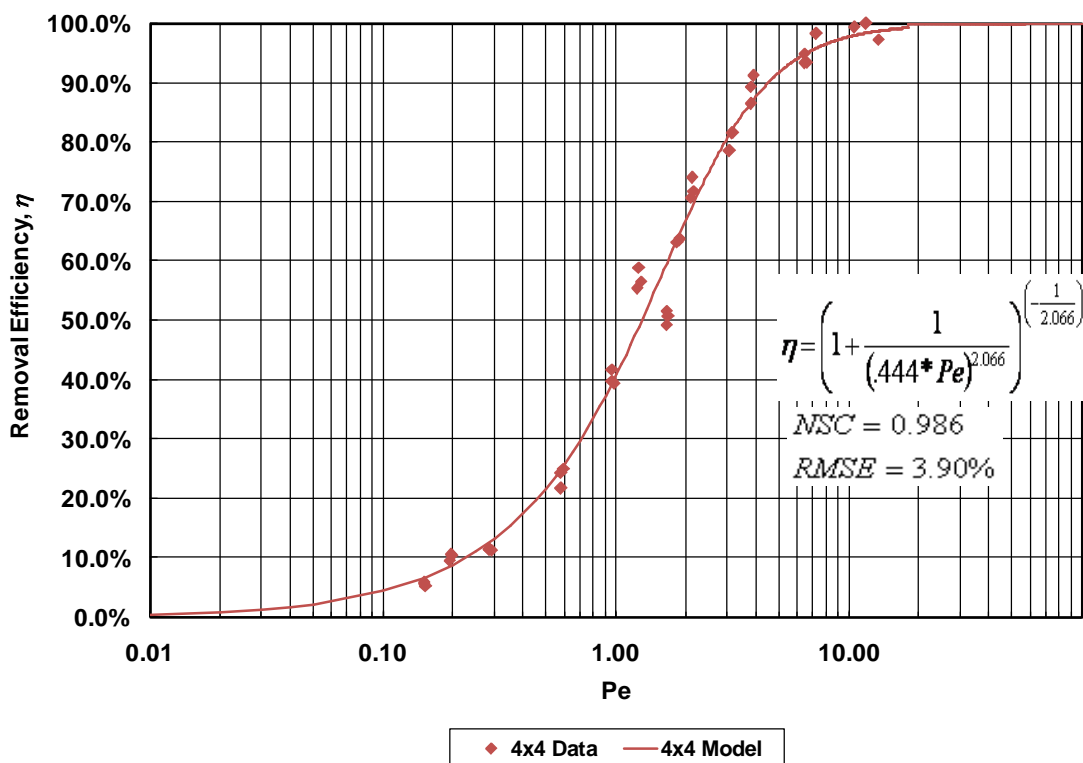
Figure G.1. 4×4 ft Standard Sump Removal Efficiency Results
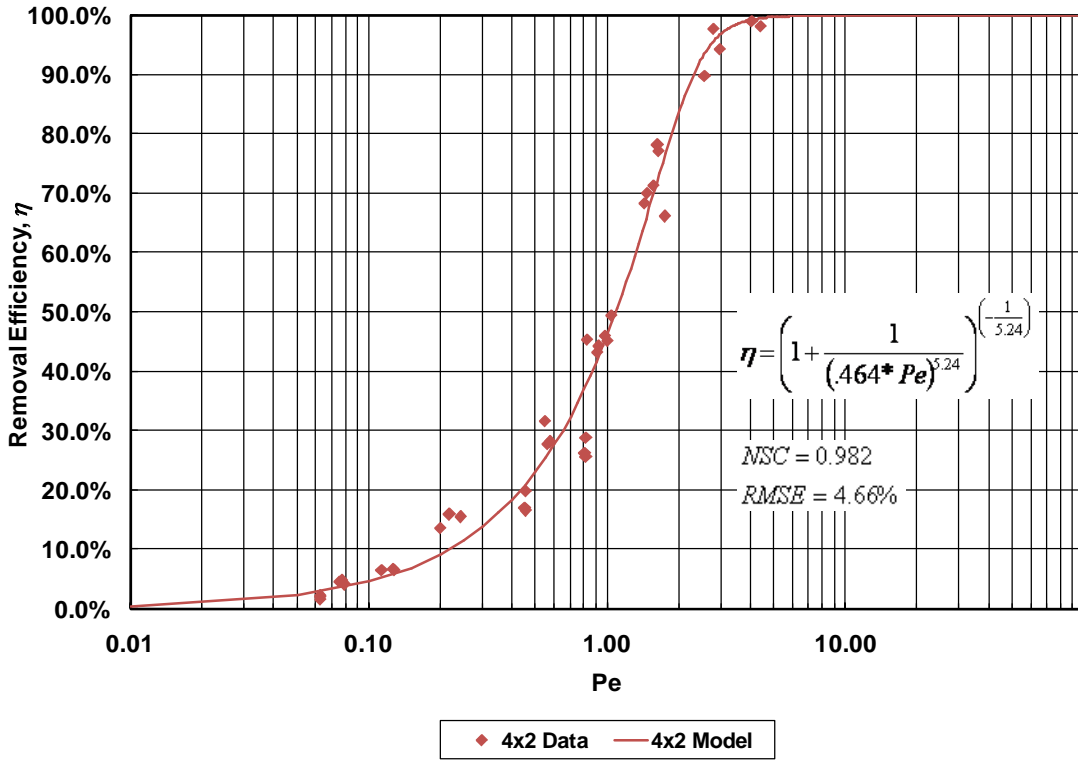
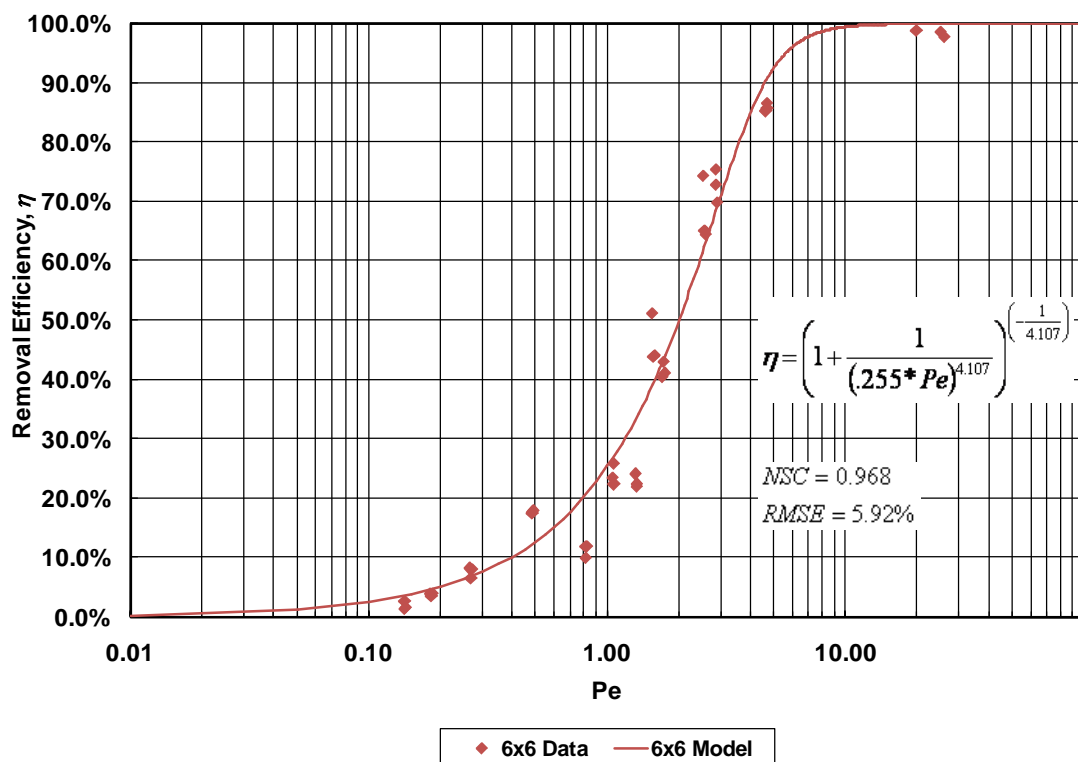**Figure G.2.** 4×2 ft Standard Sumps Removal Efficiency Results

Figure G.3. 6×6 ft Standard Sumps Removal Efficiency Results
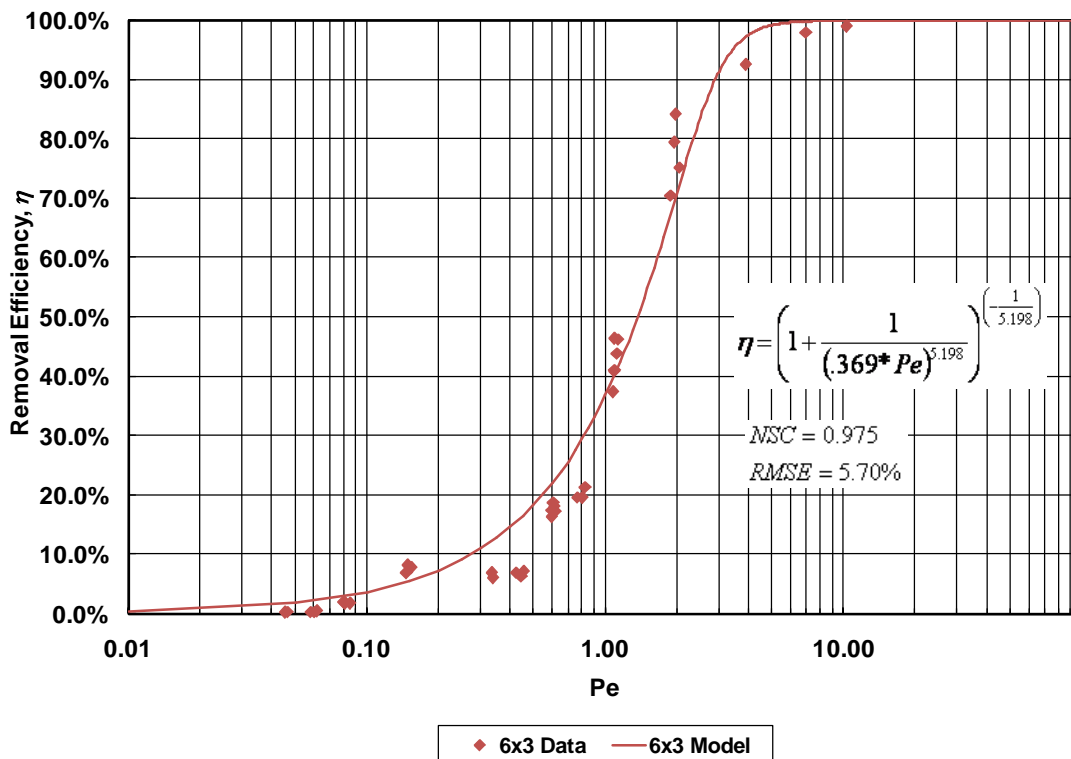
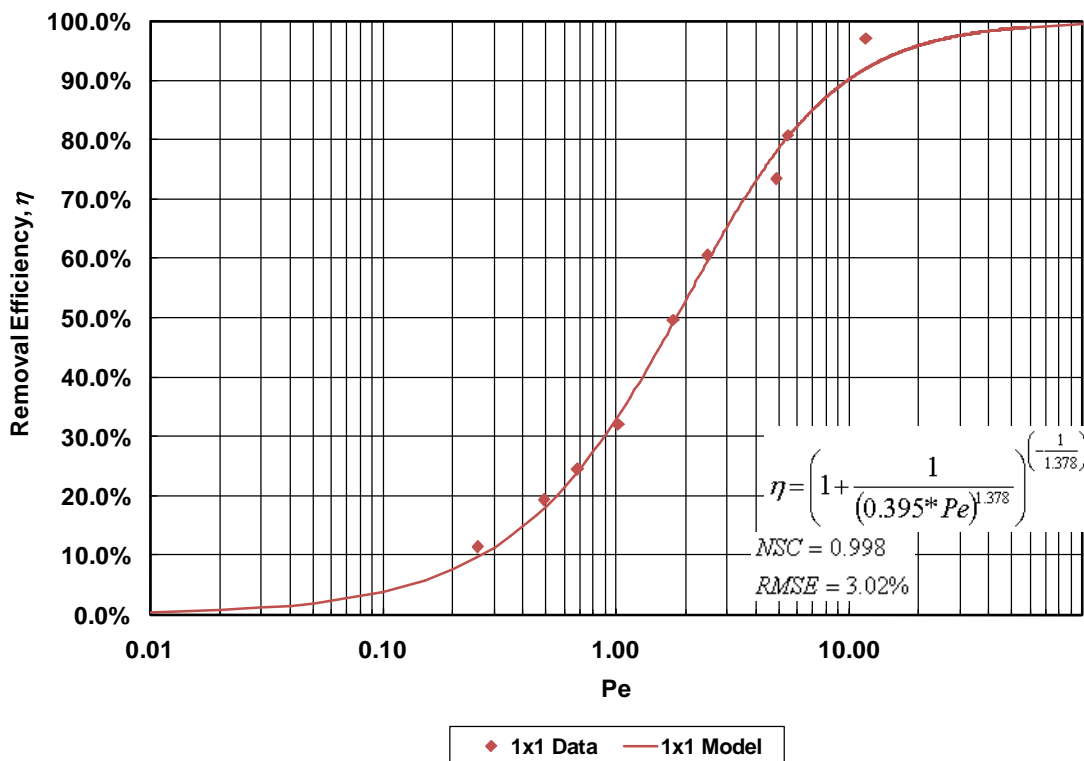**Figure G.4.** 6×3 ft Standard Sumps Removal Efficiency Results

Figure G.5. 1×1 ft Standard Sumps Removal Efficiency Results

Figure G.6 is a removal efficiency versus Péclet number plot for two repeat tests of the 4ft (1.2m) by 4ft (1.2m) sump and the 95% confidence intervals for the initial test. The first test series was completed in January and the second in May. This plot shows that the Péclet number works well for the comparison of the results from tests conducted under different flow rates and water temperatures in the same sump design. In addition, since the tests were conducted at two different times of year, the water temperature was about 30 degrees warmer for the repeated test series. The flow rates were slightly different. The tests proved very repeatable; the results of the second test series landed within the 95% confidence intervals for the initial test series model.
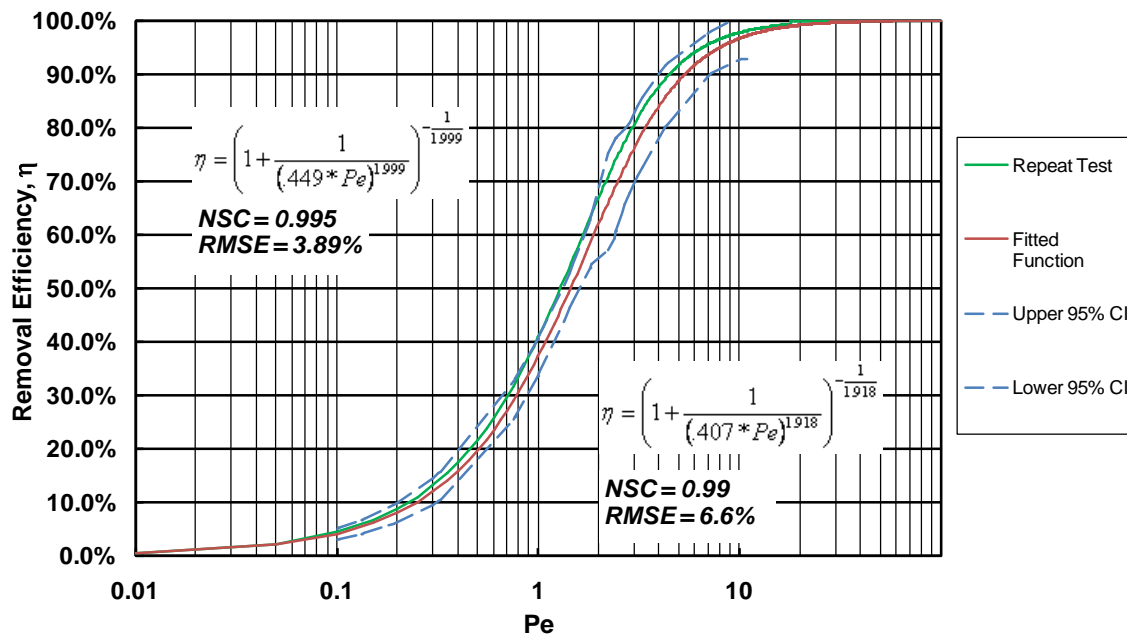

The equations shown in the figure are:

$$\eta = \left(1 + \frac{1}{(449 * Pe)^{1.999}}\right)^{-\frac{1}{1.999}}$$

NSC = 0.995
RMSE = 3.89%

$$\eta = \left(1 + \frac{1}{(407 * Pe)^{1.918}}\right)^{-\frac{1}{1.918}}$$

NSC = 0.99
RMSE = 6.6%

Legend: Repeat Test; Fitted Function; Upper 95% CI; Lower 95% CI

Figure G.6. Repeatability of Removal Efficiency Results for 4×4 ft Sump

G.2. *Scaling Improvement by Péclet Number Adjustment*

The major issue with the Péclet number as the predictor variable for the calculation of removal efficiency was its poor ability to scale varying sump sizes and depth to diameter ratios. If standard sumps have identical flow patterns, it should be expected that the data will collapse on one curve if the correct scaling variable, in this case the Péclet number is used.

As can be seen in Figures F.7 and F.8 deep sumps and shallow sumps have systematically different removal efficiencies. Comparing the 4ft (1.2m) by 2ft (0.6m) and the 4ft (1.2m) by 4ft (1.2m) sumps in Figure G.1, as well as the 6ft (1.2m) by 3ft (0.9m) and 6ft (1.8m) by 6ft (1.8m) sumps in Figure G.8 shows that for the same Péclet number the shallower sump has a higher removal efficiency. This is not meaningful from a physical point of view. Instead it is caused by the reduction in the Péclet number (Equation 4.1) caused by the reduction in the depth h of the sump. The Péclet number of the shallow sump is half that of the deep sump. An 'accurate' comparison of the shallow and deep sump would require the shallow sump to be moved to the right by a factor of 2 which is the inverse ratio of the sum depths. It is interesting to note in

Figures G.7 and G.8 that the shift between the two curves is by about a factor of 2, but only above a threshold which is about *Pe = 1* and *Pe = 0.1* for the 4-ft and the 6-ft diameter sumps, respectively. It is only above those Péclet numbers that the sump depth appears to have a physical effect.

At the very least, the sumps with geometric similitude, i.e. the 4ft (1.2m) by 4ft (1.2m), 1ft (0.3m) by 1ft (0.3m), and 6ft (1.8m) by 6ft (1.8m) sumps, should fit on one line. Or the 6ft (1.8m) by 3ft (0.9m) and the 4ft (1.2m) by 2ft (0.6m) sumps should give removal efficiencies that fit on one line. This did occur, but with a margin of error up to 20% for removal efficiency, as is shown in Figure G.9.

In order to solve this dilemma, an empirical approach was taken to make the data from different sump designs collapsed on the same curve. It was found that geometric mean of the Péclet number and the Hazen number produced very accurate results for the comparison of the sumps with different depth to diameter ratios. The Péclet number was defined by Equation 4.1, and the Hazen number is defined as

$$Ha = \frac{U_s D^2}{Q} \tag{G.1}$$

The formula produced by finding the geometric mean of the Péclet and Hazen numbers is

$$\sqrt{PeHa} = \frac{U_s h^{0.5} D^{1.5}}{Q} \tag{G.2}$$

Figures G.10 and G.11 are plots of the removal efficiency versus the geometric mean of the Péclet and Hazen numbers for all 4-ft (1.2 m) and 6-ft (1.8 m) sumps tested.
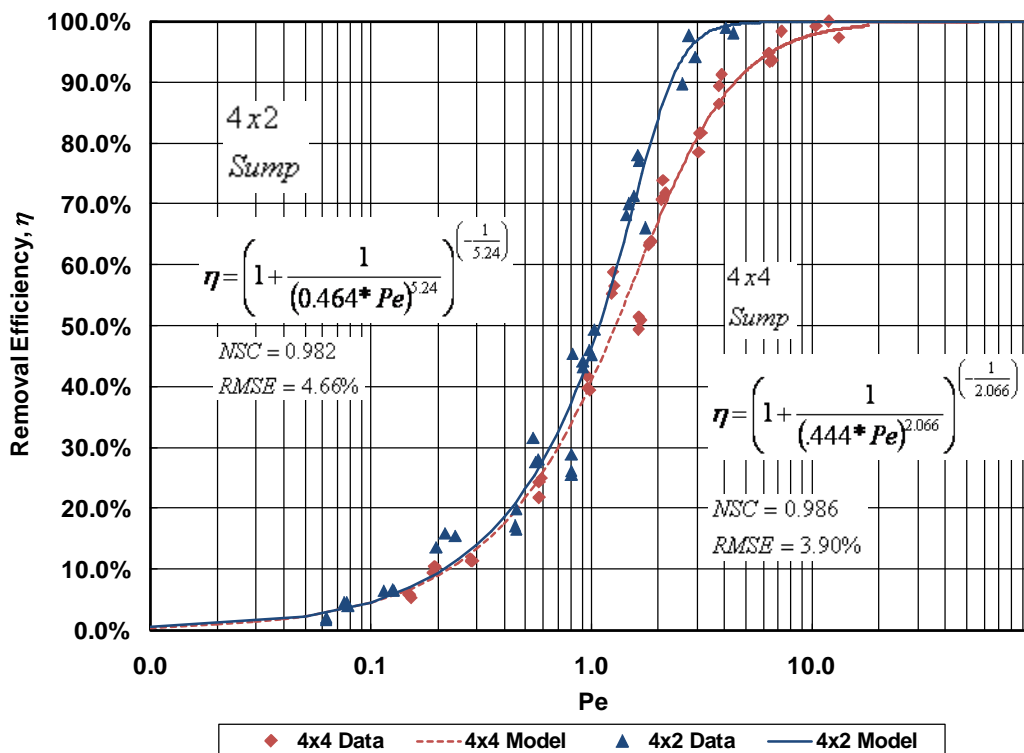
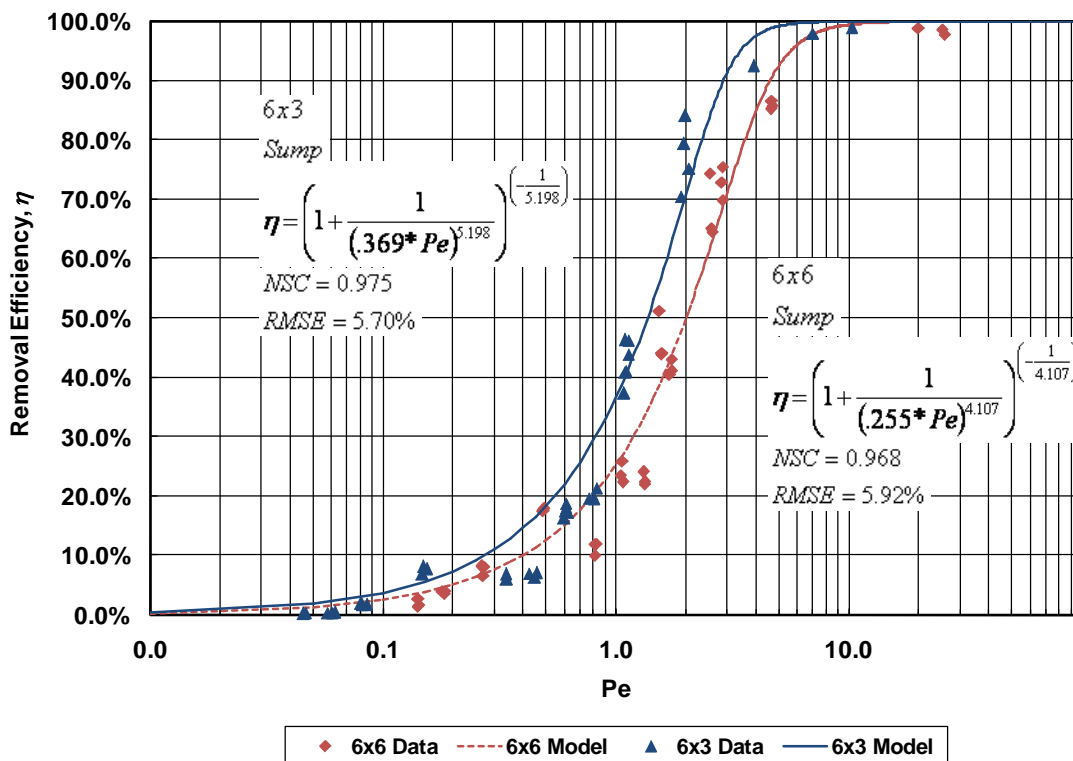**Figure G.7.** Comparison of the Removal Efficiency Results for 4×4ft and 4×2ft Sumps

Figure G.8. Comparison of the Removal Efficiency Results for 6×6ft and 6×3ft Sumps
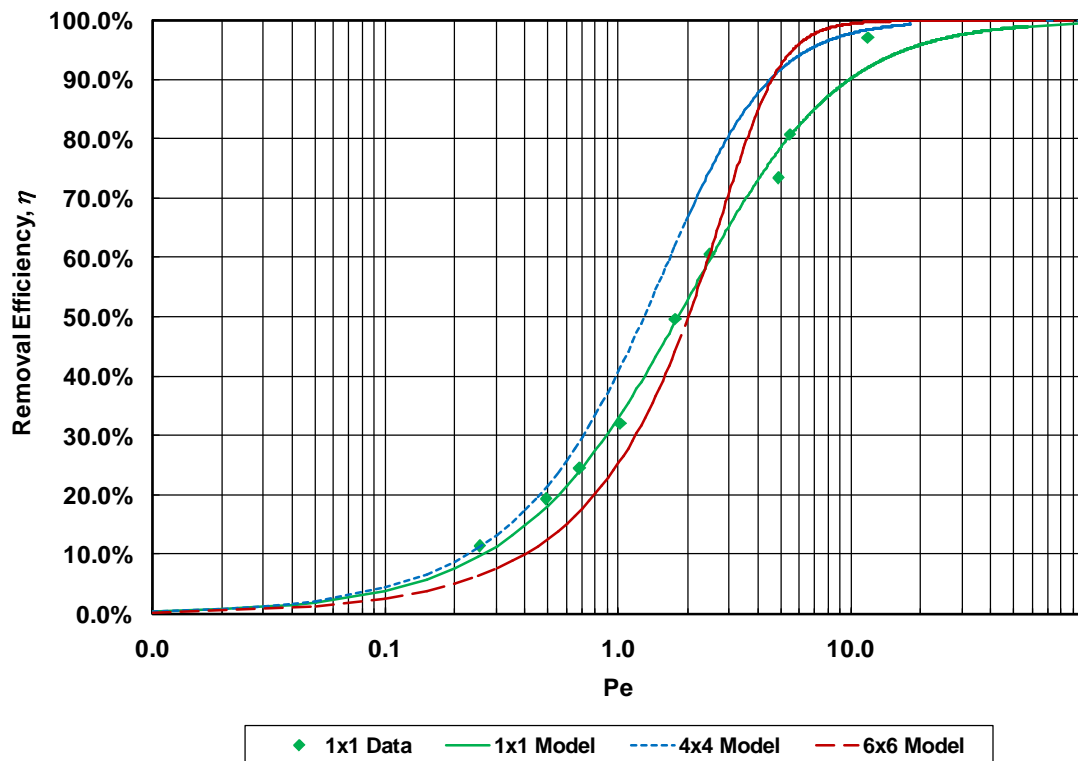
Figure G.9. Comparison of the Removal Efficiency Result Models for the 6×6ft, 4×4ft, and 1×1ft Sumps
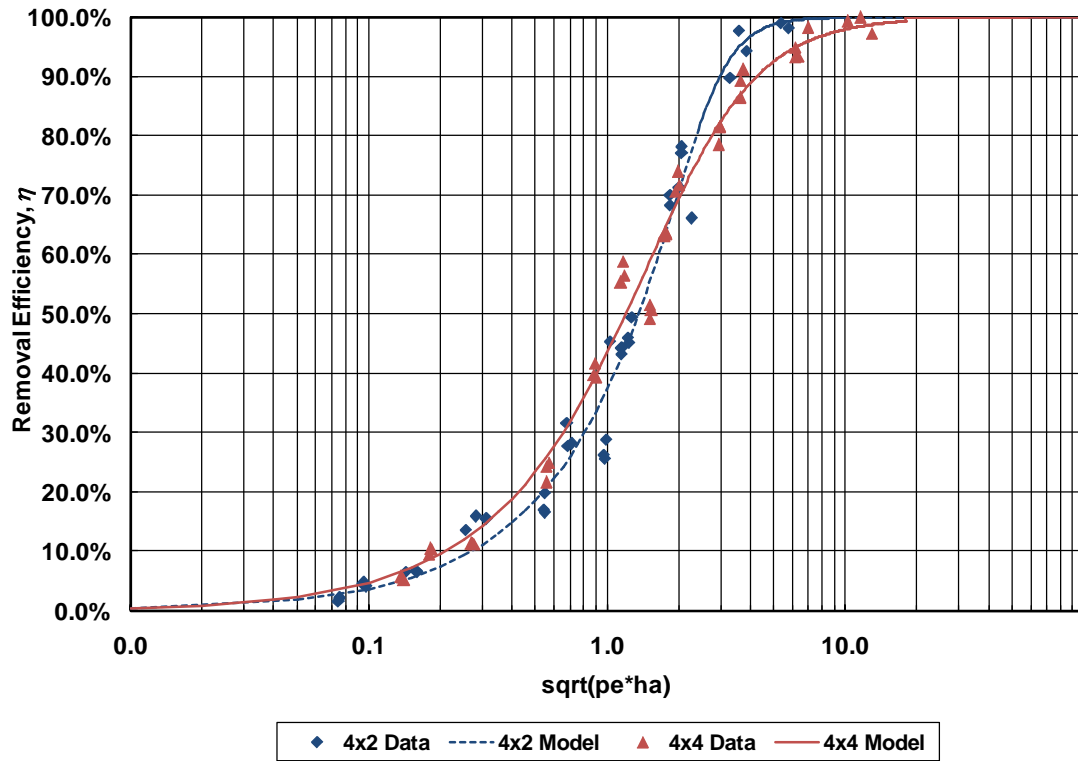

Figure G.10. Comparison of the Removal Efficiency for the 4×2ft and 4×4ft Sumps using the Geometric Mean of the Péclet and Hazen numbers
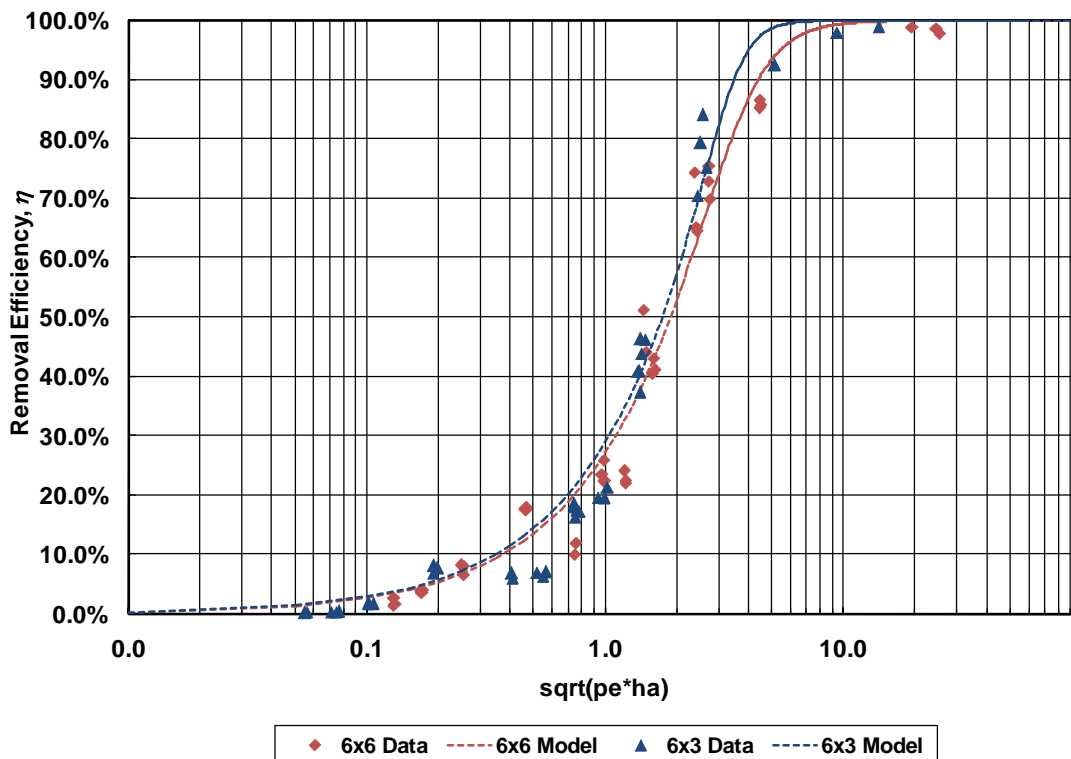
Figure G.11. Comparison of the Removal Efficiency for the 6×3 ft and 6×6 ft Sumps Using the Geometric Mean of the Péclet and Hazen Numbers.

G.3. Scaling of 1×1 ft (0.3×0.3 m) Scale Model Results

Substantial effort was put into measuring accurate removal efficiencies in the 1:4.17 1×1 ft (0.3×0.3 m) Scale Model. If a testing and scaling procedure can be created which produces results similar to the full scale sumps, it may be possible in the future to conduct tests at a smaller scale to decrease costs. This goal proved to be very challenging.

The scaling tests were designed using the removal efficiency curve from the full scale sump. A desired removal efficiency was chosen which provided an appropriate Péclet number. If it is possible to scale the device using the Péclet number, the data should land on the full scale curve. Given the desired value of the scaling parameter, considered to be a Péclet number, from the full scale 6× 6 ft (1.8×1.8 m) efficiency curve, and knowing the depth and diameter of the 1×1 ft (0.3×0.3 m) scale model, the appropriate flow rate for the 1×1 ft (0.3×0.3 m) scale model can be calculated and used in the model tests. Figure F.12 is a plot of the full scale sump performance function and the data from the model.
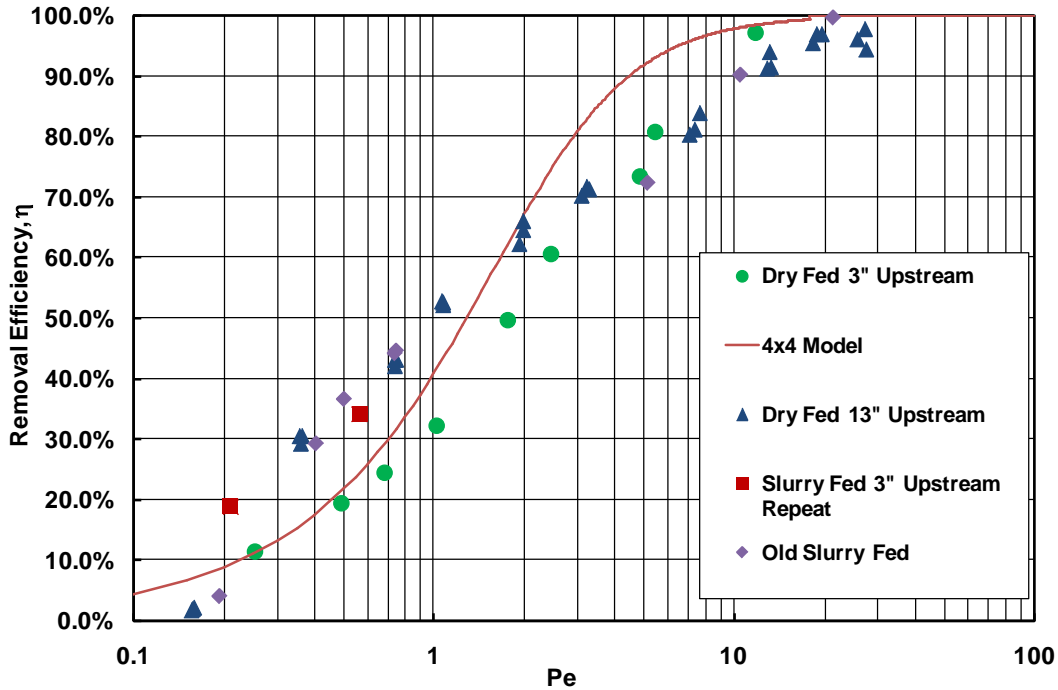
Figure G.12. 1×1 ft (0.3×0.3 m) Scale Model Performance Results with 4×4 ft Performance Model

At higher Péclet numbers the 1×1 ft (0.3×0.3 m) scale model estimates the removal consistently lower than the full scale. At lower Péclet numbers, the 1×1 ft (0.3×0.3 m) scale model data produces more scatter. Some of this scatter can be explained by the testing processes. The data above the full scale curve is data collected from tests which had the sediment either fed as a slurry 3 in (0.076 m) upstream of the device or dry fed 13 in (0.33 m) upstream of the device. The data located below the curve was collected by dry feeding sediment 3in (0.076 m) upstream of the device.

When the sediment is slurry fed, there is a deep penetration into the water column due to the high vertical velocity. The sediment which was dryfed 13in (0.33m) upstream of the device had more time to settle before reaching the sump than the sediment which was dryfed 3 in (0.076 m) upstream. Therefore particles fed as slurry or dry and further upstream will be better mixed and/or located deeper in the water column when reaching the sump compared to the particles which was dry fed 3in (0.076m) upstream of the sump. If the particles are located deeper in the water column when entering the sump, it is more probable that they will be trapped by the sump.

Typically the location of the particles in the water column when entering the sump does not have an effect on the outcome of the tests. However, in the scale of the model test, the particle size is large enough, when compared to the size of the sump, to change the outcome of the tests. This implies that it may be possible to scale sumps by length scales which are significantly different, however it may be necessary to calibrate any 1×1 ft (0.3×0.3 m) scale model test protocol with a full scale data set in order to ensure accurate results.